16 Protein Fluorescence

The biochemical applications of fluorescence often utilize intrinsic protein fluorescence. Among biopolymers, proteins are unique in displaying useful intrinsic fluorescence. Lipids, membranes, and saccharides are essentially nonfluorescent, and the intrinsic fluorescence of DNA is too weak to be useful. In proteins, the three aromatic amino acids—phenylalanine, tyrosine, and tryptophan—are all fluorescent. These three amino acids are relatively rare in proteins. Tryptophan, which is the dominant intrinsic fluorophore, is generally present at about 1 mole% in proteins. The small number of tryptophan residues is probably the result of the metabolic expense of its synthesis. A protein may possess just one or a few tryptophan residues, facilitating interpretation of the spectral data. If all twenty amino acids were fluorescent then protein emission would be more complex.

A valuable feature of intrinsic protein fluorescence is the high sensitivity of tryptophan to its local environment. Changes in the emission spectra of tryptophan often occur in response to conformational transitions, subunit association, substrate binding, or denaturation. These interactions can affect the local environment surrounding the indole ring. Tyrosine and tryptophan display high anisotropies that are often sensitive to protein conformation and the extent of motion during the excited-state lifetime. Also, tryptophan appears to be uniquely sensitive to collisional quenching, apparently due to a tendency of excited-state indole to donate electrons. Tryptophan can be quenched by externally added quenchers or by nearby groups within the proteins. There are numerous reports on the use of emission spectra, anisotropy, and quenching of tryptophan residues in proteins to study protein structure and function.

A complicating factor in the interpretation of protein fluorescence is the presence of multiple fluorescent amino acids in most proteins. The environment of each residue is distinct and the spectral properties of each residue are generally different. However, the absorption and emission spectra of tryptophan residues in proteins overlap at most usable wavelengths, and it is difficult to separate the spectral contributions of each tryptophan in a multi-tryptophan protein. Complex time-resolved intensity decays are found even for proteins that contain a single-tryptophan residue. Most single-tryptophan proteins display multi-exponential intensity decays. For this reason one cannot simply interpret the multiple decay times of a multi-tryptophan protein in terms of the individual tryptophan residues in a protein.

As a further complicating factor, tryptophan displays complex spectral properties due to the presence of two nearly isoenergetic excited states, ^1L_a and ^1L_b. The electronic transitions display distinct absorption, emission, and anisotropy spectra, and are differently sensitive to solvent polarity. The complexity of indole photophysics has stimulated detailed studies of protein fluorescence, but has also inhibited interpretation of the data.

Protein fluorescence can be complex, but considerable progress has been made in the past decade. The origin of the multi-exponential decay of tryptophan in water is now largely understood as due to the presence of rotational conformational isomers (rotamers). These rotamers have different orientations of the amino and carboxyl groups relative to the indole ring. Studies of single-tryptophan proteins have provided information on the spectral properties of tryptophan in unique environments. Widely different spectral properties have been observed for single-tryptophan proteins. The highly variable tryptophan quantum yields of proteins appear to be the result of nearby quenchers in the protein, which include lysine and histidine residues. Under appropriate conditions it appears that even amide groups in the peptide backbone can act as quenchers. The use of site-directed mutagenesis has allowed creation of mutants that contain one instead of several tryptophan residues, insertion of tryptophan at desired locations in the protein, and modification of the environment around a tryptophan residue. Examination of single-tryptophan proteins and engineered proteins has provided a more detailed understanding of how

the local environment determines the spectral properties of tryptophan. It is also possible to insert tryptophan analogues into proteins. These analogues display unique spectral features, and are observable in the presence of other tryptophan residues.

In summary, a growing understanding of indole photophysics, the ability to place the tryptophan residues at desired locations, and the availability of numerous protein structures has resulted in increased understanding of the general factors that govern protein fluorescence. The high sensitivity of the emission from tryptophan to the details of its local environment have provided numerous opportunities for studies of protein functions, folding, and dynamics.

16.1. SPECTRAL PROPERTIES OF THE AROMATIC AMINO ACIDS

Several useful reviews and monographs have summarized the spectral properties of proteins.[1–9] Proteins contain three amino-acid residues that contribute to their ultraviolet fluo-

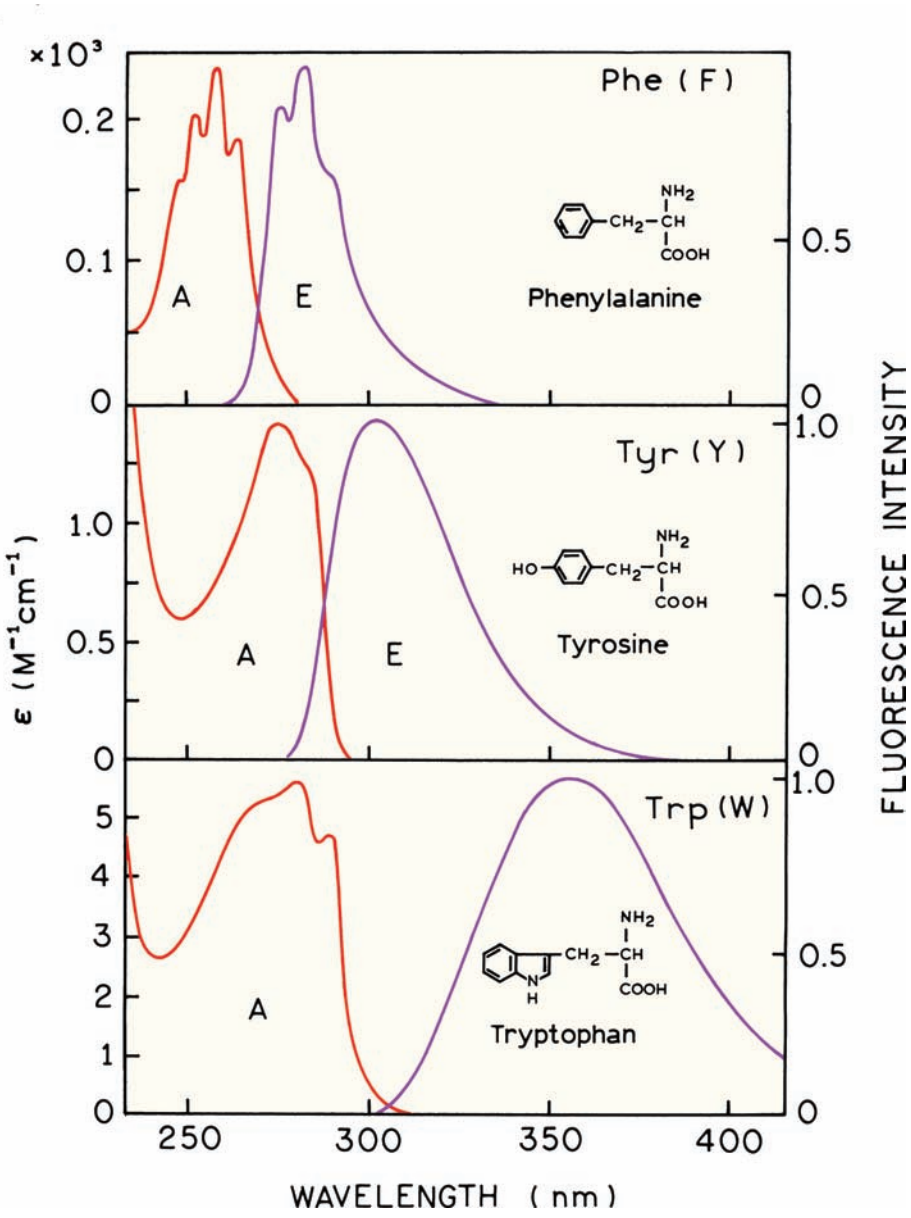

Figure 16.1. Absorption (A) and emission (E) spectra of the aromatic amino acids in pH 7 aqueous solution. Courtesy of Dr. I. Gryczynski, unpublished observations.

rescence which are usually described by their three- or one-letter abbreviations. These are tyrosine (tyr, Y), tryptophan (trp, W), and phenylalanine (phe, F). The absorption and emission spectra of these amino acids are shown in Figure 16.1. Emission of proteins is dominated by tryptophan, which absorbs at the longest wavelength and displays the largest extinction coefficient. Energy absorbed by phenylalanine and tyrosine is often transferred to the tryptophan residues in the same protein.

Phenylalanine displays the shortest absorption and emission wavelengths. Phenylalanine displays a structured emission with a maximum near 282 nm. The emission of tyrosine in water occurs at 303 nm and is relatively insensitive to solvent polarity. The emission maximum of tryptophan in water occurs near 350 nm and is highly dependent upon polarity and/or local environment. Indole is sensitive to both general solvent effects (Section 16.1.2). Indole displays a substantial spectral shift upon forming a hydrogen bond to the imino nitrogen, which is a specific solvent effect (Section 6.3). Additionally, indole can be quenched by several amino-acid side chains. As a result, the emission of each tryptophan residue in a protein depends on the details of its surrounding environment.

Protein fluorescence is generally excited at the absorption maximum near 280 nm or at longer wavelengths. Consequently, phenylalanine is not excited in most experiments. Furthermore, the quantum yield of phenylalanine in proteins is small—typically near 0.03—so emission from this residue is rarely observed for proteins. The absorption of proteins at 280 nm is due to both tyrosine and tryptophan residues. At 23°C in neutral aqueous solution the quantum yields of tyrosine and tryptophan are near 0.14 and 0.13, respectively,[10] the reported values being somewhat variable. At wavelengths longer than 295 nm, the absorption is due primarily to tryptophan. Tryptophan fluorescence can be selectively excited at 295–305 nm. This is why many papers report the use of 295-nm excitation, which is used to avoid excitation of tyrosine.

Tyrosine is often regarded as a rather simple fluorophore. However, under some circumstances tyrosine can also display complex spectral properties. Tyrosine can undergo excited-state ionization, resulting in the loss of the proton on the aromatic hydroxyl group. In the ground state the pK_A of this hydroxyl is about 10. In the excited state the pK_A decreases to about 4. In neutral solution the hydroxyl group can dissociate during the lifetime of the excited state, leading to quenching of the tyrosine fluorescence. Tyrosinate is weakly fluorescent at 350 nm, which can be confused with tryptophan fluorescence. Tyrosinate emission is observable in some proteins, but it appears that excited-state ionization is not a major decay pathway for tyrosine in proteins.

Because of their spectral properties, resonance energy transfer can occur from phenylalanine to tyrosine to tryptophan. Energy transfer has been repeatedly observed in many proteins and is one reason for the minor contribution of phenylalanine and tyrosine to the emission of most proteins. Also, blue-shifted tryptophan residues can transfer the excitation to longer wavelength tryptophan residues. The anisotropies displayed by tyrosine and tryptophan are sensitive to both overall rotational diffusion of proteins, and the extent of segmental motion during the excited-state lifetimes. Hence, the intrinsic fluorescence of proteins can provide considerable information about protein structure and dynamics, and is often used to study protein folding and association reactions. We will present examples of protein fluorescence that illustrate the use of intrinsic fluorescence of proteins. In Chapter 17 we describe time-resolved studies of protein fluorescence.

16.1.1. Excitation Polarization Spectra of Tyrosine and Tryptophan

The emission maximum of tryptophan is highly sensitive to the local environment, but tyrosine emission maximum is rather insensitive to its local environment. What is the reason for this distinct behavior? Tryptophan is a uniquely complex fluorophore with two nearby isoenergetic transitions. In contrast, emission from tyrosine appears to occur from a single electronic state.

Information about overlapping electronic transitions can be obtained from the excitation anisotropy spectra (Chapter 10). The anisotropy spectrum is usually measured in frozen solution to prevent rotational diffusion during the excited-state lifetime. For a single electronic transition the anisotropy is expected to be constant across the absorption band. The anisotropy of tyrosine (Figure 16.2) is relatively constant across the long-wavelength absorption band (260–290 nm). Most fluorophores display some increase in anisotropy as the excitation wavelength increases across the $S_0 \rightarrow S_1$ transition (260–290 nm), but such an anisotropy spectrum is usually regarded as the result of a single transition. The anisotropy data in Figure 16.2 are for N-acetyl-L-tyrosinamide (NATyrA) instead of tyrosine. Neutral derivatives of the aromatic amino acids are frequently used because the structures of these derivatives resemble those of

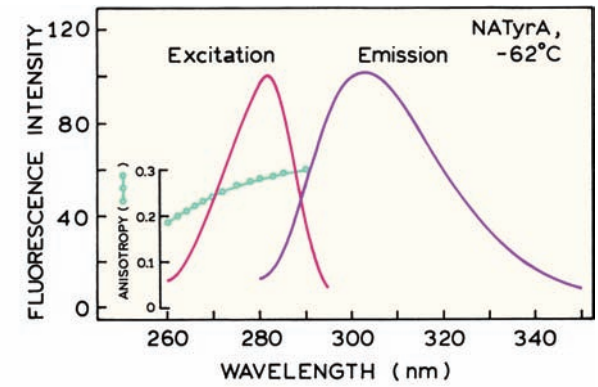

Figure 16.2. Excitation spectrum and excitation anisotropy spectra of N-acetyl-L-tyrosinamide (NATyrA). The fluorescence anisotropies (O) were measured in a mixture of 70% propylene glycol with 30% buffer at –62°C. The emission was observed at 302 nm. Data from [11–13].

the residues found in proteins. The quantum yield and lifetimes of tyrosine and tryptophan can be affected by the ionization state of the amino and carboxyl groups in tyrosine and tryptophan. These effects can be avoided by use of the neutral analogues, but it is now known that amide groups can sometimes act as quenchers.[14–15]

Interpretation of the anisotropy or anisotropy decay is aided by knowledge of the direction of the electronic transition in the fluorophore. The lowest electronic transition of tyrosine, with absorption from 260 to 290 nm, is due to the ^1L_b transition oriented across the phenol ring[16] (Figure 16.3). The ^1L_a transition is the origin of the stronger absorption below 250 nm. The anisotropy of tyrosine decreases for shorter-wavelength excitation (Figure 16.2) and becomes negative below 240 nm (not shown). This indicates that the ^1L_a transition is nearly perpendicular to the ^1L_b emitting state. For longer-wavelength excitation, above 260 nm, the anisotropy is positive, indicating the absorption transition moment is mostly parallel to the ^1L_b emission transition moment. For excitation above 260 nm the absorption and emission occur from the same ^1L_b state.

In contrast to tyrosine, indole and tryptophan do not display constant anisotropy across the long-wavelength absorption band (Figure 16.4).[17–18] On the long-wavelength side of the absorption tryptophan displays a high value of r_0 near 0.3. This indicates nearly collinear absorption and emission dipoles. The anisotropy decreases to a minimum at 290 nm, and increases at excitation wavelengths from 280 to 250 nm. This complex behavior is due to the presence of two electronic transitions to the ^1L_a and ^1L_b states in the last absorption band (Figure 16.3). These transition moments are oriented nearly perpendicular to each other,[19–23] so that the fundamental anisotropy (r_0) is strongly dependent on the fractional contribution of each state to

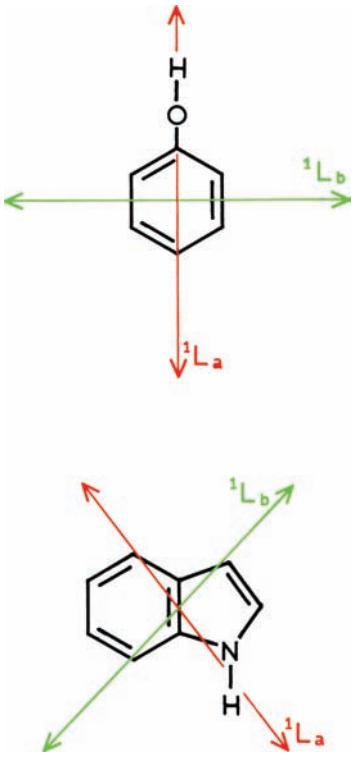

Figure 16.3. Electronic absorption transitions in tyrosine and tryptophan. Data from [16–17].

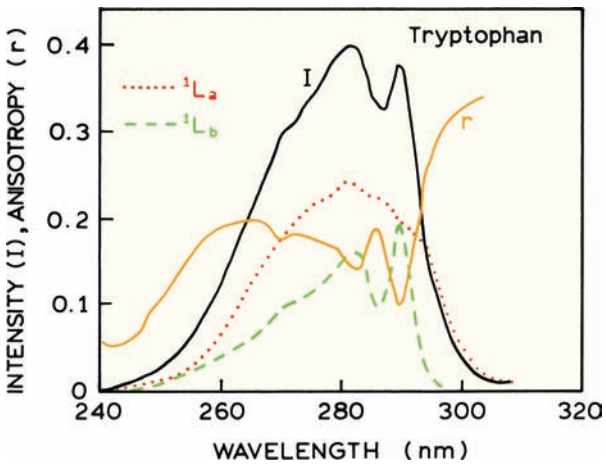

Figure 16.4. Excitation anisotropy spectra of tryptophan in propylene glycol at –50°C. Also shown are the anisotropy-resolved spectra of the ^1L_a (dotted) and ^1L_b (dashed) transitions. Data from [18].

the absorption. The minimum anisotropy near 290 nm is due to a maximum in the absorption of the ^1L_b state. The emission of tryptophan in solution and of most proteins is unstructured and due to the ^1L_a state. The anisotropy is low with 290-nm excitation, because the emission is from a state (^1L_a), which is rotated 90° from the absorbing state (^1L_b). This is another reason why protein fluorescence is often excited at 295 to 300 nm. For these excitation wavelengths only the ^1L_a state absorbs and the anisotropy is high. If emission occurs from the ^1L_b state the emission spectrum frequently displays a structured emission spectrum.

The excitation anisotropy spectra can be used to resolve the absorption spectra of the ^1L_a and ^1L_b states.[24] This procedure is based on the additivity of anisotropies (Section 10.1). This resolution assumes that the maximal anisotropy is characteristic of absorption to and emission from a single state, the ^1L_a state. A further assumption is that the transitions to the ^1L_a and ^1L_b states are oriented at 90°. Using these assumptions the ^1L_a absorption is found to be unstructured and to extend to longer wavelengths than the structured ^1L_b absorption (Figure 16.4). The dominance of ^1L_a absorption at 300 nm, and emission from the same ^1L_a state, is why proteins display high anisotropy with long-wavelength excitation.

The possible emission from two states can complicate the interpretation of time-resolved intensity decays. For example, the intensity decay of tryptophan at pH 7 is a double exponential, with decay times near 0.5 and 3.1 ns. At first it was thought that the two decay times were due to emission from the ^1L_a and ^1L_b states.[25] However, it is now thought[26–27] that the two decay times have their origin in the rotamer populations, and that tryptophan emits only from the ^1L_a state unless the local environment is completely nonpolar. An early report of 2.1 and 5.4 ns for the two decay times of tryptophan[28] is an error due to photodecomposition of the sample. Time-resolved protein fluorescence will be discussed in more detail in Chapter 17.

16.1.2. Solvent Effects on Tryptophan Emission Spectra

In order to understand protein fluorescence it is important to understand how the emission from tryptophan is affected by its local environment.[30–35] One factor affecting tryptophan emission is the polarity of its surrounding environment. The emission spectrum of tryptophan is strongly dependent on solvent polarity. Depending upon the solvent, emission can occur from the ^1L_a or ^1L_b states, but emission

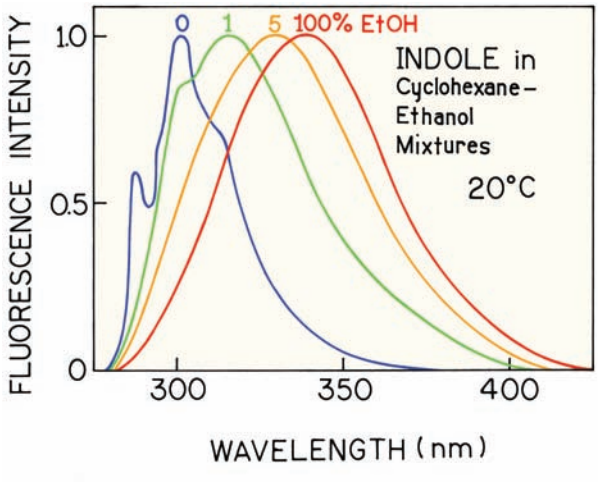

Figure 16.5. Emission spectra of indole in cyclohexane, ethanol and their mixtures at 20°C. From [29].

from the ^1L_b state is infrequent. This is because the emission of tryptophan is sensitive to hydrogen bonding to the imino group. This sensitivity is shown by the emission spectra of indole in cyclohexane, which are sensitive to trace quantities of hydrogen bonding solvent (Figure 16.5). These spectra show the presence of specific and general solvent effects.[29] In pure cyclohexane, in the absence of hydrogen bonding, the emission is structured, and seems to be a mirror image of the absorption spectrum of the ^1L_b transition (compare Figures 16.4 and 16.5). In the presence of a hydrogen-bonding solvent (ethanol) the structured emission is lost and the emission mirrors the ^1L_a transition. These structured and unstructured emission spectra indicate the possibility of emission from either the ^1L_a or ^1L_b state. The ^1L_a state is more solvent sensitive than the ^1L_b state. The ^1L_a transition shifts to lower energies in polar solvents. The higher solvent sensitivity for the ^1L_a state seems reasonable since the ^1L_a transition more directly involves the polar nitrogen atom of indole (Figure 16.3). Furthermore, the excited-state dipole moment of the ^1L_a state is near 6 debye, but the excited-state dipole moment is smaller for the ^1L_b state.[36] In a completely nonpolar environment the ^1L_b state can have lower energy and dominate the emission. In a polar solvent the ^1L_a state has the lower energy and dominates the emission. The electrical field due to the protein, or the solvent reaction field, may also influence the emission spectrum of indole.[36–37]

The different solvent sensitivities of the ^1L_a and ^1L_b states of indole can be seen in the absorption spectra of indole in the cyclohexane–ethanol mixtures (Figure 16.6).

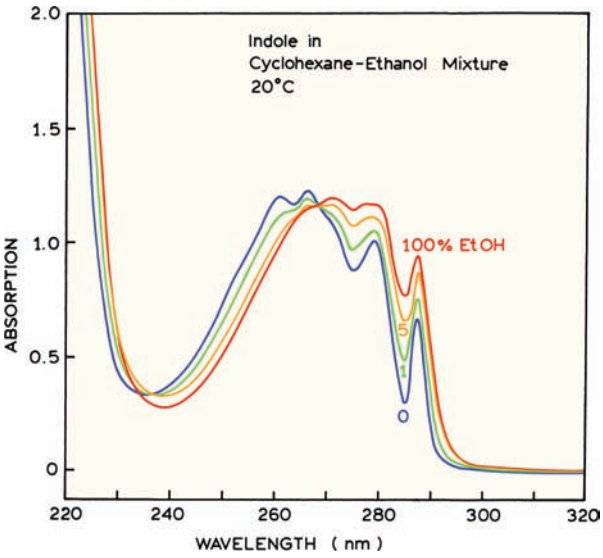

Figure 16.6. Absorption spectra of indole in cyclohexane with increasing amounts of ethanol. Data courtesy of Dr. Ignacy Gryczynski.

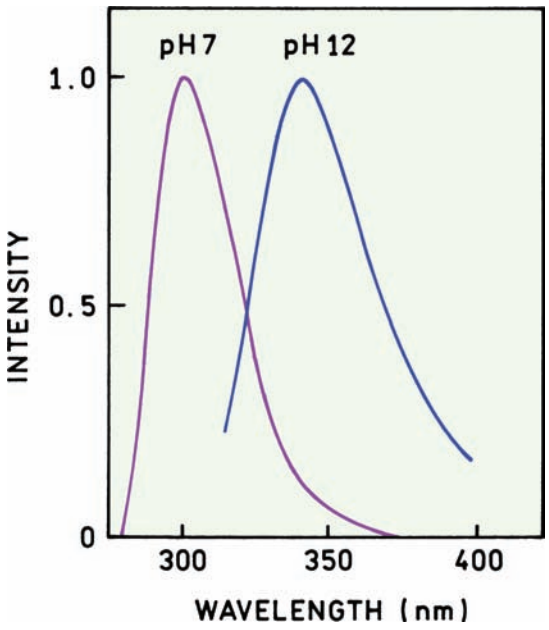

Figure 16.7. Normalized emission spectra of tyrosine at pH 7 and in 0.01 M NaOH (pH 12). Modified from [16].

As the ethanol concentration is increased the vibrational structure at 288 nm decreases. Similar results have been observed for indole derivatives.[38–39] These spectral changes can be understood as a red shift of the ^1L_a absorption spectrum due to interaction of indole with the polar solvent. This energy shift is probably due to both hydrogen bonding interactions with the imino group and the general effects of solvent polarity. The ^1L_b state is less sensitive to solvent, and its absorption is less affected by polar solvent.

The properties of the ^1L_a and ^1L_b states explain the complex emission spectra displayed by indole (Figure 16.5). In a completely nonpolar solvent the structured ^1L_b state can be the lowest energy state, resulting in structured emission. The presence of polar solvent decreases the energy level of the ^1L_a state, so that its unstructured emission dominates. At higher ethanol concentrations these specific solvent interactions are saturated, and indole displays a polarity-dependent red shift consistent with general solvent effects. Very few proteins display a structured emission, which suggests few tryptophan residues are in completely nonpolar environments.

16.1.3. Excited-State Ionization of Tyrosine

Tyrosine displays a simple anisotropy spectrum, but it is important to recognize the possibility of excited-state ionization. Excited-state ionization occurs because the pK_A of the phenolic hydroxyl group decreases from 10.3 in the ground state to about 4 in the excited state. Ionization can occur even at neutral pH, particularly if the solvent contains proton acceptors such as acetate. Tyrosinate emission is most easily observed at high pH, where the phenolic OH group is ionized in the ground state (Figure 16.7). In 0.01 M NaOH (pH 12) the emission of tyrosine is centered near 345 nm.[6,40] The emission from tyrosinate can be mistaken for tryptophan. The decay time of tyrosinate at pH 11 has been reported to be 30 ps.[41]

In Figure 16.7 the tyrosine hydroxyl group is ionized in the ground state. Tyrosinate emission can also be observed at neutral pH, particularly in the presence of a base that can interact with the excited state. One example is shown in Figure 16.8, which shows the emission spectra of tyrosine at the same pH, but with increasing concentrations of acetate buffer. The emission intensity decreases with increased acetate concentrations. This decrease occurs because the weakly basic acetate group can remove the phenolic proton, which has a pK_a of 4.2 to 5.3 in the first singlet state.[40–43] If the tyrosinate form does not emit, the acetate behaves like a collisional quencher, and the extent of excited-state ionization and quenching depends on the acetate concentration. Tyrosine can also form ground-state complexes with weak bases such as phosphate.[44–45]

Because of its low quantum yield the emission from tyrosinate is not easily seen in Figure 16.8. This emission is

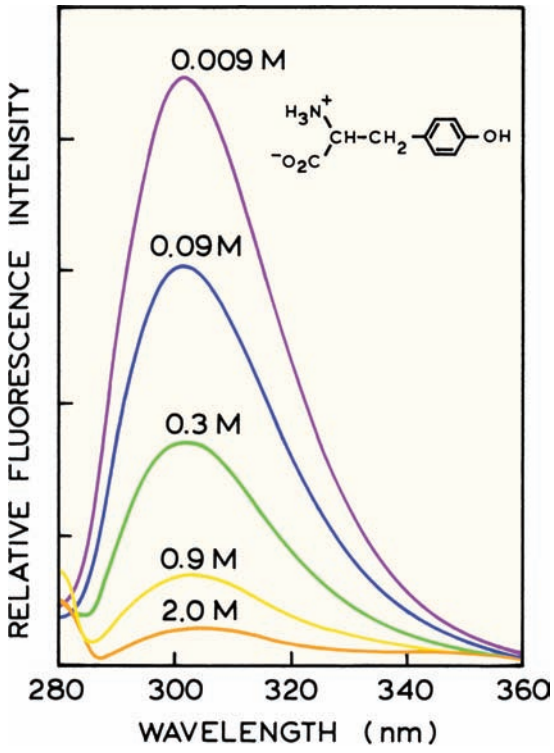

Figure 16.8. Corrected fluorescence emission spectra of tyrosine in acetate/acetic acid buffer solutions of differing ionic strength. pH = 6.05. Revised from [42].

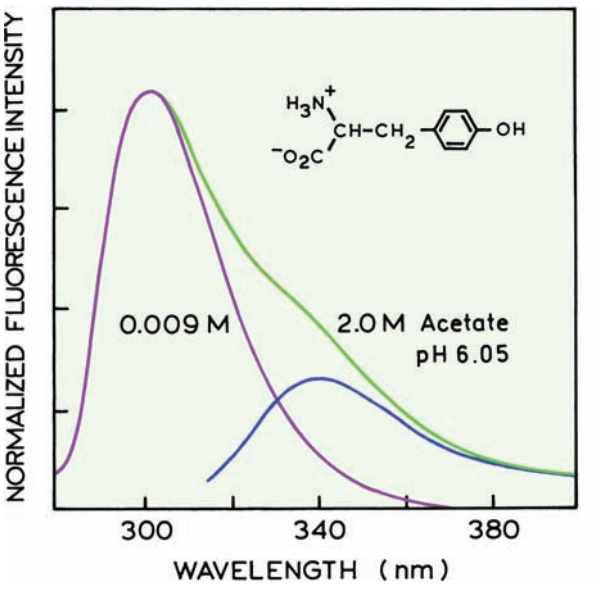

Figure 16.9. Corrected fluorescence emission spectra of tyrosine in 0.009 and 2 M acetate solutions at pH = 6.05. The difference spectrum with a maximum near 340 nm is due to tyrosinate. Revised from [42].

more easily seen in the peak-normalized emission spectra (Figure 16.9). In 2.0 M acetate tyrosine displays the usual emission maximum slightly above 300 nm. However, there is also increased intensity at 340 nm. This component is shown in the difference emission spectrum that displays a maximum near 345 nm. The important point is that the phenolic group of tyrosine can ionize even at neutral pH, and the extent to which this occurs depends on the base concentration and exposure of tyrosine to the aqueous phase.

In the example shown in Figure 16.9, tyrosinate was formed in the excited state, following excitation of un-ionized tyrosine. More complex behavior is also possible. The extent of excited-state ionization is limited by the short decay time of tyrosine and occurs to a limited extent under most conditions. Tyrosine can form a ground-state complex with weak bases.[46–47] In these complexes the hydroxyl group is not ionized, but is prepared to ionize immediately upon excitation. Quenching of tyrosine by phosphate and other bases can thus proceed by both static complex formation and by a collisional Stern-Volmer process.[46–47]

16.1.4. Tyrosinate Emission from Proteins

Tyrosinate emission has been reported for a number of proteins that lack tryptophan residues.[48–52] Several examples are shown in Figure 16.10. Crambin contains two tyrosine residues that emit from the un-ionized state. Purothionines are toxic cationic proteins isolated from wheat. α_1- and β-purothionin have molecular weights near 5000 daltons and do not contain tryptophan. The emission spectrum of β-purothionin is almost completely due to the ionized tyrosinate residue, and the emission from α_1-purothionin shows emission from both tyrosine and tyrosinate. The emission from cytotoxin II, when excited at 275 nm, shows contributions from both the ionized and un-ionized forms of tyrosine. For three proteins the tyrosinate emission is thought to form in the excited state, but may be facilitated by nearby proton acceptor side chains. Examination of the emission spectra in Figure 16.10 shows that tyrosinate emission can appear similar to and be mistaken for tryptophan emission, or conversely that tryptophan contamination in a sample can be mistaken for tyrosinate emission.

16.2. GENERAL FEATURES OF PROTEIN FLUORESCENCE

The general features of protein fluorescence have been described in several reviews.[53–56] Most proteins contain

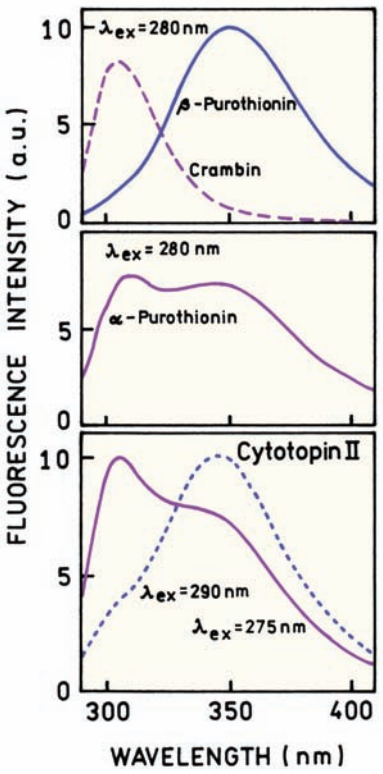

Figure 16.10. Emission spectra of proteins that lack tryptophan residues. Neutral pH. Revised from [48–49].

multiple tryptophan residues, and the residues contribute unequally to the total emission. There have been attempts to divide proteins into classes based on their emission spectra.[56–59] The basic idea is that the tryptophan emission spectrum should reflect the average environment of the tryptophan. For tryptophan in a completely apolar environment a blue-shifted structured emission characteristic of indole in cyclohexane can be observed. As the tryptophan residue becomes hydrogen bonded or exposed to water, the emission shifts to longer wavelengths (Figure 16.11). In fact, individual proteins are known that display this wide range of emission spectra.[60–61] For example, later in this chapter we will see that azurin displays an emission spectrum characteristic of a completely shielded tryptophan residue. The emission from adrenocorticotropin hormone (ACTH) is characteristic of a fully exposed tryptophan residue.

The emission maximum and quantum yield of tryptophan can vary greatly between proteins. Denaturation of proteins results in similar emission spectra and quantum yields for the unfolded proteins. Hence, the variations in tryptophan emission are due to the structure of the protein. We are not yet able to predict the spectral properties of proteins using the known structures, but some efforts are underway.[61] One might expect that proteins that display a blue-shifted emission spectrum will have higher quantum yields (Q) or lifetimes (τ). Such behavior is expected from

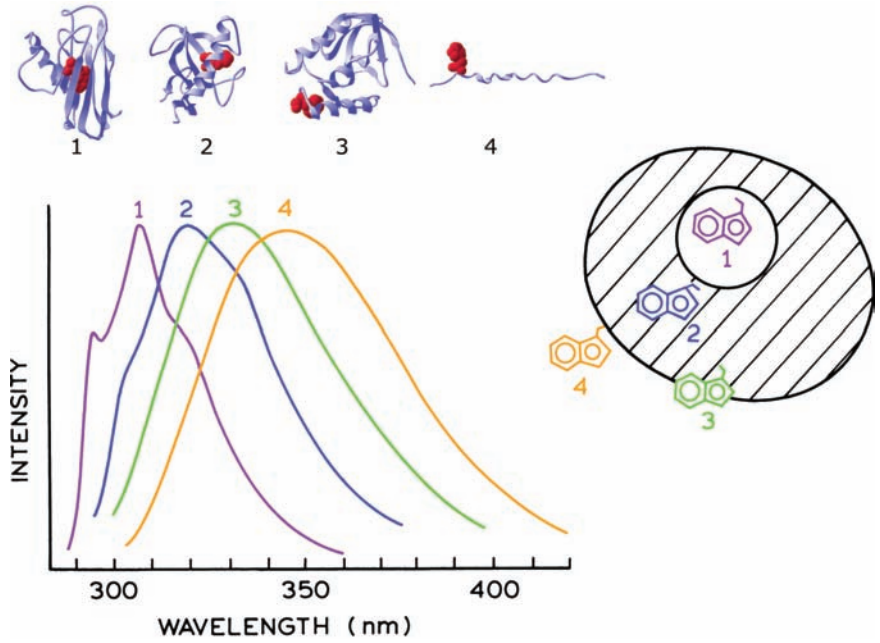

Figure 16.11. Effect of tryptophan environment on the emission spectra. The emission spectra are those of apoazurin Pfl, ribonuclease T_1, staphylococcal nuclease, and glucagon, for 1 to 4, respectively. Revised from [59] and [60].

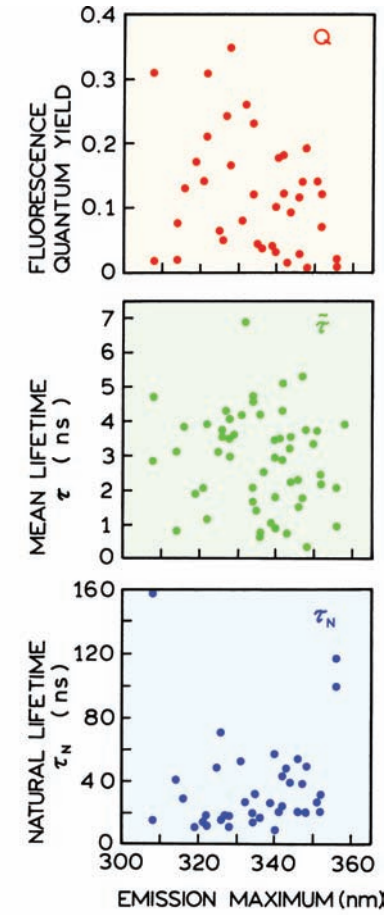

Figure 16.12. Relationship of the emission maximum of proteins to the quantum yield Q (top), mean lifetime $\bar{\tau}$ (middle), and natural lifetime τ_N (bottom). Courtesy of Dr. Maurice Eftink, University of Mississippi.

the usual increase in quantum yield when a fluorophore is placed in a less polar solvent. For instance, the lifetime of indole decreases from 7.7 ns in cyclohexane to 4.1 ns in ethanol.[29] However, for single-tryptophan proteins there is no clear correlation between quantum yields and lifetimes (Figure 16.12). As described in Chapter 1, the natural lifetime (τ_N) of a fluorophore is the reciprocal of the radiative decay rate, which is typically independent of the fluorophore environment. The value of τ_N can be calculated from the measured lifetime (τ) and quantum yield (Q), $\tau_N = \tau/Q$. Surprisingly, the apparent values of τ_N vary considerably for various proteins. Apparently, the complexity of the protein environment can override the general effects of polarity on the lifetime of tryptophan.

Why should the natural lifetimes of proteins be variable? One explanation is that some tryptophan residues are completely quenched in a multi-tryptophan protein, and thus do not contribute to the measured lifetime and the emission maximum. For instance, indole is known to be partially quenched by benzene. Hence, indole may be quenched by nearby phenylalanine residues in proteins. The nonfluorescent residues still absorb light, and thus result in highly variable quantum yields for the different proteins. The residues that are completely quenched will not contribute to the measured lifetime. As a result the apparent value of the natural lifetime τ_N will be larger than the true value. The lack of correlation between emission spectra and lifetimes of proteins is probably due to the effects of specific protein environments that quench particular tryptophan residues. One can imagine the proteins to be in slightly different conformations that bring the residue closer or further from a quenching group. Under these conditions only a fraction of the protein population would be fluorescent. This fluorescent fraction would display a longer lifetime than expected from the quantum yield.

The variability of the lifetimes and quantum yields of proteins has been a puzzle for the last several decades. The reasons for this variability are now becoming understood, but there is no single factor that explains the spectral properties summarized in Figure 16.12. There are several factors that determine the emission from tryptophan residues.[62–70] These are:

- quenching by proton transfer from nearby charged amino groups,
- quenching by electron acceptors such as protonated carboxyl groups,
- electron transfer quenching by disulfides and amides,
- electron transfer quenching by peptide bonds in the protein backbone, and
- resonance energy transfer among the tryptophan residues.

These interactions are strongly dependent on distance, especially the rate of electron transfer, which decreases exponentially with distance. The extent of electron transfer quenching can also depend on the location of nearby charged groups that can stabilize or destabilize the charge transfer state.[64] The rates of electron transfer and resonance energy transfer can be large, so that some tryptophan residues can be essentially nonfluorescent. Additionally, a protein may exist in more than a single conformation, with each displaying a different quantum yield. Proteins are known in which specific tryptophan residues are quenched, and examples where normally fluorescent tryptophan residues transfer energy to nonfluorescent tryptophan residues (Chapter 17). In summary, the variability in the quantum

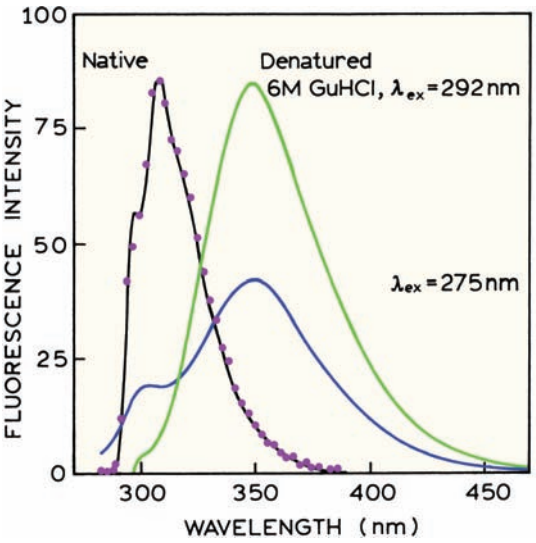

Figure 16.13. Emission spectra of *Pseudomonas fluorescens* (ATCC-13525-2) azurin Pfl. The solid lines show emission spectra for native (0.01 M cacodylate, pH 5.3) and denatured (6 M GuHCl) azurin Pfl for λ_{ex} = 292. Also shown is the emission spectrum of denatured azurin excited at 275 nm. The dots show the emission spectrum of 3-methyl-indole in methylcyclohexane. Data from [73].

yields and lifetimes of proteins is due to a number of interactions, all of which depend on the details of the protein structure.

16.3. TRYPTOPHAN EMISSION IN AN APOLAR PROTEIN ENVIRONMENT

Interpretation of protein fluorescence is hindered by the presence of multiple-tryptophan residues in most proteins. This has resulted in studies of single-tryptophan proteins. Fluorescence studies of azurins have been uniquely informative. These are small copper-containing proteins with molecular weights near 15,000 daltons. These proteins are involved in the electron transfer system of denitrifying bacteria. Some of the azurins contain a single-tryptophan residue that displays the most blue-shifted emission observed for a tryptophan residue in proteins.

Emission spectra of the single-tryptophan azurin Pfl from *Pseudomonas fluorescens* is shown in Figure 16.13. In contrast to the emission from most proteins, the emission spectrum of the wild-type (WT) proteins shows structure characteristic of the ^1L_b state.[71–74] In fact, the emission spectrum of native azurin is nearly identical with that of the tryptophan analogue 3-methyl-indole in the nonpolar solvent methylcyclohexane (●). This indicates that the indole residue is located in a completely nonpolar region of the protein, most probably without a polar group for a hydrogen bond. These results agree with x-ray studies, which show the indole group is located in the hydrophobic core of the protein.[75]

If the structure of azurin is responsible for the tryptophan emission, then disruption of the protein structure should result in a more typical emission spectrum. In the presence of 6 M guanidine hydrochloride the tryptophan emission loses its structure and shifts to 351 nm, characteristic of a fully exposed tryptophan residue. The emission spectra of denatured azurin (Figure 16.13) illustrate another typical spectral property of proteins. The emission spectra are different for excitation at 275 and 292 nm. For 275-nm excitation a peak is observed near 300 nm, which is due to the tyrosine residue(s). The occurrence of tyrosine emission indicates that resonance energy transfer from tyrosine to tryptophan is not complete in denatured azurin. In the native conformation there is no tyrosine emission with 275-nm excitation. Either the tyrosines are quenched in the native structure or energy transfer to the tryptophan residue is highly efficient. For the denatured protein, excitation at 292 nm results in emission from only the tryptophan residue. These spectra demonstrate the wide range of tryptophan spectral properties that can be observed for proteins, and show that changes in the emission spectra can be used to follow protein unfolding.

16.3.1. Site-Directed Mutagenesis of a Single-Tryptophan Azurin

Molecular biology provides a powerful tool for unraveling the complexities of protein fluorescence. Site-directed mutagenesis and expression of mutant proteins allow the amino-acid sequence of proteins to be altered.[76–77] Amino-acid residues in the wild-type sequence can be substituted with different amino acids. Site-directed mutagenesis was used to determine the effects of amino acids near the tryptophan 48 (W48) on the emission spectra of azurin Pae from *Pseudomonas aeruginosa*.[78] The three-dimensional structure of the protein consists of an α-helix plus eight β-strands that form a hydrophobic core, the so called β-barrel (Figure 16.14). The single-tryptophan residue W48 is located in the hydrophobic region. The wild-type protein, with no changes in the amino-acid sequence, displays the structured emission characteristic of indole in a nonpolar solvent (Figure 16.15).

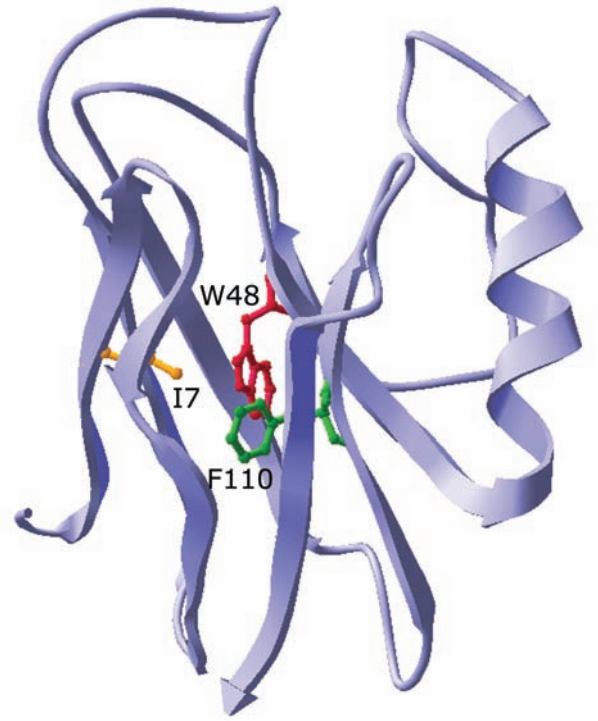

Figure 16.14. α-Carbon backbone of wild-type azurin from *Pseudomonas aeruginosa*. The environment around the single-tryptophan residue (W48) was varied by mutating isoleucine (I7) or phenylalanine (F110).

Site-directed mutagenesis of azurin was used to change amino acids located near the tryptophan residue. A single amino acid substitution was found to eliminate the structured emission spectrum of tryptophan. In a mutant protein the nonpolar amino acid isoleucine (I) at position 7 was replaced with serine (S). This mutant protein is referred to as I7S. The amino acid serine contains a hydroxyl group, which might be expected to form a hydrogen bond to indole and thus mimic ethanol in cyclohexane (Figure 16.5). This single amino acid substitution resulted in a complete loss of the structured emission (Figure 16.15). The emission maximum is still rather blue shifted (λ_{max} = 313 nm), reflecting the predominantly nonpolar character of the indole environment. The emission of tryptophan 48 was also found to be sensitive to substitution of the phenylalanine residue at position 110 by serine (F110S, Figure 16.15). These studies demonstrate that just a single hydrogen bond can eliminate the structured emission of indole, and that the emission spectra of indole are sensitive to small changes in the local environment.

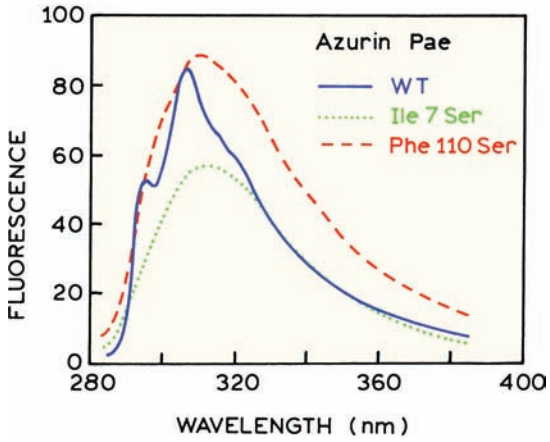

Figure 16.15. Corrected steady-state fluorescence spectra of holoazurin Pae: WT (solid), I7S (dotted), F110S (dashed). Data were collected at 298°K in 20 mM Hepes buffer at pH 8.0. The excitation wavelength was 285 nm. Reprinted with permission from [79]. Copyright © 1987, American Chemical Society.

16.3.2. Emission Spectra of Azurins with One or Two Tryptophan Residues

The azurins also provide examples of single-tryptophan proteins with the tryptophan residues located in different regions of the protein.[79] Azurins isolated from different microorganisms have somewhat different sequences. Azurin Pae has a single buried tryptophan residue at position 48. Azurin Afe has a single tryptophan on the surface at position 118, and azurin Ade has tryptophan residues at both positions 48 and 118. Each of these azurins displays distinct emission spectra (Figure 16.16). The emission of the buried residue W48 is blue shifted, and the emission of the exposed residue W118 displays a red-shifted featureless spectrum. The emission spectrum of azurin Ade with both residues is wider and shows emission from each type of tryptophan residue. Hence, a wide range of environments can exist within a single protein.

16.4. ENERGY TRANSFER AND INTRINSIC PROTEIN FLUORESCENCE

Resonance energy transfer can occur between the aromatic amino acids in proteins. Transfer is likely to occur because of spectral overlap of the absorption and emission spectra of phe, trp, and trp (Figure 16.1). The local concentrations of these residues in proteins can be quite large. Consider a typical globular protein with a molecular weight near

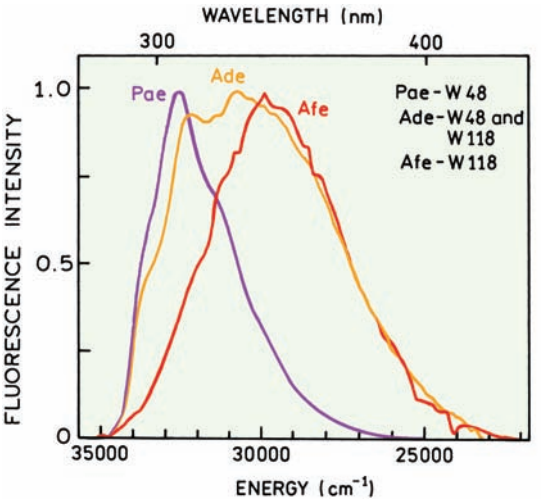

Figure 16.16. Fluorescence spectra of apo Pae azurin, apo Ade azurin, apo Afe azurin. The fluorescence spectra of the holoproteins only differ from that of the apoproteins in that they have a reduced intensity. Data reprinted with permission from [79]. Copyright © 1987, American Chemical Society.

50,000 daltons. Such a protein contains approximately 450 amino-acid residues (about 110 daltons per amino-acid residue), about 10 of which will be one of the aromatic amino acids. Using a typical density of proteins near 1.4 g/ml, one can calculate a protein radius near 24 Å. The concentration of aromatic amino acids in this protein is near 0.28 M = 280 mM.

Typical Förster distances (R_0) and characteristic concentration values (A_0) for energy transfer between the aromatic amino acids are listed in Table 16.1. These values illustrate the range of distances and concentrations typical of RET between the fluorescent amino acids. For any given donor–acceptor pair the actual distances will depend on the quantum yield and emission spectrum of the donor, which can vary in different protein environments. Absorption spectra are typically less sensitive to the environment, so the emission spectrum and quantum yield of the donor are the dominant origin of the range of R_0 values. From the values in Table 16.1 it is evident that RET can be expected between the aromatic amino acids in proteins.

The Förster distance for tryptophan-to-tryptophan homotransfer is particularly variable. This is because the extent of spectral overlap is strongly dependent on solvent polarity. In polar solvents the emission spectrum of tryptophan is shifted away from the absorption spectrum and the Förster distances are smaller. For instance, for the fully exposed tryptophan residues in melittin the Förster distance was estimated to be just 4 Å.[80–81] At low temperature in viscous solvent, where the Stokes shift was smaller, the R_0 value for tryptophan homotransfer[12] was found to be as large as 16 Å. Hence trp-to-trp transfer can be expected in proteins, particularly if some of the residues display a blue-shifted emission.

Table 16.1. Förster Distances and Critical Concentrations for Resonance Energy Transfer in Proteins

Donor	Acceptor	R_0 (Å)	A_0 (M)[a]	Ref.
Phe	Tyr	11.5–13.5	0.29–0.18	82–84
Tyr	Tyr	9–16	0.61–0.11	12, 13
Tyr	Trp	9–18	0.61–0.08	12, 85–88
Trp	Trp	4–16	7.0–0.11	12, 89

[a]The critical concentration (A_0) in moles/liter can be calculated from $A_0 = 447/R_0^3$, where R_0 is in Å. See Chapter 13.

16.4.1. Tyrosine to Tryptophan Energy Transfer in Interferon-γ

The most commonly observed resonance energy transfer in proteins is from tyrosine to tryptophan. This is because most proteins contain both of these amino acids, and both are readily excited at 275 nm. One example of tyr-to-trp transfer is human interferon-γ, whose emission spectrum depends on the extent of self-association. Interferon-γ is produced by activated lymphocytes and displays antiviral and immunoregulator activity. Its activity depends on the extent of association to dimers. The intrinsic fluorescence of interferon-γ was used to study its dissociation into monomers.

Interferon-γ is usually a dimer of two identical 17, kDa polypeptides, each containing one tryptophan residue at position 36 and four tyrosine residues (Figure 16.17).[90] The emission spectrum of the interferon-γ dimer (Figure 16.18, top) displays emission from both tyrosine and tryptophan when excited at 270 nm. Only tryptophan emission is seen for 295-nm excitation. To compare the relative intensities of tyrosine and tryptophan the spectra were normalized at long emission wavelengths where only tryptophan emits, followed by subtraction of the spectrum with 295-nm excitation from the spectrum with 270-nm excitation. This difference spectrum is seen to be that expected for tyrosine. When incubated under the appropriate conditions, interferon-γ dissociates into monomers. The relative intensity of the tyrosine increases in the monomeric state (Figure 16.18, lower panel). In the monomeric state the relative tyrosine intensity is about half that of tryptophan. In the dimer the

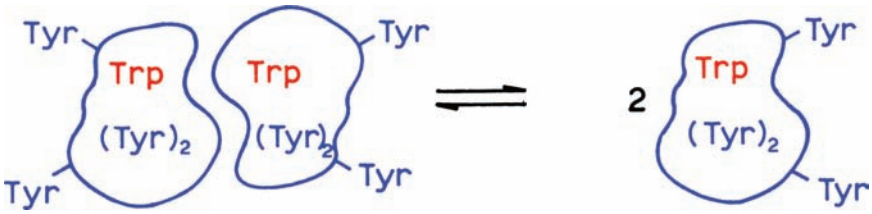

Figure 16.17. Schematic of the interferon-γ dimer. Each monomer contains one tryptophan and four tyrosines.

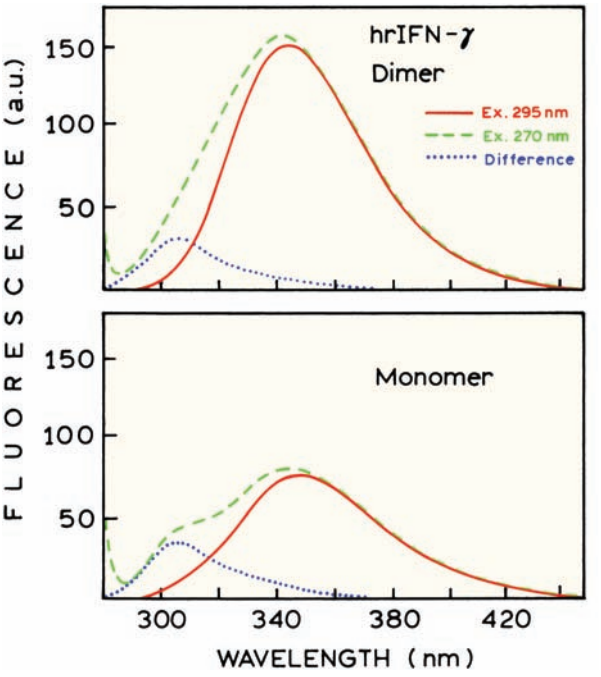

Figure 16.18. Emission spectra of human recombinant interferon-γ (hrIFN-γ), 10 mM tris, pH 7.7. Revised from [90].

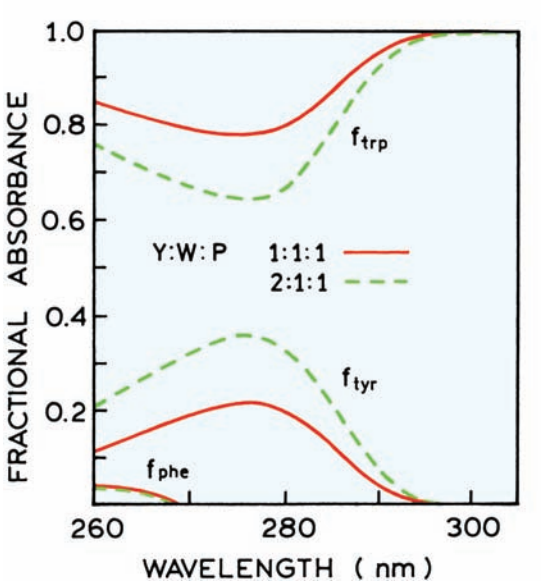

Figure 16.19. Fractional absorption of tyrosine, tryptophan and phenylalanine in a mixture of amino acids. The molar ratio of Tyr:Trp:Phe (Y:W:P) are 1:1:1 (solid) and 2:1:1 (dashed). Revised from [85].

relative tyrosine intensity is about 20%. The relative increase in tyrosine fluorescence in the monomeric state occurs because the four tyrosines are more distant from the tryptophan acceptors that are on the dissociated subunit. This result shows that RET can occur between the subunits; otherwise, the extent of tyr-to-trp energy transfer would be independent of association.

16.4.2. Quantitation of RET Efficiencies in Proteins

In the previous paragraph we explained the emission spectra of interferon-γ in terms of energy transfer, but we did not consider the effect of dimer dissociation on the fluorescence intensity of the tryptophan residue. In fact, the tryptophan emission intensity decreases approximately twofold on dissociation.[90] Fortunately, there is a means to measure the efficiency of tyrosine-to-tryptophan energy transfer that is independent of the tryptophan quantum yield. This approach depends on the relative absorbance of the aromatic amino acids at various wavelengths[85] (Figure 16.19). The fraction of total absorbance due to each type of amino acid can be calculated from the extinction coefficients in Figure 16.1. Above 295 nm only tryptophan absorbs, and its fractional absorbance is 1.0. This is the basis for selective excitation of tryptophan for wavelengths of 295 nm and longer. As the wavelength decreases the fractional absorption of tryptophan decreases and the fractional absorption of tyrosine increases. At a higher relative concentration of tyrosine its fractional absorbance is larger.

The extent of tyr-to-trp energy transfer can be found by measuring the relative tryptophan quantum yield for various excitation wavelengths. The relative quantum yield is deter-

mined from the intensity observed with a given excitation wavelength, divided by the absorbance at the excitation wavelength. If energy transfer is 100% efficient, then the tryptophan emits irrespective of whether tyrosine or tryptophan is excited. In this case the relative quantum yield $Q(\lambda)$ is independent of excitation wavelength. If there is no tyr-to-trp energy transfer then the relative tryptophan quantum yield decreases at shorter wavelengths. This decrease occurs because light absorbed by the tyrosine does not result in emission from the tryptophan. This can be understood by recognizing that the absorbance is below 290 nm due to both tyrosine and tryptophan. In the absence of energy transfer only absorption by tryptophan results in tryptophan emission.

The fractional absorbance of each type of amino acid can be calculated from the absorbance due to each amino acid. The fractional absorbance due to tryptophan is given as follows:

$$f_{trp}(\lambda) = \frac{a_{trp}(\lambda)}{a_{trp}(\lambda) + a_{tyr}(\lambda)} \qquad (16.1)$$

where $\varepsilon_i(\lambda)$ is the absorbance of the individual residues at wavelength λ. For simplicity we deleted from this expression the minor term due to absorption by phenylalanine. Figure 16.19 shows that only tryptophan absorbs at wavelengths longer than 295 nm. The relative quantum yield at 295-nm excitation is taken as a reference point at which all the light is absorbed by tryptophan. The fluorescence is monitored at 350 nm or longer to avoid tyrosine emission. The relative quantum yield at any excitation wavelength is given by

$$Q(\lambda) = \frac{a_{trp}(\lambda) + Ea_{tyr}(\lambda)}{a_{trp}(\lambda) + a_{tyr}(\lambda)} \qquad (16.2)$$

If E is 100% then the relative quantum yield of tryptophan fluorescence is independent of excitation wavelength. If E is zero then the relative quantum yield is given by the fractional absorption due to tryptophan.

Equation 16.1 is written in terms of absorbance due to each type of residues. If the number of tyrosine and tryptophan residues is known the fractional absorbance of tryptophan can be approximated from

$$f_{trp}(\lambda) = \frac{n\varepsilon_{trp}(\lambda)}{n\varepsilon_{trp}(\lambda) + m\varepsilon_{tyr}(\lambda)} \qquad (16.3)$$

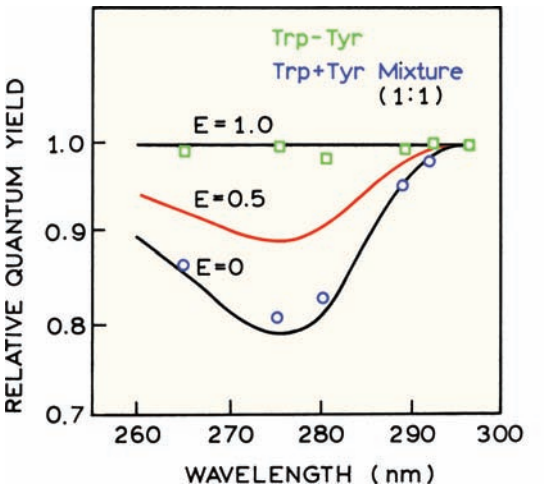

Figure 16.20. Excitation wavelength dependence of the relative quantum yield of the dipeptide tryptophanyltyrosine and an equimolar mixture of tyrosine and tryptophan. The lines correspond to transfer efficiencies of 0, 50, and 100%. Reprinted with permission from [85]. Copyright © 1969, American Chemical Society.

where $\varepsilon_i(\lambda)$ are the extinction coefficients, n is the number of tryptophan residues per protein, and m is the number of tyrosine residues per protein. This expression can be slightly in error due to shifts in the absorption of the residues in different environments.

The use of the relative quantum yield to determine the energy transfer efficiency is illustrated by data for a dipeptide—tyr–trp—and for an equimolar mixture of tyrosine and tryptophan (Figure 16.20). In the dipeptide the donor and acceptor are well within the Förster distance and the transfer efficiency is expected to be near 100%. This prediction is confirmed by the independence of the tryptophan quantum yield from the excitation wavelength. All the energy absorbed by tyrosine or tryptophan appears as tryptophan fluorescence. For the mixture of unlinked tyrosine and tryptophan the relative quantum yield closely follows the fractional absorbance due to tryptophan ($E = 0$), indicating the absence of significant energy transfer.

Such data can be used to estimate the efficiency of tyrosine–tryptophan energy transfer in proteins. The excitation wavelength-dependent tryptophan quantum yields are shown for interferon-γ in Figure 16.21. These values are measured relative to the quantum yield at 295 nm, where only tryptophan absorbs. The relative quantum yield decreases with shorter excitation wavelengths in both the monomeric and dimeric states. The quenching efficiency (E) is estimated by comparison with curves calculated for various transfer efficiencies. Using this approach the trans-

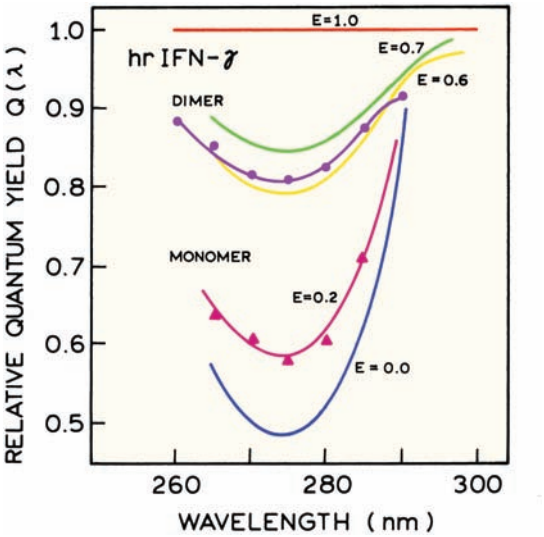

Figure 16.21. Wavelength-dependence of the relative quantum yield $Q(\lambda)$ of 1 μM hrIFN-γ in the monomer and dimer states. All theoretical and experimental data are normalized to absorbance at 295 nm. Revised and reprinted with permission from [90]. Copyright © 1996, American Chemical Society.

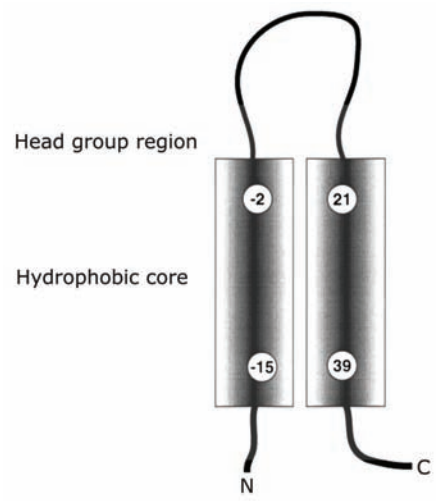

Figure 16.22. Schematic structure of membrane-bound M13 procoat protein. The numbers refer to the positions in the sequence related to residue 0 near the top of the left-side helix. Reprinted with permission from [91]. Copyright © 2001, American Chemical Society.

fer efficiency is estimated to be 20 and 60% in the monomer and dimer, respectively. The decrease in relative quantum yield is less in the dimeric state, indicating more efficient tyr-to-trp energy transfer in the dimer. This implies that the tyrosine residues in one subunit transfer to the tryptophan residue in the other subunit. The larger decrease in relative quantum yield for the monomer at 270 nm can be understood as due to the lower transfer efficiency, so that fewer of the photons absorbed by tyrosine appear as tryptophan emission.

16.4.3. Tyrosine-to-Tryptophan RET in a Membrane-Bound Protein

Tyrosine-to-tryptophan RET was used to study folding of the M13 procoat protein when bound to membranes. The final M13 coat protein is inserted into the inner membrane of *E. coli* prior to assembly of the M13 phage particle. The procoat protein is thought to form two closely spaced α-helices when bound to membranes (Figure 16.22). In order to use tyr-to-trp RET the two natural tyrosine residues and one tryptophan residue were mutated to phenylalanines. Tyr and trp were then inserted at desired locations in the sequence near the ends of the α-helical segments. The residues are numbered relative to a residue above the left-hand helix, which is taken as zero.

Emission spectra of three mutants are shown in Figure 16.23 for excitation at 280 and 295 nm.[91] In the W21Y24 mutant, where the tyrosine and tryptophan are located only three residues apart, there is no detectable tyrosine emission. For the W21Y(-15) mutant a tyrosine component is seen on the short-wavelength side of the tryptophan emission. The W39Y(-15) mutant shows a smaller tyrosine component.

It is difficult to use the emission spectra to determine the tyr-to-trp RET efficiencies. The RET efficiencies were determined from the excitation spectra (Figure 16.24). These spectra (top panel) show higher amplitude at 280 nm for the peptide that showed the lowest tyrosine emission (W21Y24), and a lower intensity for 280-nm excitation for the W21Y(-15) mutant. The transfer efficiencies can be determined by comparison with normalized intensities (lower panel). These results show the RET efficiency varies from 0 to 100% depending on the location of the tyrosine and tryptophan residues. The results of this analysis are shown in Figure 16.25. The 0% transfer efficiency for W21Y(-15) and the 50% transfer efficiency for W39Y(-15) shows that this protein binds to membranes as a pair of helices. Otherwise there would have been less efficient transfer between W39 and Y(-15).

16.4.4. Phenylalanine to Tyrosine Energy Transfer

Resonance energy transfer can also occur from phenylalanine to tyrosine. Such transfer is rarely reported because

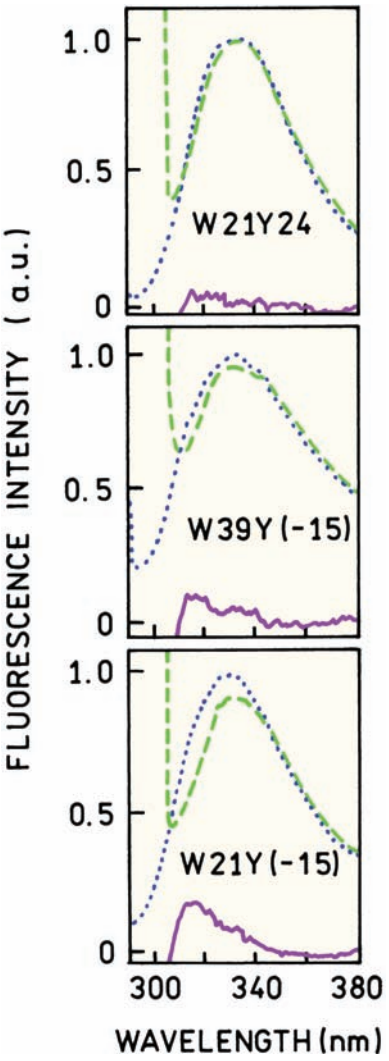

Figure 16.23. Emission spectra of the M13 procoat protein. The positions of the tyrosine and tryptophan residues are shown on the figure. Excitation at 280 (dashed) or 295 nm (dotted). The difference spectra are shown as solid lines. Revised from [91].

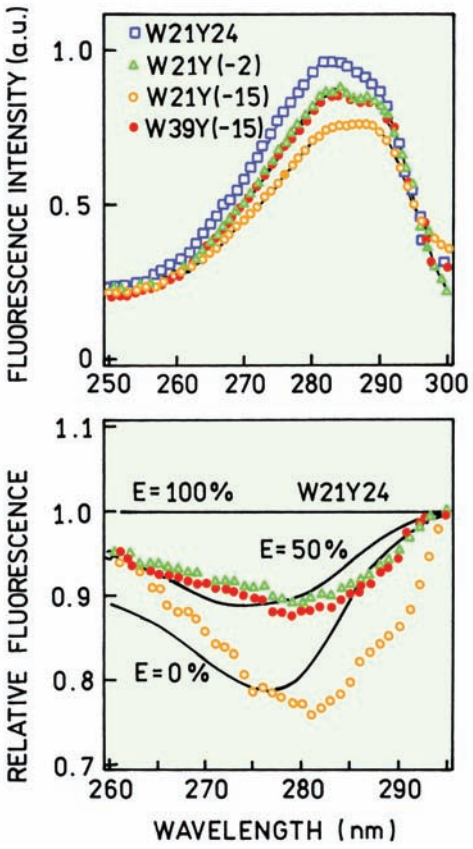

Figure 16.24. Excitation spectra of mutant M13 procoat proteins. The lower panel shows the quantum yields normalized according to eq. 16.2. Revised from [91].

tyrosine and tryptophan dominate the emission of most proteins, and proteins are usually not excited at 260 nm where phenylalanine absorbs. Phenylalanine emission was detected from an unusual histone-like protein, HTa, from the thermophilic archaebacterium *Thermoplasma acidophilum*.[82] HTa associates strongly with DNA to protect it from thermal degradation. This highly unusual protein is a tetramer, with five phenylalanine residues and one tyrosine residue in each monomer, and no tryptophan residues (Figure 16.26). In this class of organisms the more thermophilic variants have higher phenylalanine contents in their histone-like proteins. An experimentally useful property of this protein is the ability to remove the tyrosine residues, located at the third position from the carboxy terminus, by digestion with carboxypeptidase A.

The emission spectrum of HTa excited at 252 nm is shown in Figure 16.26 (solid, top panel). The emission

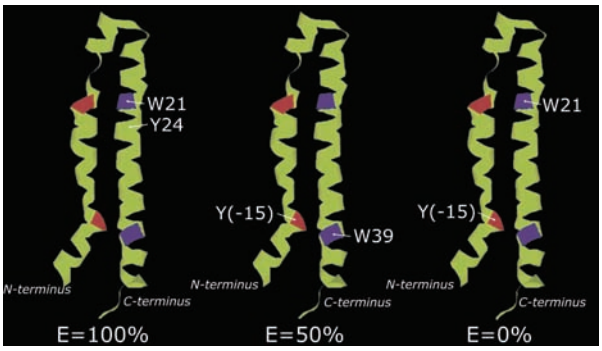

Figure 16.25. Structure and RET efficiencies for the mutant M13 procoat proteins. Data reprinted with permission from [91]. Copyright © 2001, American Chemical Society.

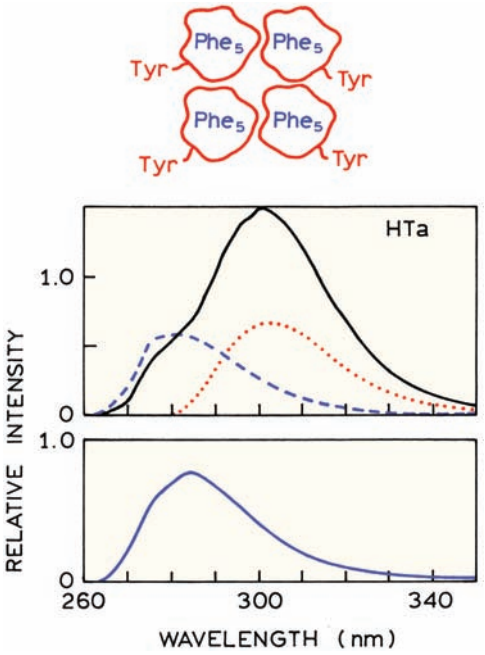

Figure 16.26. **Top**: Emission spectra of archaebacterial histone-like protein (HTa) excited at 252 nm (solid). Also shown are the emission spectra of equivalent concentrations of phenylalanine (dashed) or tyrosine (dotted). **Bottom**: Emission of HTa following removal of the tyrosine by carboxypeptidase A digestion. Revised from [82].

appears to be similar to that of tyrosine with an emission maximum near 300 nm. However, the spectrum also shows a shoulder at 280 nm that is too blue-shifted to be due to tyrosine. The origin of the dual emission was determined by a comparison with the emission from tyrosine (dotted) and phenylalanine (dashed) at equivalent concentrations. These spectra show that the emission spectrum of HTa is due to contributions from both the phe and tyr residues. Assignment of the 280-nm emission to phenylalanine was also accomplished by removal of the tyrosine residue by digestion with carboxypeptidase A. This emission spectrum (Figure 16.23, lower panel) is identical to that found for phenylalanine, identifying the emission at 280 nm as due to phenylalanine.

The presence of phe-to-tyr energy transfer in HTa was detected from the excitation spectra. Figure 16.27 shows the corrected excitation spectrum of HTa, which was superimposed on the absorption spectra of tyrosine alone and a 5-to-1 mixture of phenylalanine and tyrosine. The emission was measured at 330 nm, where only tyrosine emits. If there were no phe-to-tyr energy transfer the excitation spectrum would be the same as the absorption spectrum of tyrosine. If phe-to-tyr RET was 100% efficient then the excitation spectrum would be the same as the 5-to-1 phe-tyr mixture. Hence the transfer efficiency is near 50%. Given R_0 = 13.5 Å for phe-to-tyr energy transfer,[82] and the diameter expected for a protein with a molecular weight of 9934 daltons, which is near 28 Å, it is not surprising that phenylalanine fluorescence is partially quenched in HTa. While most proteins are larger, they may also contain multiple phenylalanine and tyrosine residues. Phenylalanine-to-tyrosine energy transfer is probably a common occurrence in proteins when excited at 260 nm.

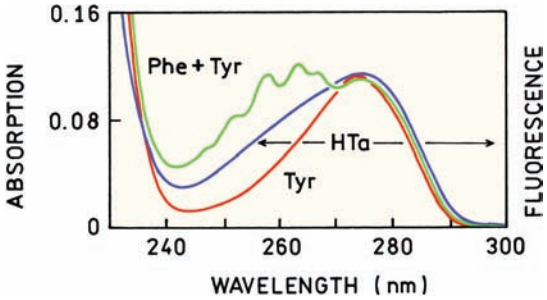

Figure 16.27. Corrected fluorescence excitation spectrum of HTa superimposed upon the ultraviolet absorbance spectra of a mixture of phenylalanine and tyrosine (5 to 1) or of tyrosine alone. Fluorescence emission was measured at 330 nm. Revised from [82].

Removal of tyrosine from HTa provided a protein without tyrosine or tryptophan and an opportunity to study the emission of phenylalanine in a protein. The lifetime of phenylalanine was near 22 ns, which is considerably longer than the 2- to 5-ns values typical of tyrosine and tryptophan. This lifetime of 22 ns is comparable to a measured value of 20 ns for a constrained analogue of phenylalanine.[92] In HTa and in the presence of tyrosine the lifetime of phenylalanine is decreased to near 12 ns. This value is consistent with 50% energy transfer from phenylalanine to tyrosine. It is interesting to notice that the 12-ns decay time is observed at all emission wavelengths, even those where only tyrosine is expected to emit.[82] Such long decay times are unlikely for directly excited tyrosine. In this protein the excited phenylalanines continue to transfer to tyrosine during their decay, resulting in an apparent 12-ns tyrosine lifetime. This phenomenon was described in Chapter 7 on excited-state reactions.

16.5. CALCIUM BINDING TO CALMODULIN USING PHENYLALANINE AND TYROSINE EMISSION

Calmodulin functions as a calcium sensor in all vertebrate cells and regulates a large number of target enzymes. Calmodulin consists of a single polypeptide chain folded into

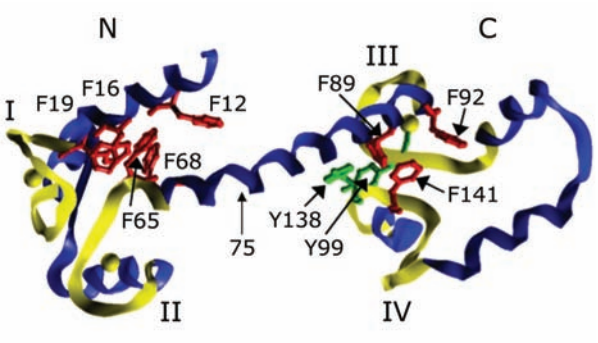

Figure 16.28. Ribbon structure for rat calmodulin saturated with calcium. The phenylalanine residues are shown in red and the tyrosine residues in green. Figure from [94] provided by Dr. Madeline A. Shea from the University of Iowa.

two domains connected by a flexible α-helical linker (Figure 16.28). Each domain contains two calcium-binding sites (I-IV). Most calmodulins lack tryptophan residues. Rat calmodulin contains five phenylalanines in the N-terminal domain (N) and three in the C domain, which also contains two tyrosine residues. When calmodulin is excited at 250 nm, in the absence of calcium, emission from both phe and tyr is observed (Figure 16.29, bottom panel). This emission

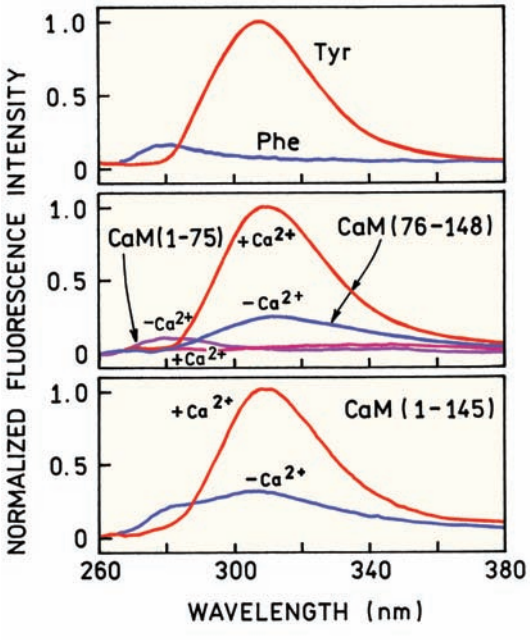

Figure 16.29. Emission spectra for excitation at 250 nm. Top: phe or tyr. Middle and bottom: rat calmodulin (CaM) with and without calcium. The numbers indicate the amino-acid residues in the calmodulin fragments. Revised from [94].

spectrum shows components similar to that observed for a mixture of these two amino acids (top panel). Addition of calcium to calmodulin (1–145) results in disappearance of the phe emission and an increase in the tyr emission.[93,94] At first glance it appears that energy transfer is increased in the presence of calcium, which is expected to decrease the phe emission and increase the tyr emission. However, an increase in RET was not expected because calmodulin is more elongated in the presence of calcium than in the absence of calcium. The middle panel shows studies of the individual domain. The N domain consisting of residues 1–75 shows only phe emission, which is quenched upon addition of calcium. The C domain consists of residues 76–145 and showed an increase in tyrosine emission upon binding calcium but no phe emission. Hence the intensity changes seen for the entire molecule CaM 1–145 are probably not due to changes in RET. This is not a disappointment, but in fact an advantage, because calcium binding to each domain can be studied independently using the intrinsic phe and tyr emission of calmodulin.

16.6. QUENCHING OF TRYPTOPHAN RESIDUES IN PROTEINS

Collisional quenching of proteins is used to determine the extent of tryptophan exposure to the aqueous phase.[95–102] The basic idea is shown in Figure 16.30, which depicts quenching by a water-soluble quencher that does not easily penetrate the protein matrix. Collisional quenching is essentially a contact phenomenon, so that the fluorophore and quencher need to be in molecular contact for quenching to occur. Consequently, if the tryptophan residue is buried inside the protein (W_1), quenching is not expected to occur. If the tryptophan residue is on the protein surface (W_2), then quenching is expected.

One example of selective quenching is shown for apoazurin Ade, which is azurin lacking copper. Apoazurin Ade has two tryptophan residues: one surface residue and one buried residue.[101] The emission spectra of this protein, along with those of its single-tryptophan variants, are shown in Figure 16.16. For our present purposes the properties of the protein with or without (apo) copper are the same.

Emission spectra were recorded in the absence and presence of 0.45 M iodide, which is a collisional quencher (Figure 16.31). The intensity decreases in the presence of iodide. The emission spectrum changes in the presence of iodide, and resembles the structured emission seen from the

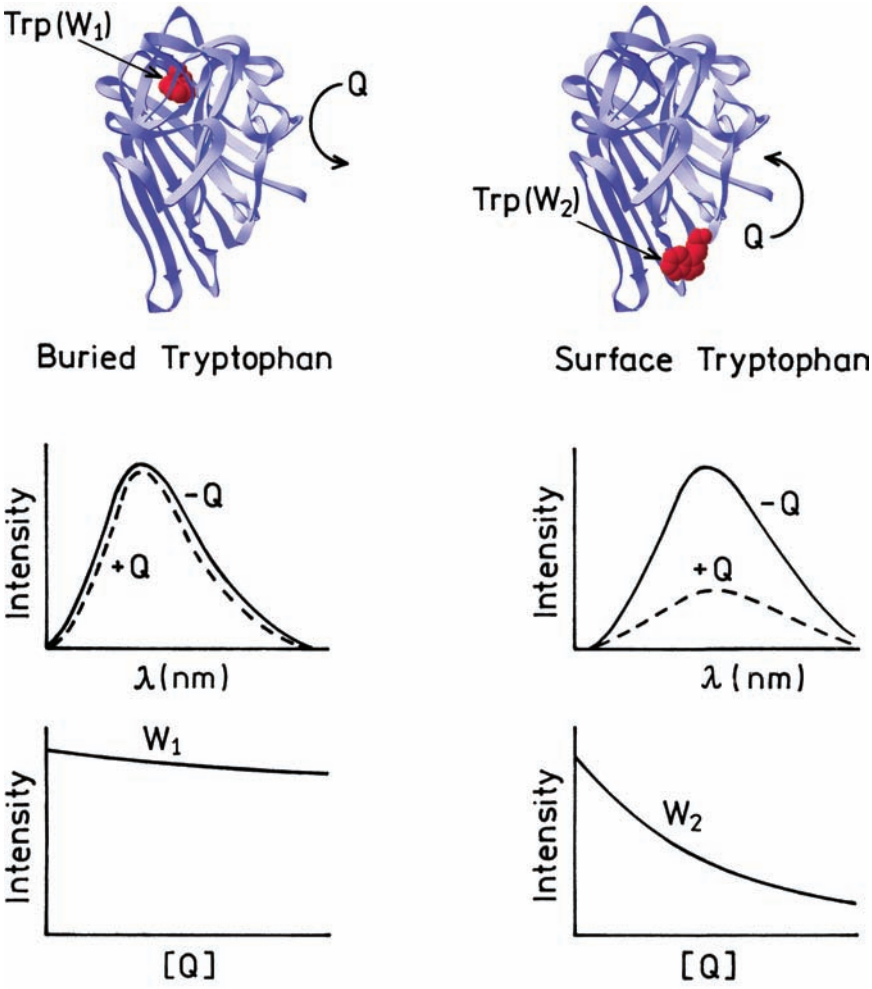

Figure 16.30. Collisional quenching of buried (W_1) and surface accessible (W_2) tryptophan residues in proteins.

single-tryptophan azurin Pae. The spectrum of the quenched tryptophan residue can be seen from the difference spectrum, and is characteristic of an exposed residue in a partially hydrophobic environment. In this favorable case, one residue is quenched and the other is not, providing resolution of the two emission spectra.

16.6.1. Effect of Emission Maximum on Quenching

Water-soluble quenchers, including iodide and acrylamide, do not readily penetrate the hydrophobic regions of proteins. There is a strong correlation between the emission maximum and quenching constant.[101–102] Blue-shifted tryptophan residues are mostly inaccessible to quenching by acrylamide, and red-shifted residues are nearly as accessible as tryptophan in water. This correlation can be seen in the acrylamide quenching of several proteins (Figure 16.32). The emission of azurin is essentially unchanged in up to 0.8 M acrylamide. In contrast, the exposed tryptophan residue in adrenocorticotropin hormone (ACTH) is almost completely quenched at 0.4 M acrylamide (Figure 16.32, left panel).

Quenching data are typically presented as Stern-Volmer plots, which are shown for several single-tryptophan proteins (Figure 16.32, right panel). In these plots the larger slopes indicate larger amounts of quenching and can be used to calculate the bimolecular quenching constant (k_q). The buried single-tryptophan residue in azurin Pae is not affected by acrylamide. In contrast, the fully exposed residue in ACTH is easily quenched by acrylamide. ACTH is quenched nearly as effectively as NATA. A plot of the bimolecular quenching constant (k_q) for acrylamide versus emission maximum for a group of single-tryptophan proteins is shown in Figure 16.33. These data show that k_q

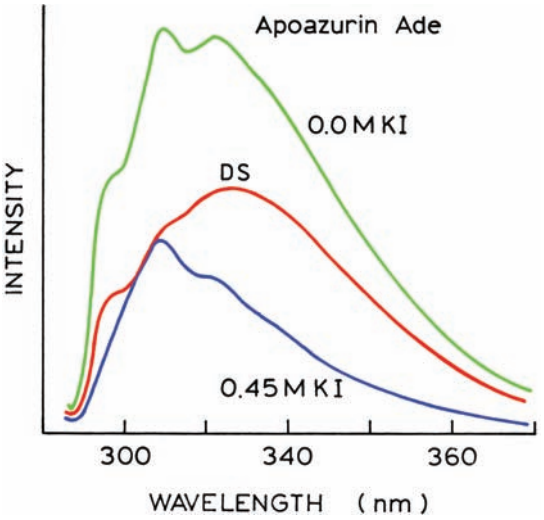

Figure 16.31. Fluorescence emission spectra of apoazurin Ade from *Alcaligenes denitrificans* in the absence (top curve) and presence (bottom curve) of 0.45 M Kl. The middle line is the difference spectrum (DS) and is due to the easily quenched emission (presumably from Trp-118). The buffer was 0.05 M sodium acetate, pH 5.0. Revised from [101].

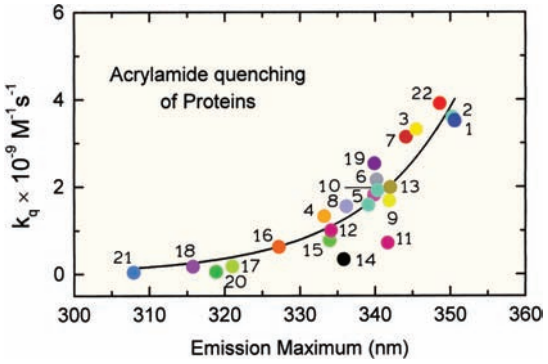

Figure 16.33. Dependence of the apparent acrylamide bimolecular quenching constant (k_q) on the emission maximum for single-tryptophan proteins: 1, glucagon; 2, adrenocorticotropin; 3, melittin monomer; 4, melittin tetramer; 5, gonadotropin; 6, phospholipase A_2; 7, human luteinizing hormone; 8,9, monellin; 10, gonadotropin; 11, human serum albumin, N form; 12, human serum albumin, F form; 13, myelin basic protein; 14, elongation factor Tu-GDP; 15, nuclease; 16, fd phage; 17, ribonuclease T_1; 18, parvalbumin; 19, calcium-depleted parvalbumin; 20, asparaginase; 21, apoazurin Pae; 22, mastopartan X. Revised from [101].

varies from almost completely inaccessible for azurin and asparaginase to completely accessible for glucagon. Glucagon is a relatively small peptide with 29 amino acids that opposes the action of insulin. Glucagon has a random structure in solution.[103–105] Hence, there is little opportunity for the protein to shield the single trp-25 residue from acrylamide quenching.

The extent of collisional quenching can also be dependent on protein conformation and/or the extent of subunit association. This effect has been observed for melittin, which is a small peptide of 26 amino acids containing a single-tryptophan residue at position 19. Depending on ionic strength, melittin can exist as a monomer or tetramer. In the tetramer, the four tryptophan residues, one per monomer, are located in a hydrophobic pocket between the helices.[106] The tryptophan residues in melittin are more easily quenched when melittin is in the monomer state (Figure 16.33).

Acrylamide and iodide are polar molecules, and do not readily penetrate the nonpolar regions of proteins. However, small nonpolar oxygen molecules readily penetrate all

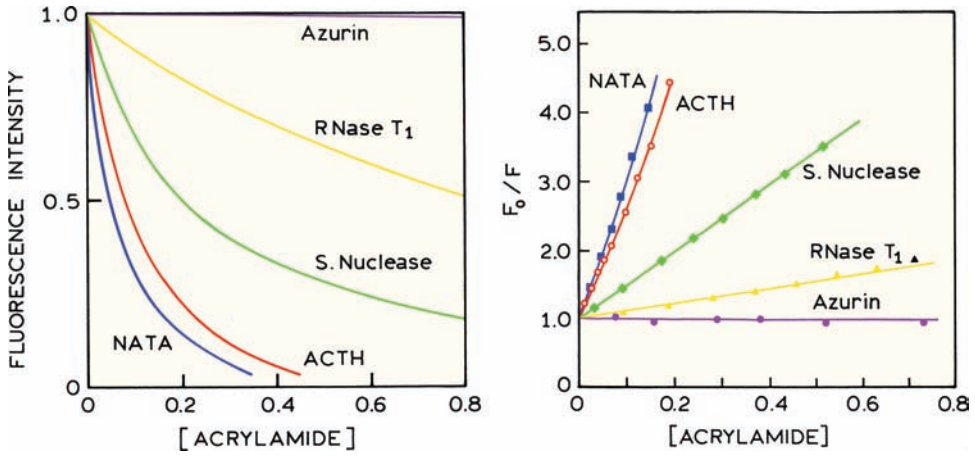

Figure 16.32. Acrylamide quenching of representative single-tryptophan proteins and NATA. Left: intensity versus acrylamide concentration. Right: Stern-Volmer plots. Data from [80], [86], and [99].

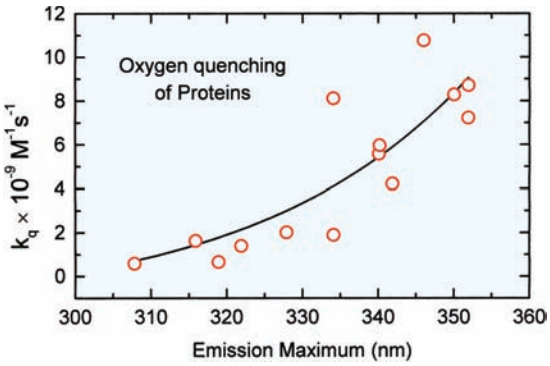

Figure 16.34. Correlation of emission maxima of multi-tryptophan proteins with the oxygen bimolecular quenching constants. Data from [107].

regions of proteins. The oxygen bimolecular quenching constants for a number of proteins show weaker correlation with the emission maxima (Figure 16.34). It is known from the x-ray structures of proteins that the interiors are densely packed, similar to crystals of organic molecules, so that there is little room for oxygen within the center of most proteins. Surprisingly, the bimolecular quenching constants for oxygen are 20 to 50% of the value for tryptophan in water (near 1 x 10^{10} M^{-1} s^{-1}). These results indicate that proteins undergo rapid structural fluctuations that allow the oxygen molecules to penetrate during the ns excited-state lifetime.[107–109] Structural fluctuations on the ns timescale are consistent with the anisotropy decays of most proteins, which typically show ns or subnanosecond components.[110–111] Acrylamide and iodide are less effective quenchers than oxygen because it is energetically unfavorable for them to enter nonpolar regions of proteins. Also, acrylamide is larger than oxygen or iodide, which also plays a role in its more selective quenching.

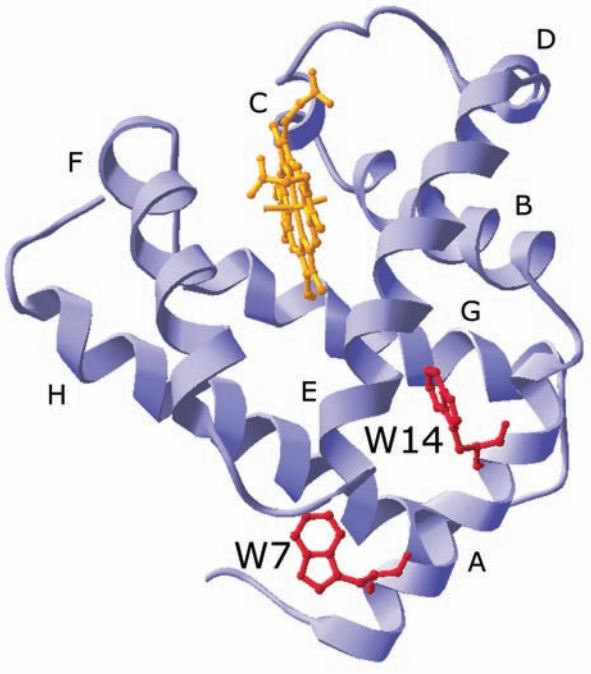

Figure 16.35. Ribbon structure of horse myoglobin showing the location of tryptophans 7 and 14. The letters denote the helices.

16.6.2. Fractional Accessibility to Quenching in Multi-Tryptophan Proteins

The selective quenching of surface tryptophan residues suggests the use of quenching to resolve the contributions of surface and buried tryptophans to the total fluorescence of a protein.[112–113] One example is apomyoglobin, which contains two tryptophan residues (Figure 16.35). Apomyoglobin refers to myoglobin without the heme group, which quenches tryptophan fluorescence by RET. In this protein W7 appears to be exposed to the aqueous phase, and W14 appears to be buried among the helices. The Stern-Volmer plots for quenching by iodide or trichloroethanol (TCE) both show downward curvature, indicating that some fraction of the total emission may be inaccessible to quenching (Figure 16.36).

The fraction of accessible fluorescence (f_a) can be obtained from a modified Stern-Volmer plot, in which $F_0/\Delta F$ is plotted versus reciprocal quencher concentration (Section 8.8). The y-intercept represents extrapolation to infinite quencher concentration. Complete quenching is expected for an accessible fluorophore, so the extrapolated value of $F_0/\Delta F$ is unity. If a portion of the fluorescence is not accessible, ΔF is smaller than F_0, and the intercept (f_a^{-1}) is greater than unity. Figure 16.36 shows an intercept near 2, so that about half of the total fluorescence is assessable to quenching.

The fractional accessibility to quenchers can be measured for each emission wavelength (Figure 16.37, lower panel). The fractional accessibility is higher on the long-wavelength side of the emission spectrum. These fractions, when multiplied by the total intensity at each wavelength, yield the emission spectra of the quenched and unquenched components from apomyoglobin (top panel). The higher accessibility at longer wavelengths results in a red-shifted spectrum for the accessible fraction. It seems probable that the accessible and inaccessible components are from W7 and W14, respectively.

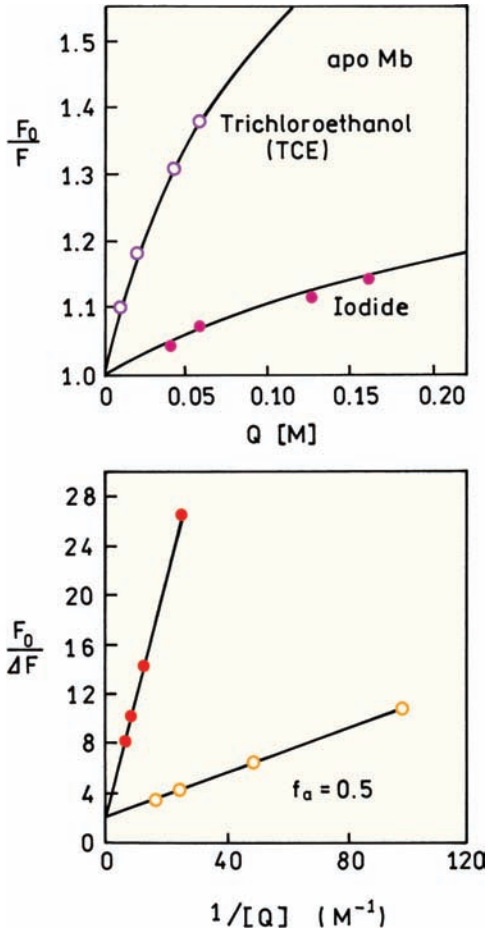

Figure 16.36. Stern-Volmer and modified Stern-Volmer plots for apomyoglobin quenching by iodide or trichloroethanol (TCE). The data in the upper panel was reconstructed from the data in the lower panel. Data from [113].

16.6.3. Resolution of Emission Spectra by Quenching

Selective quenching of tryptophan residues allows resolution of the emission spectra of the quenched and unquenched components. For apomyoglobin we assumed that some fraction of the emission was completely inaccessible to quenching. A more general procedure allows the emission spectra to be resolved even when both residues are partially accessible to quenching.[114–116] The basic approach is to perform a least-squares fit to the quenching data to recover the quenching constant and fractional intensity at each wavelength (λ):

$$\frac{F(\lambda)}{F_0} = \sum_i \frac{f_i(\lambda)}{1 + K_i(\lambda)[Q]} \qquad (16.4)$$

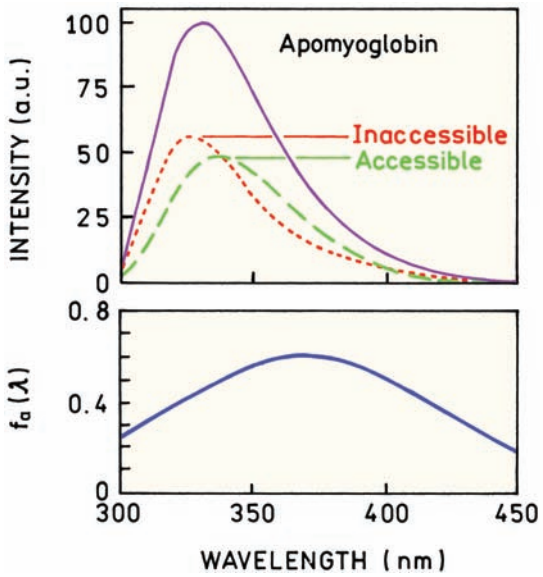

Figure 16.37. Emission spectra of apomyoglobin and of the accessible and inaccessible components. The lower panel shows the wavelength-dependent fractional accessibility to quenching. Revised from [113].

In this expression the values of $f_i(\lambda)$ represent the fraction of the total emission quenchable at wavelength λ with a value $K_i(\lambda)$ (Section 8.8).

This procedure was applied to a metalloprotease from *S. aureus* that contains two tryptophan residues.[116] For all emission wavelengths the Stern-Volmer plot is curved due to the different accessibilities of each residue (Figure 16.38). The data are fit by least-squares methods to obtain the values of $K_i(\lambda)$ and $f_i(\lambda)$. Similar data are collected for a range of emission wavelengths. These data can be used to calculate the emission spectra of each component:

$$F_i(\lambda) = F_0(\lambda) f_i(\lambda) \qquad (16.5)$$

where $F_0(\lambda)$ is the unquenched emission spectrum. For metalloprotease this procedure yielded two well-resolved emission spectra (Figure 16.39).

The use of quenching-resolved spectra may not always be successful. One possible reason for failure would be if a tryptophan residue was not in a unique environment. In this case each tryptophan residue may display more than one emission spectrum, each of which would be quenched to a different extent. Quenching-resolved spectra have been obtained for proteins that contain a single-tryptophan residue.[116–117] These results have been interpreted as due to the protein being present in more than a single conformational

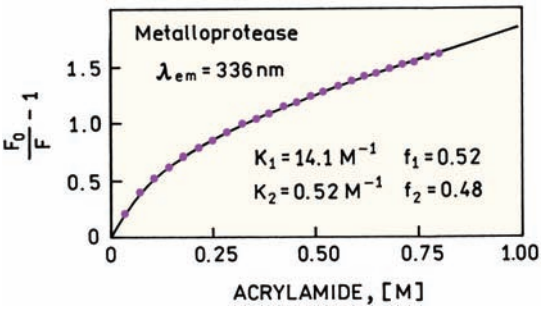

Figure 16.38. Stern-Volmer plot for acrylamide quenching of *S. aureus* metalloprotease (dotted). Excitation wavelength was 297 nm and emission was observed at 336 nm. The solid line shows the least-squares fit with parameters K_1 = 14.1 M^{-1}, K_2 = 0.52 M^{-1}, f_1 = 0.52, and f_2 = 0.48. Revised from [116].

state. A single-tryptophan residue can display a multi-exponential decay, and the decays can depend on wavelength. Hence, there is no a priori reason to assume the residue is quenched with the same quenching constants at all emission wavelengths.

16.7. ASSOCIATION REACTION OF PROTEINS

An important use of intrinsic protein fluorescence is to study binding interactions of proteins.[118–120] Such measurements take advantage of the high sensitivity of fluorescence and the ability to perform measurements on dilute protein solutions. Detection of protein association reactions by fluorescence is made possible by the high sensitivity of tryptophan to its local environment. A change in exposure to solvent or a change in proximity to a quenching group can often change the emission maximum or quantum yield of tryptophan residues.

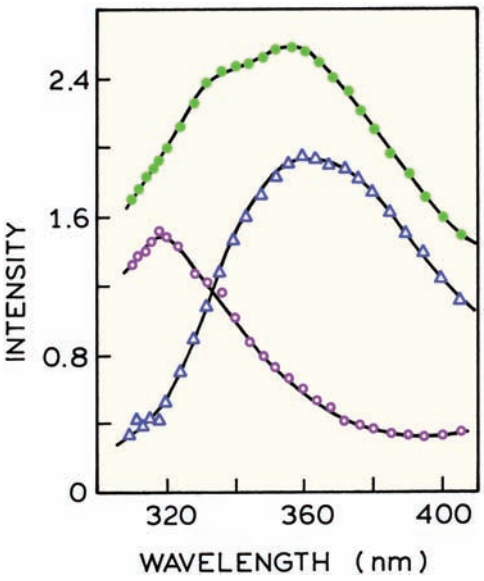

Figure 16.39. Resolution of the two tryptophan emission spectra from *S. aureus* metalloprotease. ○, component with K_1 = 0.52 M^{-1}; Δ, component with K_2 = 14.1 M^{-1}; ●, steady-state spectrum. Revised from [116].

16.7.1. Binding of Calmodulin to a Target Protein

Intrinsic protein fluorescence was used to study binding of calmodulin to a target protein. The target protein was a peptide fragment from a glutamate receptor. Glutamate is the dominant neurotransmitter in the human brain. The neuronal receptor peptide (NRP) contains a single-tryptophan residue. Calmodulin does not contain tryptophan, which allowed emission from the NRP to be observed selectively using 297-nm excitation. The intrinsic tryptophan emission of the NRP was used to study its binding to calmodulin in the absence and presence of calcium. It is frequently assumed that calmodulin does not interact with target proteins until it binds calcium. However, the absence of any interaction in the absence of calcium could result in a slow cellular response to calcium because of the time needed for diffusive encounters to occur. Pre-association of target proteins with calmodulin could increase the response speed to calcium transients.

Emission spectra of the NRP are shown in Figure 16.40. Upon addition of calcium and calmodulin to the NRP there was an increase in intensity and a blue shift of its tryptophan emission,[120] showing that calcium-saturated calmodulin binds to the NRP (lower left). Surprisingly, there was also an increase in intensity and blue shift of the NRP emission with calmodulin in the absence of calcium (upper left), showing that binding occurs without calcium. This result indicated that calmodulin pre-associates with the receptor, presumably to provide a more rapid response to calcium transients.

If calmodulin binds to the receptor without calcium then how does calcium trigger the receptor? This question was partially answered by studies of the N and C domains of calmodulin. The C domain alone was found to interact with the NRP in the absence of calcium (Figure 16.40, upper right). Interaction between the C domain and calmodulin was increased by calcium. The N domain was found to interact with the NRP only in the presence of calcium (middle panels). These results suggest that the C domain is responsible for pre-association and the N domain for signal-

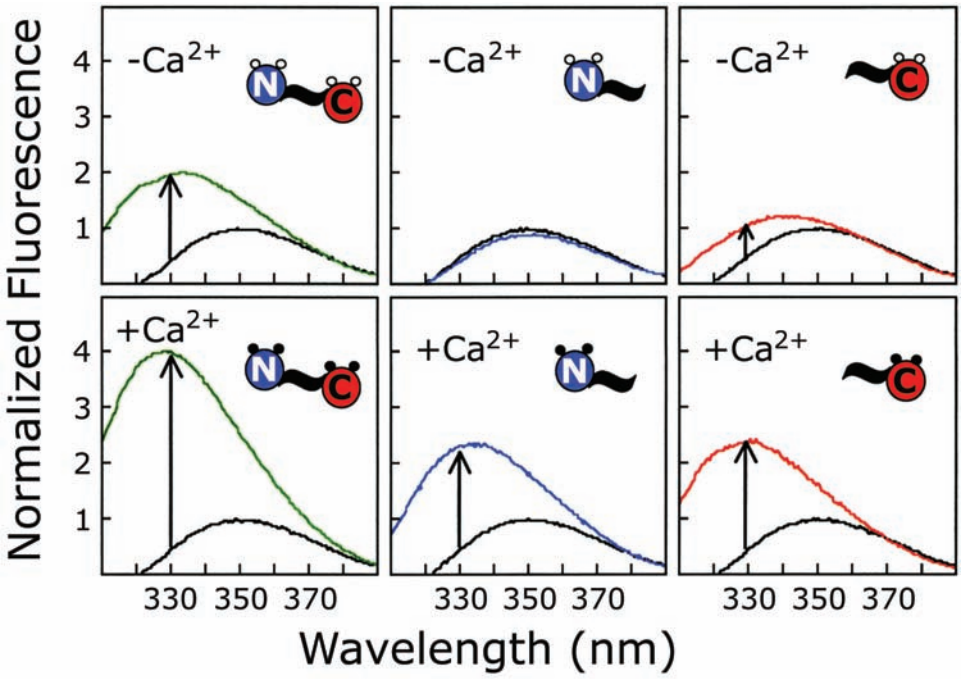

Figure 16.40. Emission spectra of a neuronal receptor peptide NRP in the presence of calmodulin and the N and C domains of calmodulin. Excitation was at 297 nm. Revised from [120].

ing. The high sensitivity of tryptophan emission to its local environment can provide detailed information on protein–protein interactions.

16.7.2. Calmodulin: Resolution of the Four Calcium-Binding Sites Using Tryptophan-Containing Mutants

Site-directed mutagenesis allows single-tryptophan residues to be placed at desired locations in the protein. This approach was applied to calmodulin and resulted in an ability to detect binding of calcium to each of the four binding sites. Calmodulin has four binding sites for calcium, but little was known about the sequence of binding and possibility of cooperativity between the four binding sites. Other studies of calcium binding were not adequate to distinguish between various models for Ca^{2+} binding. Bulk measurements of binding can reveal only the total amount of bound calcium and do not indicate the sequence of calcium binding.

This problem was solved by the creation of single-tryptophan mutants.[121] Calmodulin contains several tyrosine residues, but it does not contain tryptophan. This allowed the insertion of tryptophan residues into the sequence to probe various regions of the protein, and the use of these residues to probe local regions of the calmodulin structure. The tryptophan residues were inserted near each of the four Ca^{2+} binding sites, one trp residue per mutant. The normalized intensity changes for each tryptophan residue are shown in Figure 16.41. These measurements revealed the sequence of calcium binding to calmodulin, and revealed interactions between the various binding sites. Protein engineering and fluorescence spectroscopy can provide detailed information on the solution behavior of a protein. Similar tryptophan-containing calmodulin mutants were used to study binding of peptides to calmodulin.[122]

16.7.3. Interactions of DNA with Proteins

Intrinsic protein fluorescence can be used to study binding of DNA to proteins.[123–129] These studies typically rely on quenching of intrinsic tryptophan fluorescence by the DNA bases. One example is the single-stranded DNA binding protein (SSB) from *E. coli* (Figure 16.42). This protein is a member of a class of proteins that bind ssDNA with high affinity but low specificity. Proteins that destabilize double-helical DNA are required for DNA replication and repair. SSB is a homotetramer that binds about 70 nucleotides.

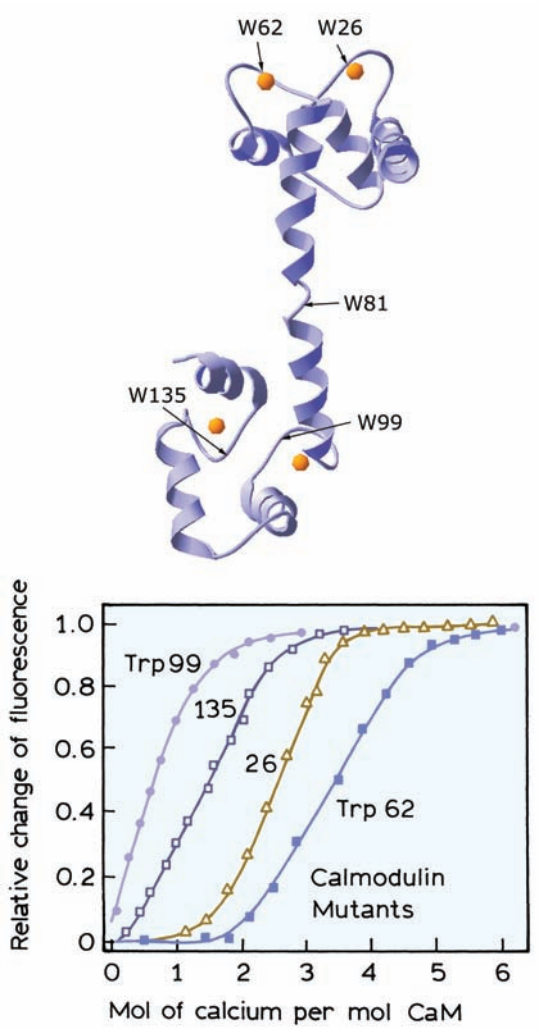

Figure 16.41. Relative changes in the fluorescence intensity of Trp 99 (●), Trp 135 (□), Trp 26 (Δ), and Trp 62 (■) in single-tryptophan mutants of calmodulin with changes in the amount of bound calcium. The arrows show the location of the tryptophan residues and the orange dots are calcium atoms. Reprinted with permission from [121]. Copyright © 1992, American Chemical Society.

Figure 16.42. Ribbon structure for the *E. coli* single-stranded binding protein (SSB) with a bound 70-mer. Figure from [128] and provided by Dr. Alexander Kozlov and Dr. T. Lohman, Washington University, MO.

DNA is tightly packed in chromatin, but DNA replication occurs rapidly nonetheless. Hence it is of interest to determine the rates of DNA folding around the SSB. This can be accomplished using rapid mixing stopped-flow measurements, while monitoring the intrinsic tryptophan fluorescence of SSB (Figure 16.43). Upon mixing with $(dT)_{70}$ there is a rapid decrease in the tryptophan emission.[128] By studies with various concentrations of DNA and different lengths of DNA it was possible to determine the rate constants for initial DNA binding and subsequent folding of DNA around the protein. The rates of DNA folding around the protein were also measured using RET between DNA oligomers labeled with Cy5 and Cy3 at the 5' and 3' ends, respectively. These probes were brought into closer contact when DNA wrapped around SSB (not shown). The changes in RET and intrinsic protein fluorescence occurred on the same timescale, indicating that wrapping of DNA around the protein proceeds very rapidly after binding occurs.

The intensity changes can be used to determine the fraction of the total emission that is quenched by DNA. The Myb oncoprotein is associated with chromatin and appears to function as a regulator of gene expression. The N-terminal region of this protein, which contains the DNA binding region, consists of three domains: R_1, R_2, and R_3. The subscripts refer to the domain number, not the number of domains. Each domain contains three highly conserved tryptophan residues, which suggests these residues are involved in binding to DNA.

The intrinsic protein fluorescence of the R_2R_3 fragment of the Myb oncoprotein is partially quenched by DNA.[129]

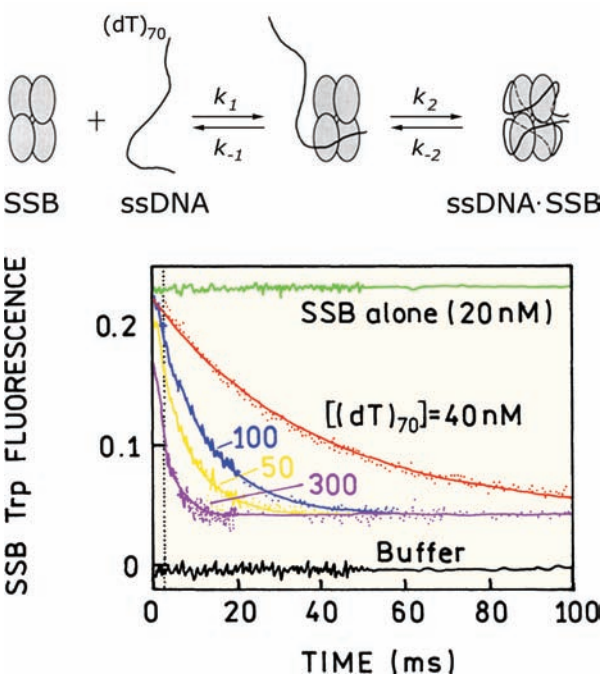

Figure 16.43. Stopped-flow intrinsic tryptophan emission of SSB upon mixing with $(dT)_{70}$. Revised from [128].

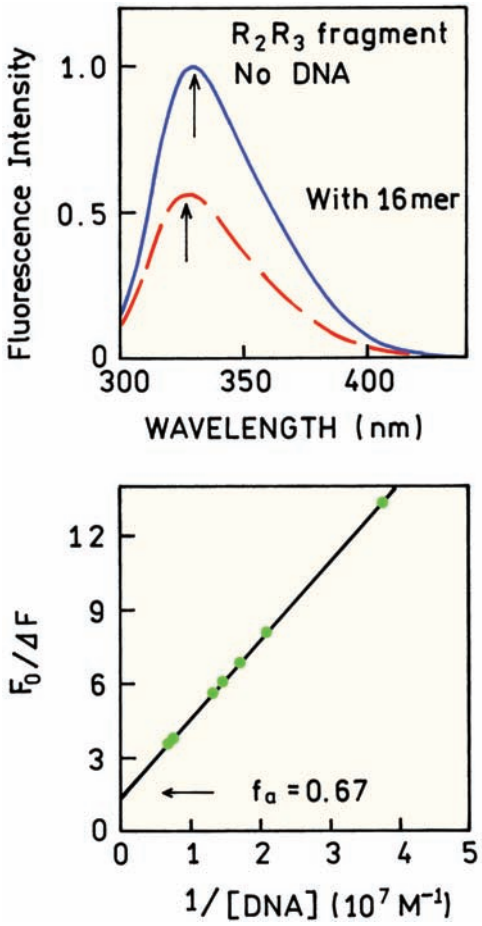

Figure 16.44. Emission spectra and modified Stern-Volmer plot for quenching of the tryptophan emission of the R_2R_3 domain of the Myb oncoprotein by DNA. Revised from [129].

This fragment contains six tyr residues, three in each domain. Addition of a 16-mer results in quenching of the emission of R_2R_3 and a small blue shift in the emission (Figure 16.44). The tryptophan intensities were measured for a number of 16-mer concentrations, and plotted in modified Stern-Volmer format. Extrapolation to high DNA concentrations shows that a fraction of 0.67 of the total intensity was quenched by DNA. Assuming all the tryptophans have the same quantum yield, this result indicates that 2 of the 3 trp residues in each domain are quenched by contact with DNA.

16.8. SPECTRAL PROPERTIES OF GENETICALLY ENGINEERED PROTEINS

Interpretation of intrinsic protein fluorescence is complicated by the presence of multiple-tryptophan residues. When the intrinsic fluorescence of a multi-tryptophan protein is first measured it is not known whether all the trp contributes equally to the emission and the emission maxima of the emitting residues. Site-directed mutagenesis provides an approach to determining the spectral properties of each trp residue. For example, suppose the protein of interest contains two tryptophan residues in the wild-type sequence. One can attempt to use quenching or time-resolved methods with the wild-type protein to resolve the emission spectra of the two residues. However, success requires that the residues have very different lifetimes or accessibilities to quenchers. Even if the resolution appears to be successful it may not reveal interactions between the two residues. That is, the emission from the wild-type protein may not be the same as the sum of the emission from the two single-tryptophan mutants.

A powerful approach to resolving the contributions of each tryptophan, and the interactions between the tryptophans, is by examination of the two single-tryptophan mutants. Each tryptophan residue is replaced in turn by a similar residue, typically phenylalanine. This approach to resolving protein fluorescence has been used in many laboratories.[130–137] It is not practical to describe all these results. Rather, we have chosen a few representative cases. These examples show simple non-interactive tryptophans and the

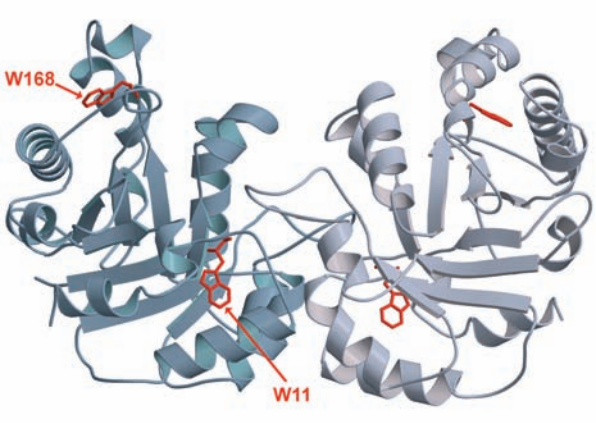

Figure 16.45. Structure of triosephosphate isomerase. Courtesy of Dr. Hema Balaram from the Jawaharlal Nehru Center for Advanced Scientific Research, India.

more complex cases in which there is trp-to-trp energy transfer.

16.8.1. Single-Tryptophan Mutants of Triosephosphate Isomerase

Triosephosphate isomerase (TPI) is a protein that catalyzes isomerization of dihydroxyacetone phosphate and glyceraldehyde phosphate. The enzyme from the malarial parasite *Plasmodium falciparum* contains two tryptophan residues, at positions 11 and 168. The enzyme exists as a homodimer with each monomer containing W11 and W168 (Figure 16.45). The monomer structure consists of a central β-sheet surrounded by α-helices, which is a common structural feature in this class of enzymes. It is difficult to judge the degree of exposure of each residue to water. Depending on the viewing angle, W168 appears to be either exposed to water (left monomer) or shielded from water (right monomer).

The contributions of each tryptophan emission to the total emission of TPI were determined by construction of the single-tryptophan mutants.[138] In each mutant one of the tryptophans was replaced with phenylalanine (F). The W168F mutant contains only W11 and the W11F mutant contains only W168. Emission spectra of the wild-type and mutant proteins are shown in Figure 16.46 (top panel). The emission from W168 is strongly blue shifted with an emission maximum at 321 nm, and the emission maximum of W11 is 332 nm. In this example the emission of the wild-type protein appears to be the sum of the emission from the two single-tryptophan mutants. This result indicates the

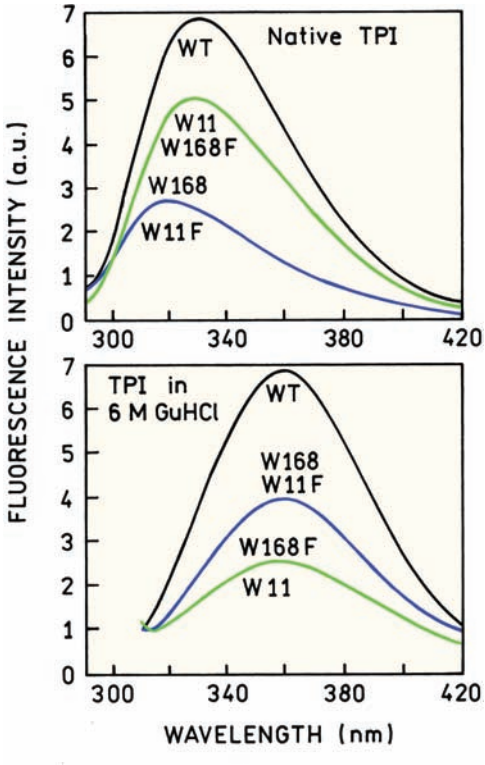

Figure 16.46. Emission spectra of wild-type triosephosphate isomerase and the two single-tryptophan mutants. Revised from [138].

tryptophan residues do not interact with each other. Denaturation of the protein in 6 M GuHCl equalized the emission maxima of both tryptophan residues to 357 nm (lower panel). The red shifts upon unfolding show that both residues are shielded from water to some extent in the native protein structure.

The emission spectra of the TPI mutants showed that both tryptophans are sensitive to the protein structure, and that these residues do not interact in the native protein. This result suggests that each tryptophan residue could be used to detect the effects of the trp-to-phe mutation on stability of TPI. Figure 16.47 shows the effects of the denaturant guanidine hydrochloride (GuHCl) on the emission maxima of the wild-type TPI and the two single-tryptophan mutants. The W168F mutant with W11 has the same stability as TPI. In contrast, the W11F mutant with W168 denatures more rapidly in GuHCl, which indicates lower protein stability. Hence, substitution of W11 with a phenylalanine destabilizes the protein. This is a surprising result because the emission spectra (Figure 16.46) showed that W168 is buried more deeply in the protein. One may have expected the buried residue to contribute more to the protein stability.

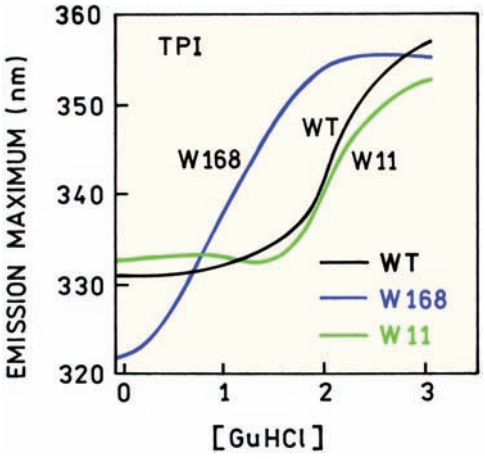

Figure 16.47. Effect of guanidium hydrochloride on the wild-type triosephosphate isomerase and the two single-tryptophan mutants. Revised from [138].

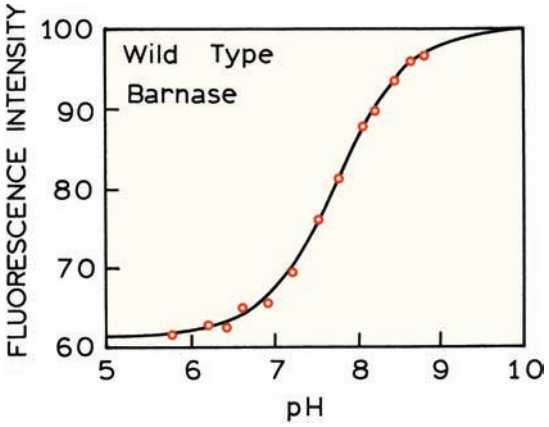

Figure 16.49. pH-dependent intensity of the tryptophan emission of wild-type barnase. Excitation, 295 nm; emission, 340 nm. Revised and reprinted with permission from [139]. Copyright © 1991, American Chemical Society.

16.8.2. Barnase: A Three-Tryptophan Protein

Barnase is an extracellular ribonuclease that is often used as a model for protein folding. It is a relatively small protein: 110 amino acids, 12.4 kDa. The wild-type protein contains three tryptophan residues (Figure 16.48), one of which is located close to histidine 18 (H18). Examination of the three single-tryptophan mutants of barnase provides an example of energy transfer between tryptophan residues and the quenching effects of the nearby histidine.[139]

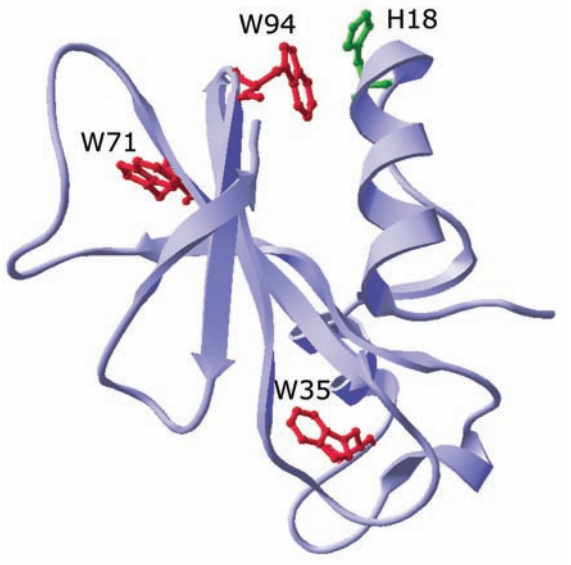

Figure 16.48. Structure of barnase showing the positions of the three tryptophan residues and histidine 18.

The emission intensity of wild-type barnase, which contains all three tryptophan residues, increases nearly twofold as the pH is increased from 7 to 8.5 (Figure 16.49). This increase in fluorescence is due to the presence of W94 and the histidine. Only mutants containing both his-18 and trp-94 showed pH dependent intensities. Tryptophan residues are known to be quenched by the protonated form of histidine.[140–141] This is not surprising given the sensitivity of indole to electron deficient molecules.

Emission spectra of barnase and its mutants at pH 5.5 and 9.4 are shown in Figure 16.50. At first glance these spectra appear complex. First consider the contribution of W71. Substitution of W71 with tyrosine (W71Y) has little effect on the spectra. Hence, W71 is weakly fluorescent. It appears that weakly fluorescent or nonfluorescent trp residues is a common occurrence in proteins. Such effects may contribute to the frequent observation of longer-than-expected lifetimes of proteins that display low quantum yields and long apparent natural lifetimes (Figure 16.12).

The effect of H18 is immediately apparent from the glycine mutant H18G. The intensity at pH 5.5 increases 2.6-fold over that for the wild-type protein (Figure 16.50), and the intensity at pH 9.4 increases by about 70%. This result indicates that both the protonated and neutral forms of histidine quenched W94, but that quenching by the electron-deficient protonated form present at pH 5.5 is more efficient quencher.

Surprising results were found when W94 was replaced with leucine in W94L. The intensity of the protein increased even though the number of tryptophan residues decreased. These effects were not due to a structural change

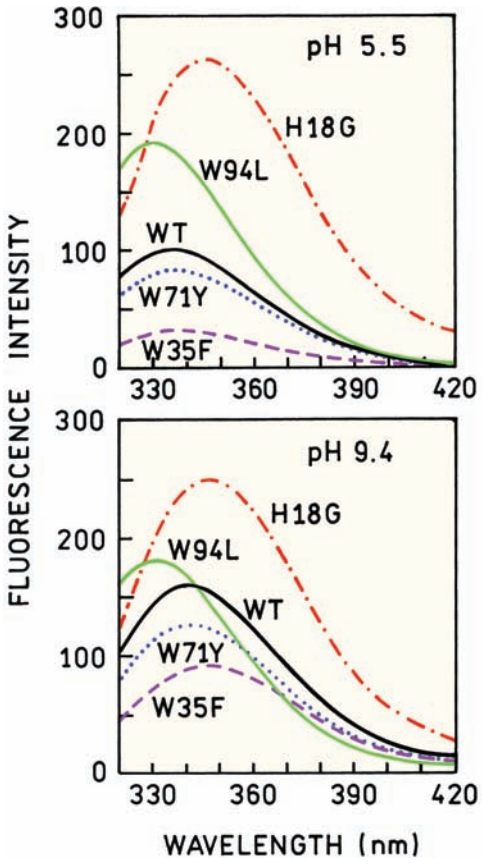

Figure 16.50. Fluorescence emission spectra of the wild-type (WT) barnase and its mutants in buffer at pH 5.5 (top), where histidine 18 is protonated and at pH 9.4 where histidine is neutral (bottom). Also shown are the emission spectra of the single-tryptophan mutants at these pH values. Revised and reprinted with permission from [139]. Copyright © 1991, American Chemical Society.

in the protein.[139] The increase in intensity upon removal of W94 is due to energy transfer from the other trp residues to W94. Tryptophan 94 serves as an energy trap for the other trp residues. The emission spectrum of trp94 is red shifted relative to W35 and W71, as seen in the H18G mutants. When W94 is removed (W94L), the blue-shifted emission from the other residues increases since they no longer transfer energy to the quenched residue W94. Examination of the structure (Figure 16.48) suggests that W94 is located on the surface of barnase, whereas W71 and W35 appear to be buried. Tryptophan 94 is red shifted and serves as an acceptor for the other two tryptophan residues. Trp-94 is also quenched by the presence of a nearby histidine residue. Hence, the overall quantum yield of barnase is strongly influenced by just one tryptophan residue. These results for barnase illustrate the complex spectral properties of multi-tryptophan proteins, and how these properties can be understood by site-directed mutagenesis.

16.8.3. Site-Directed Mutagenesis of Tyrosine Proteins

The concept of engineered proteins has also been applied to tyrosine–only proteins.[142-143] One example is Δ^5-3-ketosteroid isomerase (KSI), which catalyzes the isomerization of steroids. The protein is a dimer and each subunit contains three tyrosine residues (Y14, Y55, and Y88). The three double tyrosine deletion mutants were prepared by substitution with phenylalanine.[143] One of the residues—Y14—displayed a normal tyrosine emission (Figure 16.51) and a good quantum yield (0.16). The other two mutants (Y55 and Y88) displayed lower quantum yields (0.06 and 0.03, respectively) and long-wavelength tails on the tyrosine spectra. These spectra were interpreted as quenching due to hydrogen-bonding interactions with nearby groups. In this protein, the emission is dominated by one of the tyrosine residues.

16.9. PROTEIN FOLDING

The intrinsic tryptophan emission of proteins has proved to be particularly valuable in studies of protein folding.[144–157] It is widely recognized that proteins must fold by a particular pathway because the process is too fast to be explained by a random conformational search. The sensitivity of tryptophan to its local environment usually results in changes in intensity or anisotropy during the folding process. One example (not shown) are kinetic studies of the refolding of

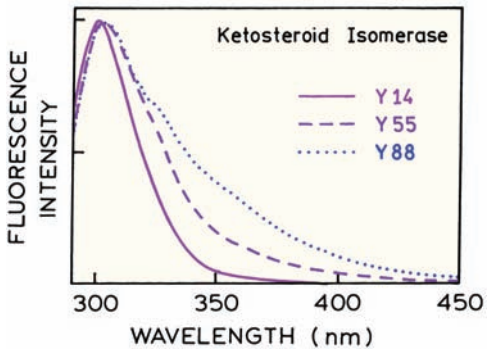

Figure 16.51. Normalized emission spectra of the single-tyrosine mutants of Δ^5-3-ketosteroid isomerase. The wild-type enzyme has three tyrosine residues per subunit. Y14, Y55F/Y88F (solid); Y55, Y14F/Y88F (dashed); Y88, Y14F/Y55F (dotted). Revised from [143].

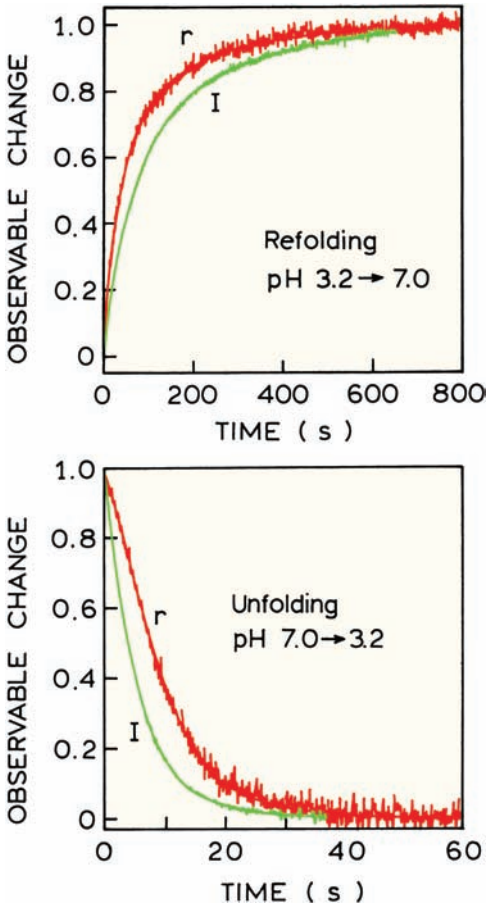

Figure 16.52. Time-dependent intensity (I) and anisotropy (r) of the single tryptophan in staphylococcal nuclease following a pH jump from 3.2 to 7.0 (top) or 7.0 to 3.2 (bottom). Revised from [150].

apomyoglobin.[151–152] In this case one of the tryptophan residues is quenched as two helices of myoglobin come into contact. This quenching is due to contact of tryptophan 14 on one helix with methionine 131 on another helix. Methionine is known to quench tryptophan fluorescence.[141]

Figure 16.52 shows stopped-flow measurements for a mutant nuclease from *Staphylococcal aureus*. This nuclease contains a single-tryptophan residue at position 140 near the carboxy terminus. This residue is mostly on the surface of the protein, but its intensity and anisotropy are sensitive to protein folding. Folding and unfolding reactions were initiated by jumps in pH from 3.2 to 7.0, and from 7.0 to 3.2, respectively. For a pH jump to 7.0 the intensity increases over several minutes, indicating the intensity is larger in the folded state. A time-dependent decrease was observed for unfolding following a pH jump from 7.0 to 3.2, showing that unfolding proceeds more rapidly than folding.

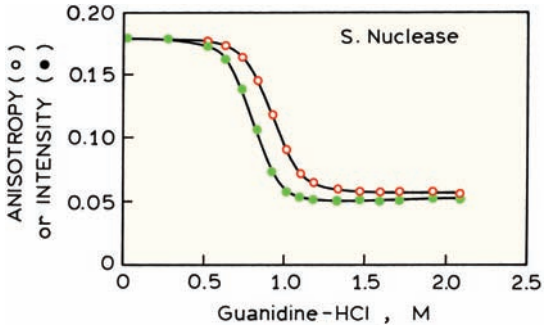

Figure 16.53. Unfolding of staphylococcal nuclease as observed by the steady-state intensity (●) or anisotropy (○). From [150].

Protein folding can be followed using fluorescence intensities, anisotropies, or lifetimes. It is important to recognize that the percent completion of the unfolding transitions may not be accurately represented by the percentage change in the lifetimes or anisotropies.[153] Suppose that the intensity and anisotropy both decrease when the protein is unfolded by denaturant. Then the folding transition seen by the anisotropy data will be weighted more toward the folded state than the unfolded state (Figure 16.53). A decrease in intensity was seen for unfolding of the staphylococcal nuclease. When the intensity decrease indicates unfolding is half complete, the anisotropy change is less than 50% because of the larger contribution of the folded state to the steady-state anisotropy. This is why the folding transition observed from the anisotropy data precedes that observed from the intensities (Figure 16.52, top). When performing measurements of protein folding it is important to remember that the anisotropy and mean lifetime are intensity-weighted parameters. For an intensity-weighted parameter the measured value depends on the relative fluorescence intensity of each state, as well as the fraction of the protein present in each state.

16.9.1. Protein Engineering of Mutant Ribonuclease for Folding Experiments

Since the classic refolding experiments of Christian Anfinsen on ribonuclease A (RNase A), this protein has been a favorite model for studies of protein folding. RNase A normally contains only tyrosine residues and no tryptophan. In order to create a unique probe to study folding,[158] a single-tryptophan residue was inserted at position 92. This position was chosen because, in the wild-type protein, the tyrosine residue at position 92 is hydrogen bonded to aspartate 38 (D38). This suggested the possibility that a tryptophan

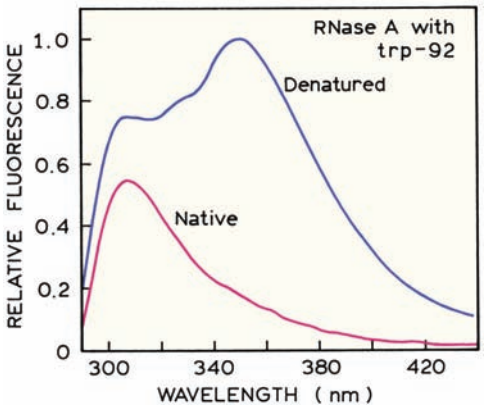

Figure 16.54. Emission spectra of the trp-92 mutant of RNase A in the native and denatured state at pH 5. Excitation at 280 nm. Revised from [158].

residue inserted at position 92 would be quenched by the nearby carboxyl group in the folded state.

Emission spectra of RNase A with the W92 insertion are shown in Figure 16.54. The excitation wavelength was 280 nm, so that both tyrosine and tryptophan are excited. The surprising feature of these spectra is that the relative tyrosine contribution is highest in the native protein. This is the opposite of what is observed for most proteins. This unusual result occurs because W92 is quenched in the folded state by the nearby aspartate residue. The large amount of quenching by D38 suggests the carboxyl group is in the protonated form, which is known to quench tryptophan.

16.9.2. Folding of Lactate Dehydrogenase

In order to determine the folding pathway it is important to examine multiple positions in a protein.[149,159] This is possible using mutant proteins. One example is the folding–unfolding transition of lactate dehydrogenase from *Bacillus stearothermophilus*. This protein typically contains three tryptophans that were replaced by tyrosines. Nine single-tryptophan mutants were produced with the residues dispersed throughout the protein matrix (Figure 16.55). These mutant proteins were studied in increasing concentrations of guanidium hydrochloride. Three of the nine unfolding curves are shown (Figure 16.56). The unfolding transitions occur at different denaturant concentrations for each of the

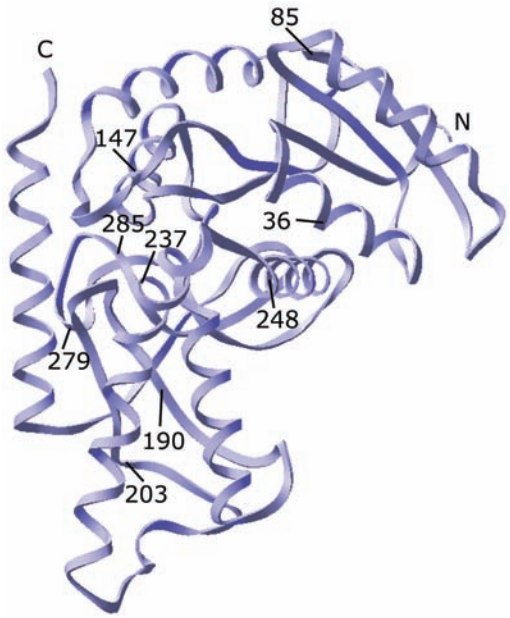

Figure 16.55. Positions of tryptophan probes in the lactate dehydrogenase subunit from *B. stearothermophilus*. The backbone of the protein is shown as a ribbon, and the positions of each single change of tyrosine to tryptophan are indicated by the residue number. Reprinted with permission from [149]. Copyright © 1991, American Chemical Society.

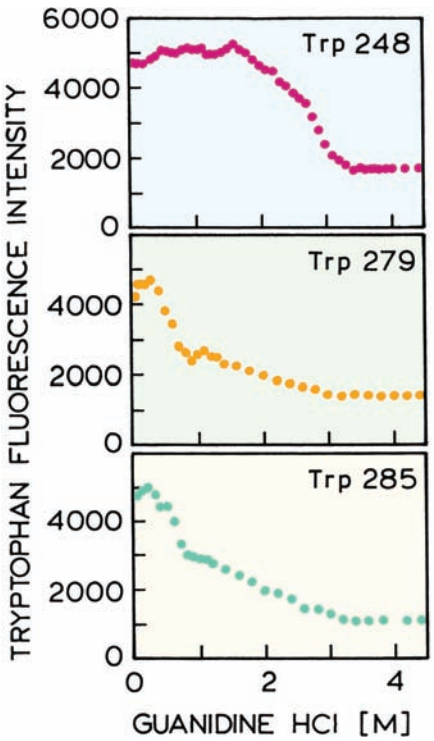

Figure 16.56. Equilibrium unfolding of a single-tryptophan mutants of lactate dehydrogenase monitored by tryptophan fluorescence intensity. Tryptophan fluorescence was excited at 295 nm and measured at 345 nm. Revised and reprinted with permission from [149]. Copyright © 1991, American Chemical Society.

three residues. For instance, the structure surrounding W248 persists to higher guanidium concentrations than the structured around residues W279 and W285. From such data it is possible to reconstruct which regions of the protein are more stable, and which are first disrupted during protein unfolding.

16.9.3. Folding Pathway of CRABPI

The folding pathway and kinetics can be studied using mutant proteins.[160–161] This was accomplished using cellular retinoic acid binding protein I (CRABPI). This protein has three tryptophan residues at positions 7, 87, and 109 (Figure 16.57). In the native state the emission spectra are strongly dependent on the excitation wavelength (not shown). This occurs because each of the tryptophan residues are present in different environments, and the absorption and emission spectra of the residues depend on the local environment. When the protein is denatured, the emission spectra becomes independent of the excitation wavelength because the three tryptophan residues are all in a similar environment.

CRABPI mutants were used to study refolding of the denatured protein. This was accomplished by initially denaturing the protein in urea. The urea was then rapidly diluted in a stopped-flow instrument, followed by measurement of the tryptophan emission (Figure 16.57). These traces show that the region surrounding W7 folds most rapidly, followed by folding of the regions around W87 and W109, which occurs several-fold more slowly.

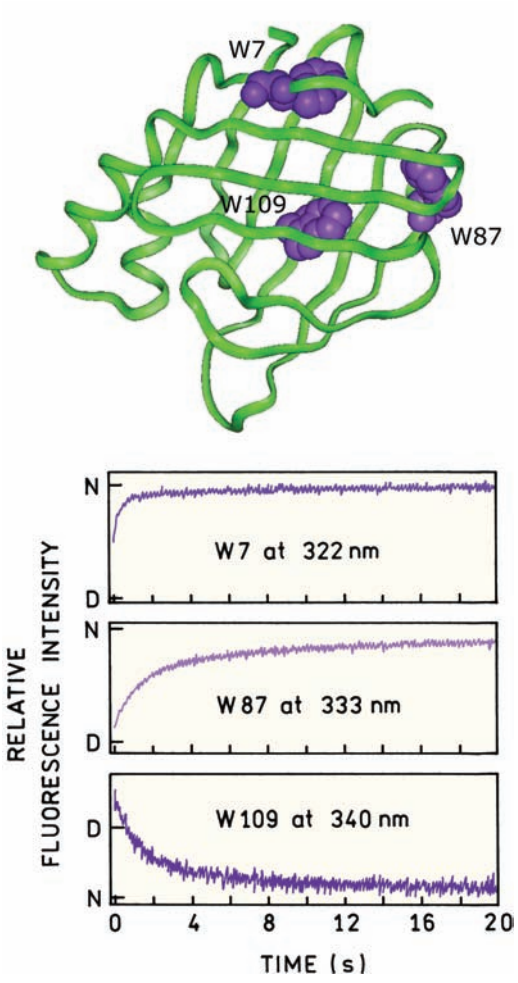

Figure 16.57. Structure (top) and refolding kinetics (bottom) of the three single-tryptophan mutants of CRABPI. Courtesy of Dr. Lila M. Gierasch from the University of Massachusetts.

16.10. PROTEIN STRUCTURE AND TRYPTOPHAN EMISSION

Numerous protein structures are known and it is now becoming possible to correlate the environment around the tryptophan residues with their spectral properties. One example is human antithrombin (Figure 16.58). Human antithrombin (AT) responds to heparin with a 200- to 300-fold increase in the rate of inhibition of clotting factor Xa. Wild-type AT contains four tryptophan residues. The contri-

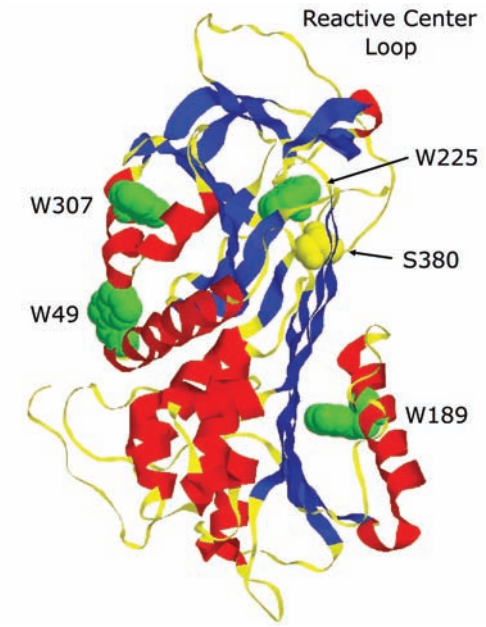

Figure 16.58. Structure of human antithrombin showing the four tryptophan residues and serine residue present in the wild-type protein. Courtesy of Dr. Peter G. W. Gettins from the University of Illinois.

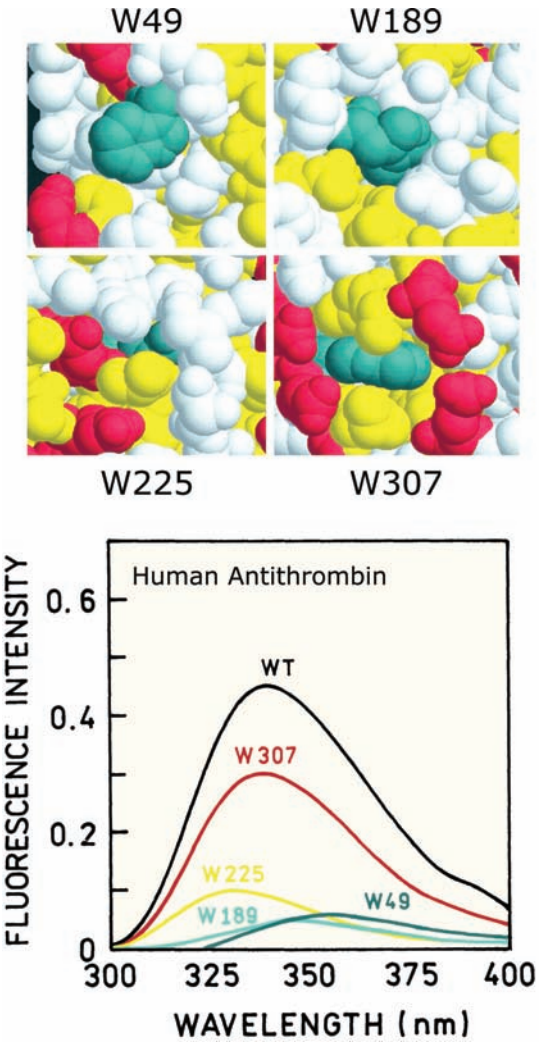

Figure 16.59. Emission spectra and local environment of each tryptophan residue in human antithrombin. Tryptophan is blue, acidic residues are red, hydrophobic residues are yellow and other residues are white. Revised from [162].

butions of each tryptophan to the total emission was determined indirectly using mutants, with a single tryptophan being substituted with phenylalanine.[162] Hence, each mutant protein contained three tryptophan residues. Since only a single mutation occurred in each protein it was more likely that AT retained its native structure than if more of the tryptophan residues were removed.

Figure 16.59 show the emission spectra recovered for each tryptophan residue in AT. These were not recorded directly but were calculated from the spectra of the mutants with three tryptophan residues. Also shown is a closeup image of each tryptophan residue as seen from outside the protein. The most exposed residue W49 has the longest-wavelength emission maximum, and the most buried residue W225 has the most blue-shifted emission. While this result may seem obvious it is only recently that such correlations of a detailed three-dimensional structure with emission spectra have been published.

Another example of correlating the structure and solvent exposure to the tryptophan emission maxima is shown in Figure 16.60. Adrenodoxin (Adx) is a 14-kD single-chain protein that plays a role in electron transport. Wild-type Adx does not contain any tryptophan residues, but contains one tyrosine and four phenylalanine residues (Figure 16.60). These aromatic residues were substituted one by one with tryptophan.[163] The closeup view of W11 shows it is buried in the protein and the closeup view of W82 shows it is on the surface of the protein. The emission spectra of these two mutants (Figure 16.61) correlate with the visual degree of exposure of each residue. The acrylamide quenching constants also correlate with the degree of exposure seen in Figure 16.60.

16.10.1. Tryptophan Spectral Properties and Structural Motifs

Intrinsic protein fluorescence with site-directed mutagenesis provides an opportunity to correlate the spectral properties of tryptophan with its location in a structural motif.[164–167] Such experiments can also provide a test of the similarity of a protein structure in solution and in a crystal. This type of experiment was performed using tear lipocalin (TL). This protein is found in tears. TL binds a wide range of hydrophobic molecules such as fatty acids, cholesterol, and phospholipids. The structure of lipocalin shows regions of α-helix and β-sheet, and regions of undefined structure (Figure 16.62). Wild-type lipocalin contains a single-tryptophan residue that was removed by making the W17Y mutant. Then about 150 mutant proteins were made with a single-tryptophan residue inserted sequentially along the sequence.[166-167]

Figure 16.63 shows the emission spectra of the mutants with tryptophan at positions 99 to 105. The emission maxima shift from shorter to longer wavelengths as the tryptophan is moved by one position along the peptide chain. Such an oscillating behavior is expected for a β-sheet structure. Lipocalin contains a β-sheet in this region. These mutant proteins were also analyzed using acrylamide quenching. The extents of quenching also oscillated with

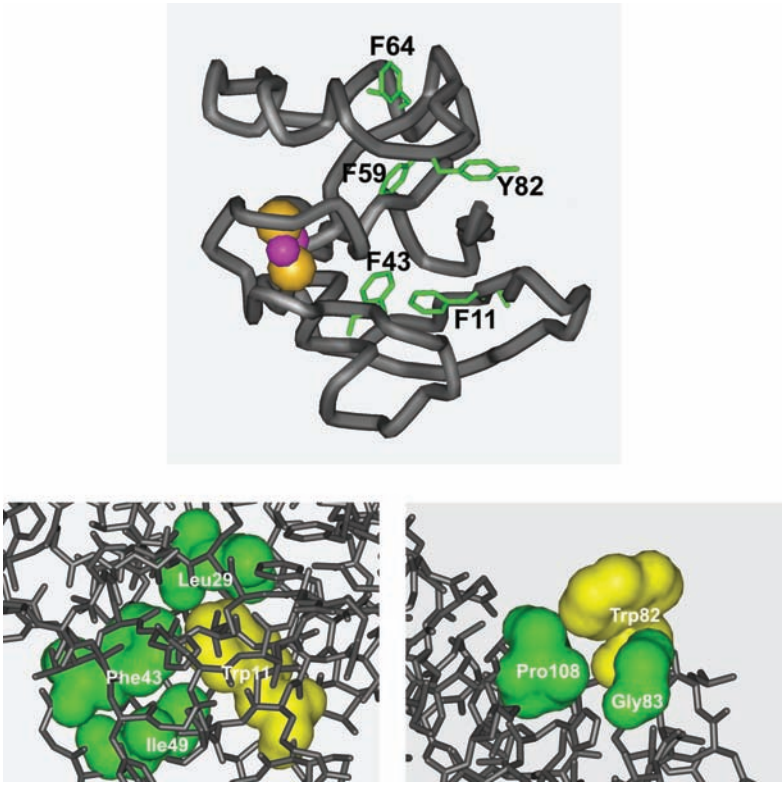

Figure 16.60. Structure of bovine adrenodoxin (top) and closeup views of W11 and W82 in the mutant proteins. Courtesy of Dr. Rita Bernhardt from Saarlandes University, Germany.

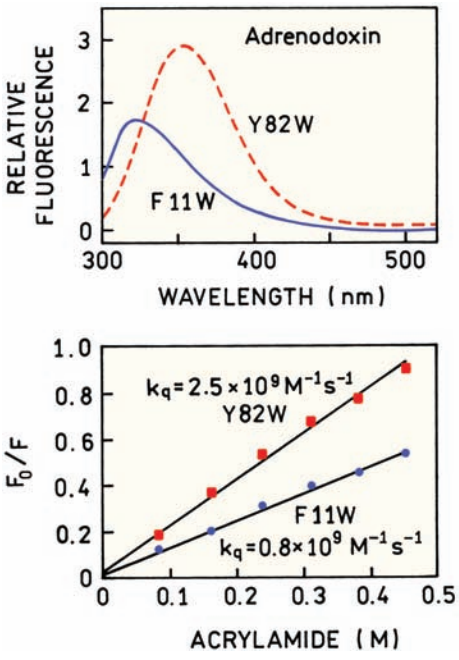

Figure 16.61. Emission spectra and acrylamide Stern-Volmer plots for adrenodoxin mutants F11W and Y82W. Revised from [163].

each step along the sequence (Figure 16.64). Hence, residues from positions 94 to 105 are alternately exposed or shielded from the solvent.

Figure 16.65 shows a summary of the tryptophan emission maxima for about 150 mutants. Also indicated are regions of α-helical and β-sheet structure. In β-sheet regions the emission maxima oscillate with each step along the sequence. For the α-helical region the emission maxima oscillates with a periodicity of about 3.6 residues per cycle. These data showed a close correlation between tryptophan emission and the x-ray structures of lipocalin.

16.11. TRYPTOPHAN ANALOGUES

Advanced Topic

For calmodulin and other tyrosine-only proteins a genetically inserted tryptophan residue can serve as a useful probe. However, most proteins contain several tryptophan residues that must all be removed to selectively observe the inserted tryptophan. It is useful to have tryptophan analogues that could be selectively observed in the presence of tryptophan-containing proteins. This can be accomplished

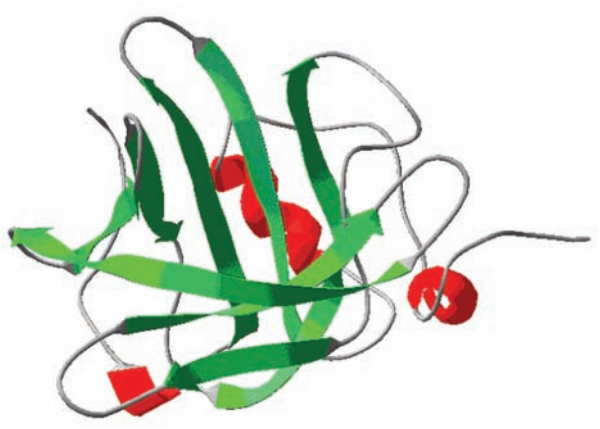

Figure 16.62. Structure of tear lipocalin. Red indicates α-helical structure, green is β-sheet and grey is undefined structure. Courtesy of Dr. Ben J. Glasgow from the University of California, Los Angeles.

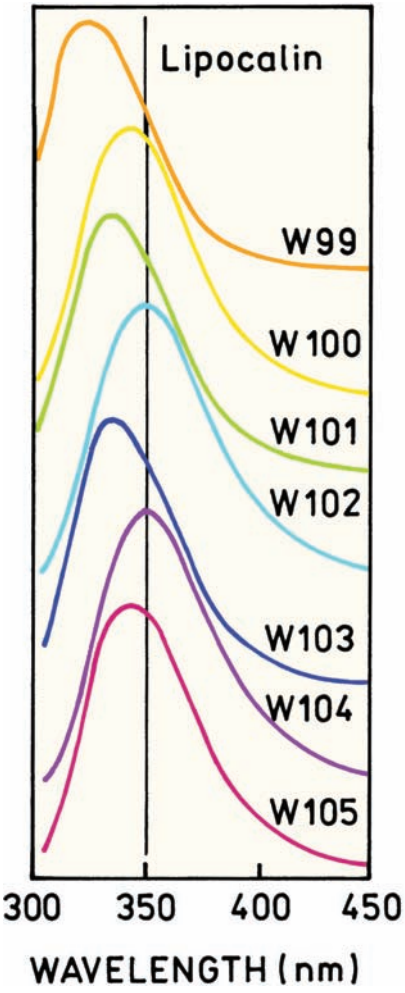

Figure 16.63. Emission spectra of tear lipocalin with single-tryptophan insertions. Revised from [166].

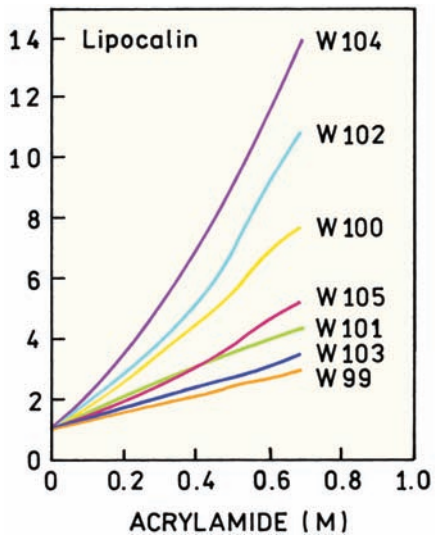

Figure 16.64. Acrylamide quenching of lipocalin with single-tryptophan insertions. Revised from [166].

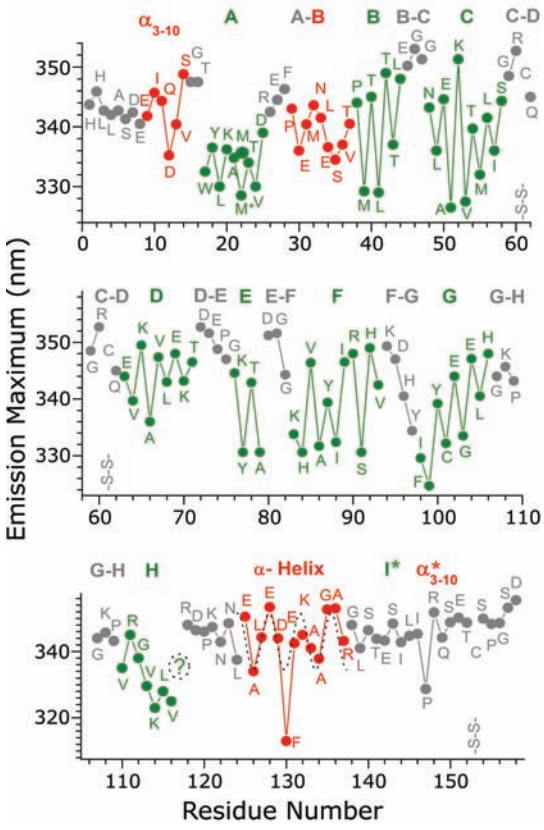

Figure 16.65. Emission maxima of lipocalin with single-tryptophan insertions. The letters indicate the amino acid in the wild-type protein. Red indicates α-helix, green indicates β-sheet, and grey indicates undefined structure. Courtesy of Dr. Ben J. Glasgow from the University of California, Los Angeles.

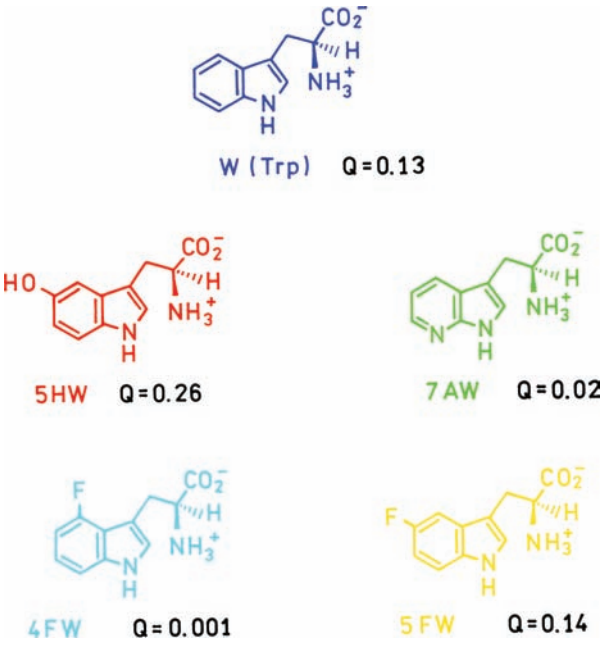

Figure 16.66. Structures of tryptophan analogues. The numbers under the structures are the quantum yields in neutral buffer [168].

using tryptophan or amino-acid analogues that absorb at longer wavelengths than tryptophan. These analogues must be inserted into the protein sequence. This can be accomplished in three ways. The entire protein can be synthesized de novo. However, this approach is limited to small peptides and proteins that will fold spontaneously after synthesis. The second approach is by incorporation into protein grown in bacteria or a cell-free system. This is typically done using tryptophan auxotrophs, which cannot synthesize their own tryptophan. The amino-acid analogue is chemically attached to the tRNA, which is then added to the sample during protein synthesis. The inserted amino acids are typically selected to have a structure similar to tryptophan. The third and most elegant approach is modification of the genetic code and protein synthesis machinery to include a new amino acid.

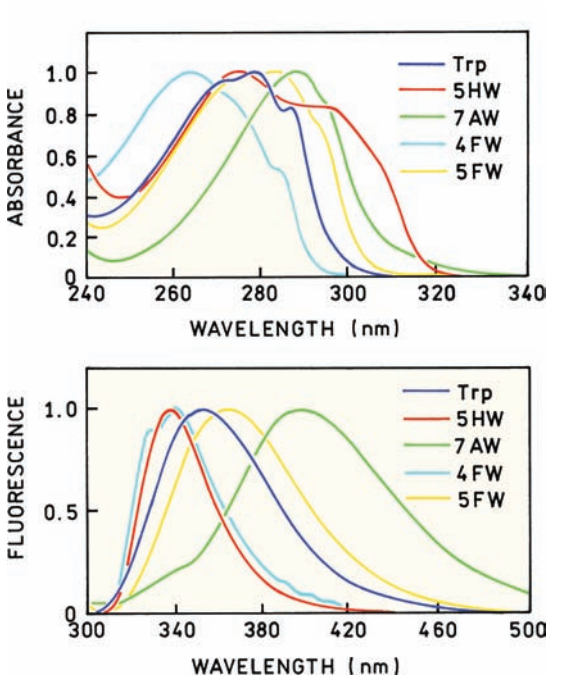

Figure 16.67. Absorption (top) and emission spectra (bottom) of tryptophan analogues. Revised from [168].

16.11.1. Tryptophan Analogues

A group of tryptophan analogues have been synthesized and incorporated into proteins using tryptophan auxotrophs[168–181] (Figure 16.66). These analogues were designed to retain a size close to tryptophan itself. Except for 4-fluorotryptophan (4FW) these analogues absorb at longer wavelengths than tryptophan (Figure 16.67).

The spectral properties of 5HW and 7AW are different from tryptophan.[178] In water, 5HW displays a higher quantum yield than tryptophan (0.275 for 5HW versus 0.13 for W). 5HW is less sensitive to solvent polarity than tryptophan, and displays an emission maximum near 339 nm (Figure 16.67). The quantum yield of 7AW is highly dependent on solvent polarity and decreases upon contact with water.[182] In water its quantum yield is low, near 0.017, with an emission maximum near 403 nm. This property of 7AW is somewhat problematic. The use of 7AW was originally proposed as an alternative to tryptophan because 7AW was thought to display a simple single exponential decay.[183–184] Unfortunately, 7AW and azaindole display complex decay kinetics due to the presence of several solvated states.[185–187] A non-exponential decay has also been observed for an octapeptide that contains a 7AW residue.[188] 7AW is a useful tryptophan analogue, but it can display complex decay kinetics.

These tryptophan analogues have been incorporated into a number of proteins. One example is substitution of 5HW and 7AW for the single-tryptophan residue in staphylococcal nuclease (Figure 16.68). In this case the emission maxima of tryptophan and 5HW are similar. The advantages of 5HW and 7AW can be seen by their use in studies of more complex biochemical mixtures. 5HW was used to replace the tyrosine residue in insulin. This allowed the fluorescence of 5HW-insulin to be used to study its binding to

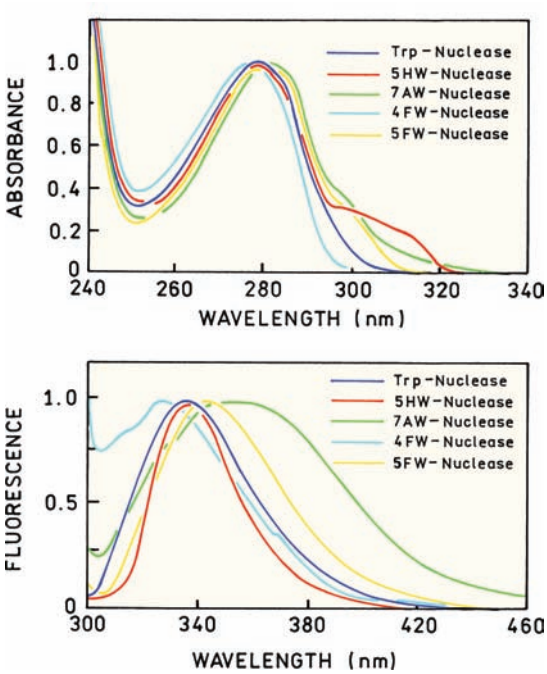

Figure 16.68. Absorption and emission spectra of wild-type staphylococcal nuclease (W140) and mutant proteins when W140 is replaced with a tryptophan analogue. Revised from [168].

the insulin receptor.[179] Such studies would not be possible using the tyrosine fluorescence of insulin because this emission is masked by the tryptophan emission of the insulin receptor protein. 5HW has proven valuable in measuring an antigen–antibody association.[173] 5HW was incorporated into the calcium-binding protein oncomodulin. Binding of

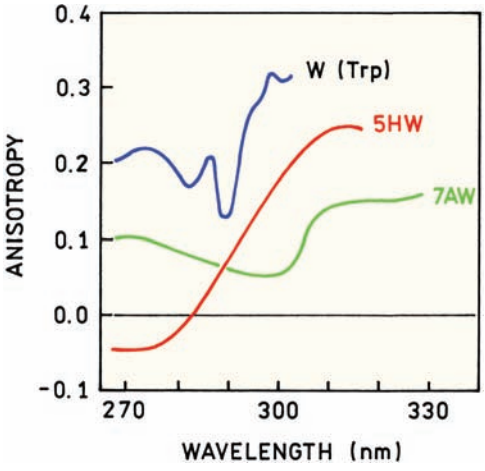

Figure 16.69. Low-temperature excitation anisotropy spectra of tryptophan, 5HW, and 7AW in 50% glycerol-phosphate buffer, 77°K. Revised and reprinted with permission from [178]. Copyright © 1997, Cambridge University Press.

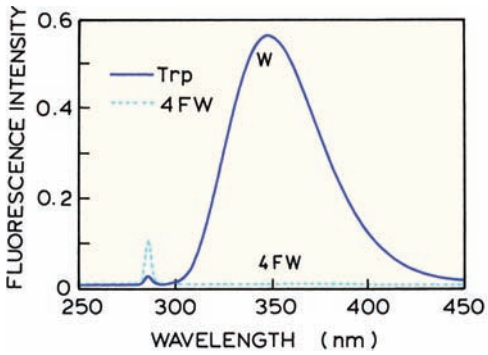

Figure 16.70. Relative fluorescence spectra in aqueous solution of tryptophan (solid) and 4-fluorotryptophan (dashed) at 25°C and 285-nm excitation. Revised from [189].

this protein to antibodies could be detected even though the antibody possessed numerous tryptophan residues.

These tryptophan analogues can be used to study protein association reactions, which are often studied using anisotropy measurements. For these purposes it is valuable to know the excitation anisotropy spectra. The anisotropy of both analogues is lower than that of tryptophan itself (Figure 16.69). The low anisotropy of 7AW is another indication of its complex spectral properties.

Another useful tryptophan analogue is 4-fluorotryptophan (4FW). This analogue is useful because it has a similar size and shape as tryptophan, but is almost nonfluorescent (Figure 16.70).[189] This analogue provides a means to eliminate the emission from a tryptophan while retaining almost the same size and shape.

16.11.2. Genetically Inserted Amino-Acid Analogues

During the past several years, a new method appeared to incorporating non-natural amino acids into proteins. This is accomplished by identifying a unique tRNA and aminoacyl-tRNA synthetase that will act independently of the other tRNAs and other enzymes.[190–195] In some cases an unused three-base codon is used, and in other cases a unique four-base codon is used.[196–198] This approach is general and can introduce a variety of amino-acid analogues, some of which are shown in Figure 16.71.

This approach was used to introduce amino-acid analogues into streptavidin.[199–200] Figure 16.72 shows the structure of a single subunit of streptavidin showing the portion of the mchAla or the 2,6-dnsAF analogues. These amino-acid analogues can be excited at wavelengths longer than

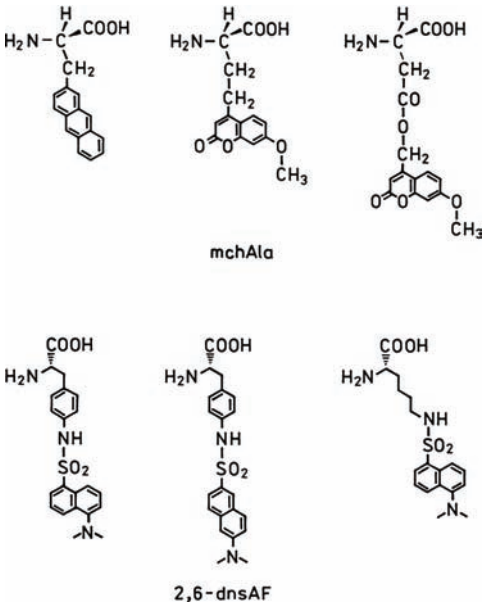

Figure 16.71. Amino-acid analogues inserted using a modified genetic code. From [196–200].

320 nm so that intrinsic tryptophans do not interfere with this probe. The mutant streptavidin with mchAla showed a change in emission intensity upon binding biotin (Figure 16.73). Streptavidin was also synthesized with the anthracene-like amino acid, yielding an unusual protein with the emission of anthracene. It seems probable that these methods for synthesis of labeled proteins will become more widely used as the methodology becomes more available.

16.12. THE CHALLENGE OF PROTEIN FLUORESCENCE

The intrinsic fluorescence of proteins represents a complex spectroscopic challenge. At the initial level one has to deal with multiple fluorophores with overlapping absorption and emission spectra. The presence of multiple fluorophores is itself a significant challenge. However, the actual situation is still more complex. The dominant fluorophore tryptophan displays complex spectral properties due to the presence of two overlapping electronic states. It is now accepted that

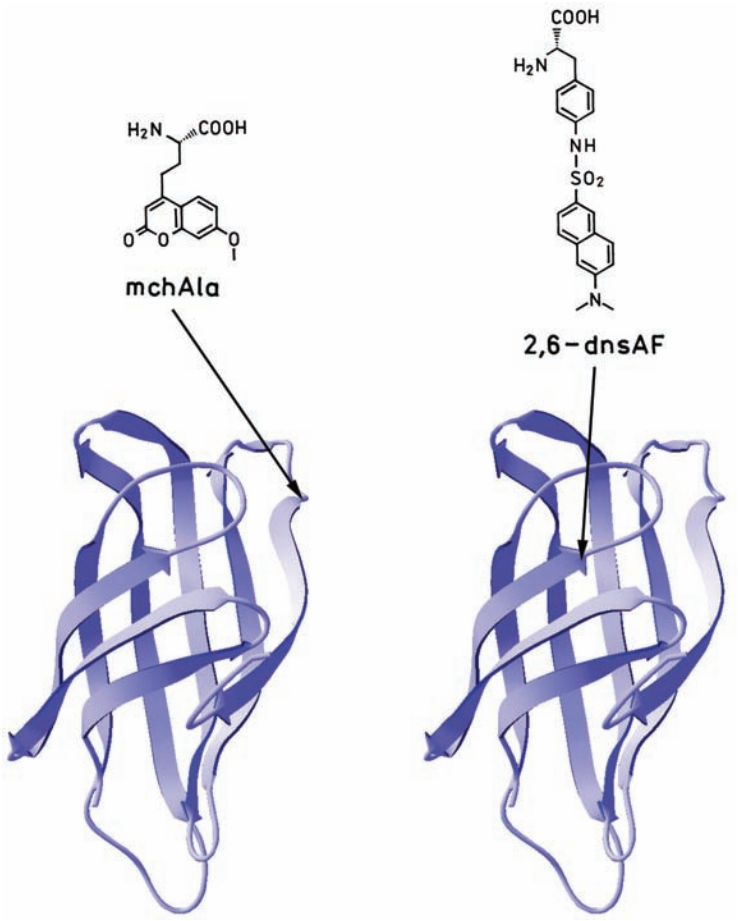

Figure 16.72. Structures of streptavidin containing mchAla at position 120 or streptavidin with 2,6-dnsAF at position 44. From [199–200].

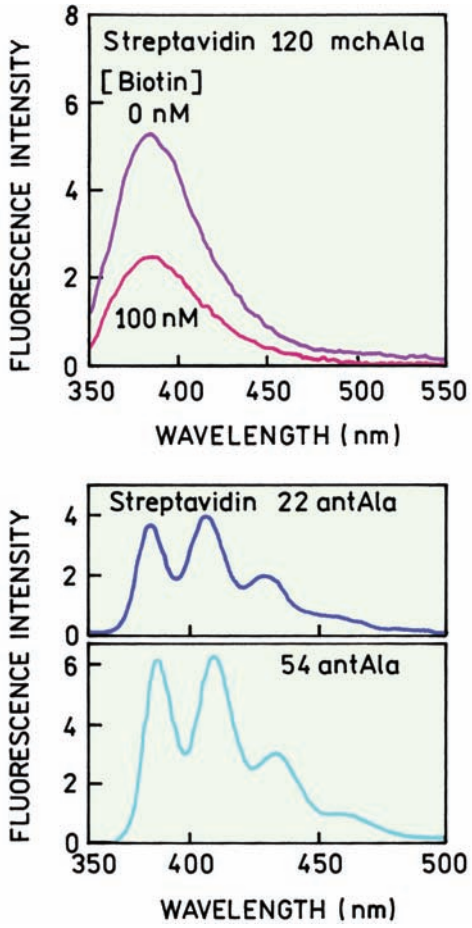

Figure 16.73. Emission spectra of streptavidin containing amino-acid analogue. Revised from [199]. Insert shows structure of streptavidin containing mchAla (red) with bound biotin (purple).

even for single-tryptophan proteins the emission often contains multiple spectral contributions due to either multiple conformations or the intrinsic heterogeneity of tryptophan itself. Tryptophan is uniquely sensitive to a variety of quenchers, many of which are present in proteins. Tryptophan is also sensitive to quenching by nearby peptide bonds. Small motions of the amino-acid side chains or backbone can apparently result in changes in tryptophan emission, and some of these motions may occur during the excited-state lifetime. And, finally, the fluorescent amino acids in proteins can interact by energy transfer. In some cases a quenched tryptophan residue can serve as a trap for normally fluorescent residues. Such effects will be highly sensitive to the conformation of the proteins and relative orientation of the fluorescent amino acids.

Given the complexity of tryptophan fluorescence, it is not surprising that the details remained elusive from studies of multi-tryptophan proteins. It was recognized that tryptophan could be quenched by nearby groups and that energy transfer could occur. However, it was not until the availability of engineered proteins of known structure that we were able to identify convincing examples of these phenomena.

REFERENCES

1. Brand L, Johnson ML, eds. 1997. *Methods in enzymology*, Vol. 278: *Fluorescence spectroscopy*. Academic Press, San Diego.
2. Ladokhin AS. 2000. Fluorescence spectroscopy in peptide and protein analysis. In *Encyclopedia of analytical chemistry*, pp. 5762–5779. Ed RA Meyers. John Wiley & Sons, New York.
3. Engelborghs Y. 2001. The analysis of time-resolved protein fluorescence in multi-tryptophan proteins. *Spectrochim Acta, Part A* **57**: 2255–2270.
4. Ladokhin AS, Jayasinghe S, White SH. 2000. How to measure and analyze tryptophan fluorescence in membranes properly, and why bother. *Anal Biochem* **285**:235–245.
5. Weinryb I, Steiner RF. 1971. The luminescence of the aromatic amino acids. In *Excited states of proteins and nucleic acids*, pp. 277–318. Ed RF Steiner, I Weinryb. Plenum Press, New York.
6. Demchenko AP. 1981. *Ultraviolet spectroscopy of proteins*. Springer-Verlag, New York.
7. Konev SV. 1967. *Fluorescence and phosphorescence of proteins and nucleic acids*. Plenum Press, New York.
8. Permyakov EA. 1993. *Luminescent spectroscopy of proteins*. CRC Press, Boca Raton, FL.
9. Longworth JW. 1983. Intrinsic fluorescence of proteins. In *Time-resolved fluorescence spectroscopy in biochemistry and biology*, pp. 651–778. Ed RB Cundall, RE Dale. Plenum Press, New York.
10. Chen RF. 1967. Fluorescence quantum yields of tryptophan and tyrosine. *Anal Lett* **1**(1):35–42.
11. Lakowicz JR, Maliwal BP. 1983. Oxygen quenching and fluorescence depolarization of tyrosine residues in proteins. *J Biol Chem* **258**(8):4794–4801.
12. Weber G. 1960. Fluorescence polarization spectrum and electronic-energy transfer in tyrosine, tryptophan, and related compounds. *Biochem J* **75**:335–345.
13. Weber G. 1966. Polarization of the fluorescence of solutions. In *Fluorescence and phosphorescence analysis*, pp. 217–240. Ed DM Hercules. Wiley Interscience, New York.
14. Noronha M, Lima JC, Lamosa P, Santos H, Maycock C, Ventura R, Macanita AL. 2004. Intramolecular fluorescence quenching of tyrosine by the peptide α-carbonyl group revisited. *J Phys Chem A* **108**: 2155–2166.
15. Guzow K, Ganzynkowicz R, Rzeska A, Mrozek J, Szabelski M, Karolczak J, Liwo A, Wiczk W. 2004. Photophysical properties of tyrosine and its simple derivatives studied by time-resolved fluorescence spectroscopy, global analysis, and theoretical calculations. *J Phys Chem B* **108**:3879–3889.
16. Ross JBA, Laws WR, Rousslang KW, Wyssbrod HR. 1992. Tyrosine fluorescence and phosphorescence from proteins and polypeptides. In *Topics in fluorescence spectroscopy*, Vol. 3: *Biochemical applications*, pp. 1–63. Ed JR Lakowicz. Plenum Press, New York.

17. Lakowicz JR, Maliwal BP, Cherek H, Balter A. 1983. Rotational freedom of tryptophan residues in proteins and peptides. *Biochemistry* **22**:1741–1752.
18. Eftink MR, Selvidge LA, Callis PR, Rehms AA. 1990. Photophysics of indole derivatives: experimental resolution of ^1L_a and ^1L_b transitions and comparison with theory. *J Phys Chem* **94**:3469–3479.
19. Yamamoto Y, Tanaka J. 1972. Polarized absorption spectra of crystals of indole and its related compounds. *Bull Chem Soc Jpn* 4**5**: 1362–1366.
20. Song P-S, Kurtin WE. 1969. A spectroscopic study of the polarized luminescence of indole. *J Am Chem Soc* **91**:4892–4906.
21. Albinsson B, Kubista M, Norden B, Thulstrup EW. 1989. Near-ultraviolet electronic transitions of the tryptophan chromophore: linear dichroism, fluorescence anisotropy, and magnetic circular dichroism spectra of some indole derivatives. *J Phys Chem* **93**:6646–6655.
22. Albinsson B, Norden B. 1992. Excited-state properties of the indole chromophore: electronic transition moment directions from linear dichroism measurements—effect of methyl and methoxy substituents. *J Phys Chem* **96**:6204–6212.
23. Callis PR. 1997. ^1L_a and ^1L_b transitions of tryptophan: applications of theory and experimental observations to fluorescence of proteins. *Methods Enzymol* **278**:113–150.
24. Valeur B, Weber G. 1977. Resolution of the fluorescence excitation spectrum of indole into the ^1L_a and ^1L_b excitation bands. *Photochem Photobiol* **25**:441–444.
25. Rayner DM, Szabo AG. 1977. Time-resolved fluorescence of aqueous tryptophan. *Can J Chem* **56**:743–745.
26. Petrich JW, Chang MC, McDonald DB, Fleming GR. 1983. On the origin of nonexponential fluorescence decay in tryptophan and its derivatives. *J Am Chem Soc* **105**:3824–3832.
27. Creed D. 1984. The photophysics and photochemistry of the near-UV absorbing amino acids, I: tryptophan and its simple derivatives. *Photochem Photobiol* **39**(4):537–562.
28. Fleming GR, Morris JM, Robbins RJ, Woolfe GJ, Thistlewaite PJ, Robinson GW. 1978. Nonexponential fluorescence decay of aqueous tryptophan and two related peptides by picosecond spectroscopy. *Proc Natl Acad Sci USA* **75**:4652–4656.
29. Gryczynski I, Wiczk W, Johnson ML, Lakowicz JR. 1988. Lifetime distributions and anisotropy decays of indole fluorescence in cyclohexane/ethanol mixtures by frequency-domain fluorometry. *Biophys Chem* **32**:173–185.
30. Walker MS, Bednar TW, Lumry R. 1966. Exciplex formation in the excited state. *J Chem Phys* 45:3455–3456.
31. Hershberger MV, Lumry R, Verral R. 1981. The 3-methylindole/n-butanol exciplex: evidence for two exciplex sites in indole compounds. *Photochem Photobiol* **33**:609–617.
32. Strickland EH, Horwitz J, Billups C. 1970. Near-ultraviolet absorption bands of tryptophan: studies using indole and 3-methylindole as models. *Biochemistry* **9**(25):4914–4920.
33. Lasser N, Feitelson J, Lumry R. 1977. Exciplex formation between indole derivatives and polar solutes. *Isr J Chem* **16**:330–334.
34. Sun M, Song P-S. 1977. Solvent effects on the fluorescent states of indole derivatives-dipole moments. *Photochem Photobiol* **25**:3–9.
35. Lami H, Glasser N. 1986. Indole's solvatochromism revisited. *J Chem Phys* **84**(2):597–604.
36. Pierce DW, Boxer SG. 1995. Stark effect spectroscopy of tryptophan. *Biophys J* **68**:1583–1591.
37. Callis PR, Burgess BK. 1997. Tryptophan fluorescence shifts in proteins from hybrid simulations: an electrostatic approach. *J Phys Chem B* **101**:9429–9432.
38. Strickland EH, Billups C, Kay E. 1972. Effects of hydrogen bonding and solvents upon the tryptophanyl ^1L_a absorption band: studies using 2,3-dimethylindole. *Biochemistry* **11**(19):3657–3662.
39. Van Duuren BL. 1961. Solvent effects in the fluorescence of indole and substituted indoles. *J Org Chem* **26**:2954–2960.
40. Willis KJ, Szabo AG. 1991. Fluorescence decay kinetics of tyrosinate and tyrosine hydrogen-bonded complexes. *J Phys Chem* **95**:1585–1589.
41. Willis KJ, Szabo AG, Krajcarski DT. 1990. The use of Stokes Raman scattering in time correlated single photon counting: application to the fluorescence lifetime of tyrosinate. *Photochem Photobiol* **51**: 375–377.
42. Rayner DM, Krajcarski DT, Szabo AG. 1978. Excited-state acid–base equilibrium of tyrosine. *Can J Chem* **56**:1238–1245.
43. Pal H, Palit DK, Mukherjee T, Mittal JP. 1990. Some aspects of steady state and time-resolved fluorescence of tyrosine and related compounds. *J Photochem Photobiol A: Chem* **52**:391–409.
44. Shimizu O, Imakuvo K. 1977. New emission band of tyrosine induced by interaction with phosphate ion. *Photochem Photobiol* **26**: 541–543.
45. Dietze EC, Wang RW, Lu AYH, Atkins WM. 1996. Ligand effects on the fluorescence properties of tyrosine-9 in alpha 1-1 glutathione S-transferase. *Biochemistry* **35**:6745–6753.
46. Behmaarai TA, Toulme JJ, Helene C. 1979. Quenching of tyrosine fluorescence by phosphate ions: a model study for protein-nucleic acid complexes. *Photochem Photobiol* **30**:533–539.
47. Schnarr M, Helene C. 1982. Effects of excited-state proton transfer on the phosphorescence of tyrosine-phosphate complexes. *Photochem Photobiol* **36**:91–93.
48. Szabo A, Lynn KR, Krajcarski DT, Rayner DM. 1978. Tyrosinate fluorescence maxima at 345 nm in proteins lacking tryptophan at pH 7. *FEBS Lett* **94**:249–252.
49. Prendergast FG, Hampton PD, Jones B. 1984. Characteristics of tyrosinate fluorescence emission in α- and β-purothionins. *Biochemistry* **23**:6690–6697.
50. Libertini LJ, Small EW. 1985. The intrinsic tyrosine fluorescence of histone H1. *Biophys J* **47**:765–772.
51. Ruan K, Li J, Liang R, Xu C, Yu Y, Lange R, Balny C. 2002. A rare protein fluorescence behavior where the emission is dominated by tyrosine: case of the 33-kDA protein from spinach photosystem II. *Biochem Biophys Res Commun* **293**:593–597.
52. Pundak S, Roche RS. 1984. Tyrosine and tyrosinate fluorescence of bovine testes calmodulin calcium and pH dependence. *Biochemistry* **23**:1549–1555.
53. Longworth JW. 1971. Luminescence of polypeptides and proteins. In *Excited states of proteins and nucleic acids*, pp. 319–484. Ed RF Steiner, I Weinryb. Plenum Press, New York.
54. Kronman MJ, Holmes LG. 1971. The fluorescence of native, denatured and reduced denatured proteins. *Photochem Photobiol* **14**:113–134.
55. Burstein EA, Vedenkina NS, Ivkova MN. 1974. Fluorescence and the location of tryptophan residues in protein molecules. *Photochem Photobiol* 18:263–279.

56. Burstein EA, Abornev SM, Reshetnyak YK. 2001. Decomposition of protein tryptophan fluorescence spectra into log-normal components, I: decomposition algorithms. *Biophys J* **81**:1699–1709.
57. Reshetnyak YK, Burstein EA. 2001. Decomposition of protein tryptophan fluorescence spectra into log-normal components, II: the statistical proof of discreteness of tryptophan classes in proteins. *Biophys J* 81:1710–1734.
58. Reshetnyak YK, Koshevnik Y, Burstein EA. 2001. Decomposition of protein tryptophan fluorescence spectra into log-normal components, III: correlation between fluorescence and microenvironment parameters of individual tryptophan residues. *Biophys J* **81**:1735–1758.
59. Eftink MR. 1990. Fluorescence techniques for studying protein structure. *Methods Biochem Anal* **35**:117–129.
60. Burstein EA. 1976. Luminescence of protein chromophores. In *Model studies: science and technology results*, Vol. 6: *Biophysics*, VINITI, Moscow.
61. Vivian JT, Callis P. 2001. Mechanisms of tryptophan fluorescence shifts in proteins. *Biophys J* **80**:2093–2109.
62. Callis FR, Liu T. 2004. Quantitative prediction of fluorescence quantum yields for tryptophan in proteins. *J Phys Chem B* **108**:4248–4259.
63. Callis PR, Vivian JT. 2003. Understanding the variable fluorescence quantum yield of tryptophan in proteins using QM-MM simulations: quenching by charge transfer to the peptide backbone. *Chem Phys Lett* **369**:409–414.
64. Ababou A, Bombarda E. 2001. On the involvement of electron transfer reactions in the fluorescence decay kinetics heterogeneity of proteins. *Protein Sci* **10**:2102–2113.
65. Adams PD, Chen Y, Ma K, Zagorski M, Sonnichsen FD, McLaughlin ML, Barkley MD. 2002. Intramolecular quenching of tryptophan fluorescence by the peptide bond in cyclic hexapeptides. *J Am Chem Soc* **124**:9278–9286.
66. Chen Y, Barkley MD. 1998. Toward understanding tryptophan fluorescence in proteins. *Biochemistry* **37**:9976–9982.
67. Chen Y, Liu B, Yu H-T, Barkley MD. 1996. The peptide bond quenches indole fluorescence. *J Am Chem Soc* **118**:9271–9278.
68. Eftink MR, Ghiron CA. 1984. Indole fluorescence quenching studies on proteins and model systems: use of the inefficient quencher succinimide. *Biochemistry* **23**:3891–3899.
69. Froehlich PM, Gantt D, Paramasigamani V. 1977. Fluorescence quenching of indoles by *N*,*N*-dimethylformamide. *Photochem Photobiol* **26**:639–642.
70. Froehlich PM, Nelson K. 1978. Fluorescence quenching of indoles by amides. *J Phys Chem* **82**(22):2401–2403.
71. Finazzi-Agro A, Rotilio G, Avigliano L, Guerrieri P, Boffi V, Mondovi B. 1970. Environment of copper in *Pseudomonas fluorescens* azurin: fluorometric approach. *Biochemistry* **9**(9):2009–2014.
72. Burstein EA, Permyakov EA, Yashin VA, Burkhanov SA, Agro AF. 1977. The fine structure of luminescence spectra of azurin. *Biochim Biophys Acta* **491**:155–159.
73. Szabo AG, Stepanik TM, Wayner DM, Young NM. 1983. Conformational heterogeneity of the copper binding site in azurin. *Biophys J* **41**:233–244.
74. Fuentes L, Oyola J, Fernández M, Quiñones E. 2004. Conformational changes in azurin from *Pseudomonas aeruginosa* induced through chemical and physical protocols. *Biophys J* **87**: 1873–1880.
75. Adman ET, Jensen LH. 1981. Structural features of azurin at 2.7 Å resolution. *Isr J Chem* **21**:8–12.
76. Aueuhel FM, Brent R, Kingston RE, Moore DD, Seidman JG, Smith JA, Struhl K, eds. 1987. *Current protocols in molecular biology*. John Wiley & Sons, New York, (see chapter 8).
77. Sambrook J, Fritsch EF, Maniatis T. 1989. *Molecular cloning*, chap. 15. Cold Spring Harbor Laboratory Press, Plainview, NY.
78. Gilardi G, Mei G, Rosato N, Canters GW, Finazzi-Agro A. 1994. Unique environment of Trp48 in *Pseudomonas aeruginosa* azurin as probed by site-directed mutagenesis and dynamic fluorescence anisotropy. *Biochemistry* **33**:1425–1432.
79. Petrich JW, Longworth JW, Fleming GR. 1987. Internal motion and electron transfer in proteins: a picosecond fluorescence study of three homologous azurins. *Biochemistry* **26**:2711–2722.
80. Lakowicz JR, Cherek H, Gryczynski I, Joshi N, Johnson ML. 1987. Enhanced resolution of fluorescence anisotropy decays by simultaneous analysis of progressively quenched samples. *Biophys J* **51**: 755–768.
81. Georghiou S, Thompson M, Mukhopadhyay AK. 1982. Melittin-phospholipid interaction studied by employing the single-tryptophan residue as an intrinsic fluorescent probe. *Biochim Biophys Acta* **688**: 441–452.
82. Searcy DG, Montenay-Garestier T, Helene C. 1989. Phenylalanine-to-tyrosine singlet energy transfer in the archaebacterial histone-like protein HTa. *Biochemistry* **28**:9058–9065.
83. Kupryszewska M, Gryczynski I, Kawski A. 1982. Intramolecular donor–acceptor separations in methionine- and leucine-enkephalin estimated by long-range radiationless transfer of singlet excitation energy. *Photochem Photobiol* **36**:499–502.
84. Gryczynski I, Kawski A, Darlak K, Grzonka Z. 1985. Intramolecular electronic excitation energy transfer in dermorphine and its analogues. *J Photochem* **30**:371–377.
85. Eisinger J. 1969. Intramolecular energy transfer in adrenocorticotropin. *Biochemistry* **8**:3902–3908.
86. Moreno MJ, Prieto M. 1993. Interaction of the peptide hormone adrenocorticotropin, ACTH(1-24), with a membrane model system: a fluorescence study. *Photochem Photobiol* **57**(3):431–437.
87. Pearce SF, Hawrot E. 1990. Intrinsic fluorescence of binding-site fragments of the nicotinic acetylcholine receptor: perturbations produced upon binding α-bungarotoxin. *Biochemistry* **29**:10649–10659.
88. Schiller PW. 1983. Fluorescence study on the conformation of a cyclic enkephalin analogue in aqueous solution. *Biochem Biophy Res Commun* 114(1):268–274.
89. Alfimova EYa, Likhtenstein GI. 1976. Fluorescence study of energy transfer as method of study of protein structure. *Mol Biol (Moscow)* **8**(2):127–179.
90. Boteva R, Zlateva T, Dorovska-Taran V, Visser AJWG, Tsanev R, Salvato B. 1996. Dissociation equilibrium of human recombinant interferon γ. *Biochemistry* **35**:14825–14830.
91. Eisenhawer M, Cattarinussi S, Kuhn A, Vogel H. 2001. Fluorescence resonance energy transfer shows a close helix–helix distance in the transmembrane M13 procoat protein. *Biochemistry* **40**:12321–12328.
92. Lankiewicz L, Stachowiak K, Rzeska A, Wiczk W. 1999. Photophysics of sterically constrained phenylalanines. In *Peptide science—present and future*, pp. 168–170. Ed Y Shimonishi. Kluwer, New York.

93. Vanscyoc WS, Shea MA. 2001. Phenylalanine fluorescence studies of calcium binding to N-domain fragments of *paramecium* calmodulin mutants show increased calcium affinity correlates with increased disorder. *Protein Sci* **10**:1758–1768.
94. VanScyoc WS, Sorensen BR, Rusinova E, Laws WR, Ross JBA, Shea MA. 2002. Calcium binding to calmodulin mutants monitored by domain-specific intrinsic phenylalanine and tyrosine fluorescence. *Biophys J* **83**:2767–2780.
95. Burshtein EA. 1996. Resolution of the fluorescence spectra by the degree of accessibility to quenchers. *Biophysics* **41**(1):235–239.
96. Raja SM, Rawat SS, Chattopadhyay A, Lata AK. 1999. Localization and environment of tryptophans in soluble and membrane-bound states of a pore-forming toxin from *Staphylococcus aureus*. *Biophys J* **76**:1469–1479.
97. Rausell C, Munoz-Garay C, Miranda-Casso Luengo R, Gomez I, Rudino-Pinera E, Soberon M, Bravo A. 2004. Tryptophan spectroscopy studies and black lipid bilayer analysis indicate that the oligomeric structure of Cry1Ab toxin from *bacillus thuringiensis* is the membrane-insertion intermediate. *Biochemistry* **43**:166–174.
98. Weber J, Senior AE. 2000. Features of F_1-ATPase catalytic and noncatalytic sites revealed by fluorescence lifetimes and acrylamide quenching of specifically inserted tryptophan residues. *Biochemistry* **39**:5287–5294.
99. Eftink MR, Ghiron CA. 1977. Exposure of tryptophanyl residues and protein dynamics. *Biochemistry* **16**(25):5546–5551.
100. Eftink MR, Ghiron CA. 1981. Fluorescence quenching studies with proteins. *Anal Biochem* **114**:199–227.
101. Eftink MR. 1991. Fluorescence quenching: theory and applications. In *Topics in fluorescence spectroscopy*, Vol. 2: *Principles*, pp. 53–126. Ed JR Lakowicz. Plenum Press, New York.
102. Vazquez-Ibar JL, Guan L, Svrakic M, Kaback HR. 2003. Exploiting luminescence spectroscopy to elucidate the interaction between sugar and a tryptophan residue in the lactose permease of *Escherichia coli*. *Proc Natl Acad Sci USA* **100**(22):12706–12711.
103. Wu C-SC, Yang JT. 1980. Helical conformation of glucagon in surfactant solutions. *Biochemistry* **19**:2117–2122.
104. Boesch C, Bundi A, Oppliger M, Wüthrich K. 1978. ^{1}H nuclear-magnetic-resonance studies of the molecular conformation of monomeric glucagon in aqueous solution. *Eur J Biochem* **91**:209–214.
105. Edelhoch H, Lippoldt RE. 1969. Structural studies on polypeptide hormones. *J Biol Chem* **244**:3876–3883.
106. Terwilliger TC, Eisenberg D. 1982. The structure of melittin. *J Biol Chem* **257**:6016–6022.
107. Lakowicz JR, Weber G. 1973. Quenching of protein fluorescence by oxygen: detection of structural fluctuations in proteins on the nanosecond timescale. *Biochemistry* **12**:4171–4179.
108. Calhoun DB, Vanderkooi JM, Englander SW. 1983. Penetration of small molecules into proteins studied by quenching of phosphorescence and fluorescence. *Biochemistry* **22**:1533–1539.
109. Calhoun DB, Englander SW, Wright WW, Vanderkooi JM. 1988. Quenching of room temperature protein phosphorescence by added small molecules. *Biochemistry* **27**:8466–8474.
110. Kouyama I, Kinosita K, Ikegami A. 1989. Correlation between internal motion and emission kinetics of tryptophan residues in proteins. *Eur J Biochem* **182**:517–521.
111. Lakowicz JR, Gryczynski I, Cherek I, Szmacinski H, Joshi N. 1991. Anisotropy decays of single tryptophan proteins measured by GHz frequency-domain fluorometry with collisional quenching. *Eur Biophys J* **19**:125–140.
112. Avigliano L, Finazzi-Agro A, Mondovi B. 1974. Perturbation studies on some blue proteins. *FEBS Lett* **38**:205–208.
113. Glandieres J-M, Twist C, Haouz A, Zentz C, Alpert B. 2000. Resolved fluorescence of the two tryptophan residues in horse apomyoglobin. *Photochem Photobiol* **71**(4):382–386.
114. Wasylewski Z, Kaszycki P, Guz A, Stryjewski W. 1988. Fluorescence quenching resolved spectra of fluorophores in mixtures and micellar solutions. *Eur J Biochem* **178**:471–476.
115. Stryjewski W, Wasylewski Z. 1986. The resolution of heterogeneous fluorescence of multitryptophan-containing proteins studied by a fluorescence-quenching method. *Eur J Biochem* **158**:547–553.
116. Wasylewski Z, Poloczek H, Wasniowska A. 1988. Fluorescence quenching resolved spectroscopy of proteins. *Eur J Biochem* **172**: 719–724.
117. Wasylewski Z, Kaszycki P, Drwiega M. 1996. A fluorescence study of Tn10-encoded tet repressor. *J Protein Chem* **15**(1):45–52.
118. Eftink MR. 1997. Fluorescence methods for studying equilibrium macromolecule-ligand interactions. *Methods Enzymol* **278**:221–257.
119. Ulrich A, Schmitz AAP, Braun T, Yuan T, Vogel HJ, Vergères G. 2000. Mapping the interface between calmodulin and MARCKS-related protein by fluorescence spectroscopy. *Proc Natl Acad Sci USA* **97**(10):5191–5196.
120. Akyol Z, Bartos JA, Merrill MA, Faga LA, Jaren OR, Shea MA, Hell JW. 2004. Apo-calmodulin binds with its C-terminal domain to the N-methyl-D-aspartate receptor NR1 C0 region. *J Biol Chem* **279**(3): 2166–2175.
121. Kilhoffer M-C, Kubina M, Travers F, Haiech J. 1992. Use of engineered proteins with internal tryptophan reporter groups and perturbation techniques to probe the mechanism of ligand-protein interactions: investigation of the mechanism of calcium binding to calmodulin. *Biochemistry* **31**:8098–8106.
122. Chabbert M, Lukas TJ, Watterson DM, Axelsen PH, Prendergast FG. 1991. Fluorescence analysis of calmodulin mutants containing tryptophan: conformational changes induced by calmodulin-binding peptides from myosin light chain kinase and protein kinase II. *Biochemistry* **30**:7615–7630.
123. Dong CZ, De Rocquigny H, Rémy E, Mellac S, Fournié-Zaluski MC, Roques BP. 1997. Synthesis and biological activities of fluorescent acridine-containing HIV-1 nucleocapsid proteins for investigation of nucleic acid-NCp7 interactions. *J Pept Res* **50**:269–278.
124. Rai SS, O'Handley D, Nakai H. 2001. Conformational dynamics of a transposition repressor in modulating DNA binding. *J Mol Biol* **312**: 311–322.
125. Lorenz M, Diekmann S. 2001. Quantitative distance information on protein-DNA complexes determined in polyacrylamide gels by fluorescence resonance energy transfer. *Electrophoresis* **22**:990–998.
126. Boyer M, Poujol N, Margeat E, Royer CA. 2000. Quantitative characterization of the interaction between purified human estrogen receptor α and DNA using fluorescence anisotropy. *Nucleic Acids Res* **28**(13):2494–2502.
127. Bombarda E, Ababou A, Vuilleumier C, Gerard D, Roques BP, Piemont E, Mely Y. 1999. Time-resolved fluorescence investigation of the human immunodeficiency virus type 1 nucleocapsid protein: influence of the binding of nucleic acids. *Biophys J* **76**:1561–1570.

128. Kozlov AG, Lohman TM. 2002. Stopped-flow studies of the kinetics of single-stranded DNA binding and wrapping around the *Escherichia coli* SSB tetramer. *Biochemistry* **41**:6032–6044.
129. Zargarian L, Le Tilly V, Jamin N, Chaffotte A, Gabrielsen OS, Toma F, Alpert B. 1999. Myb-DNA recognition: role of tryptophan residues and structural changes of the minimal DNA binding domain of c-Myb. *Biochemistry* **38**:1921–1929.
130. Pokalsky C, Wick P, Harms E, Lytle FE, Van Etten RL. 1995. Fluorescence resolution of the intrinsic tryptophan residues of bovine protein tyrosyl phosphatase. *J Biol Chem* **270**(8):3809–3815.
131. Ramos P, Coste T, Piemont E, Lessinger JM, Bousquest JA, Chapus C, Kerfelec B, Ferard G, Mely Y. 2003. Time-resolved fluorescence allows selective monitoring of Trp30 environmental changes in the seven-trp-containing human pancreatic lipase. *Biochemistry* **42**:12488–12496.
132. Cheung C-W, Mas MT. 1996. Substrate-induced conformational changes in yeast 3-phosphoglycerate kinase monitored by fluorescence of single tryptophan probes. *Protein Sci* **5**:1144–1149.
133. Pham AS, Reinhart GD. 2003. Quantification of allosteric influence of *escherichia coli* phosphofructokinase by frequency domain fluorescence. *Biophys J* **85**:656–666.
134. Takita T, Nakagoshi M, Inouye K, Tonomura B. 2003. Lysyl-tRNA synthetase from *bacillus stearothermophilus*: the Trp314 residue is shielded in a non-polar environment and is responsible for the fluorescence changes observed in the amino acid activation reaction. *J Mol Biol* **325**:677–695.
135. Tang L, van Merode AEJ, Spelberg JHL, Fraaije MW, Janssen DB. 2003. Steady-state kinetics and tryptophan fluorescence properties of halohydrin dehalogenase from *agrobacterium radiobacter*: roles of W139 and W249 in the active site and halide-induced conformational change. *Biochemistry* **42**:14057–14065.
136. Clark EH, East JM, Lee AG. 2003. The role of tryptophan residues in an integral membrane protein: diacylglycerol kinase. *Biochemistry* **42**:11065–11073.
137. Van Duffelen M, Chrin LR, Berger CL. 2004. Nucleotide dependent intrinsic fluorescence changes of W29 and W36 in smooth muscle myosin. *Biophys J* **87**:1767–1775.
138. Pattanaik P, Ravindra G, Sengupta C, Maithal K, Balaram P, Balaram H. 2003. Unusual fluorescence of W168 in *plasmodium falciparum* triosephosphate isomerase, probed by single-tryptophan mutants. *Eur J Biochem* **270**:745–756.
139. Loewenthal R, Sancho J, Fersht AR. 1991. Fluorescence spectrum of barnase: contributions of three tryptophan residues and a histidine-related pH dependence. *Biochemistry* **30**:6775–6779.
140. Shopova M, Genov N. 1983. Protonated form of histidine 238 quenches the fluorescence of tryptophan 241 in subtilisin novo. *Int J Pept Res* **21**:475–478.
141. Eftink MR. 1991. Fluorescence quenching reactions. In *Biophysical and biochemical aspects of fluorescence spectroscopy*, pp. 1–41. Ed TG Dewey. Plenum Press, New York.
142. Lux B, Baudier J, Gerard D. 1985. Tyrosyl fluorescence spectra of proteins lacking tryptophan: effects of intramolecular interactions. *Photochem Photobiol* **42**(3):245–251.
143. Wu P, Li Y-K, Talalay P, Brand L. 1994. Characterization of the three tyrosine residues of Δ^5-3-ketosteroid isomerase by time-resolved fluorescence and circular dichroism. *Biochemistry* **33**:7415–7422.
144. Canet D, Doering K, Dobson CM, Dupont Y. 2001. High-sensitivity fluorescence anisotropy detection of protein-folding events: application to α-lactalbumin. *Biophys J* **80**:1996–2003.
145. Ghaemmaghami S, Word JM, Burton RE, Richardson JS, Oas TG. 1998. Folding kinetics of a fluorescent variant of monomeric λ repressor. *Biochemistry* **37**:9179–9185.
146. Tcherkasskaya O, Uversky VN. 2001. Denatured collapsed states in protein folding: example of apomyoglobin. *Proteins: Struct Funct Genet* **44**:244–254.
147. Gilmanshin R, Gulotta M, Dyer RB, Callender RH. 2001. Structures of apomyoglobin's various acid-destabilized forms. *Biochemistry* **40**: 5127–5136.
148. Jones BE, Beechem JM, Matthews CR. 1995. Local and global dynamics during the folding of *Escherichia coli* dihydrofolate reductase by time-resolved fluorescence spectroscopy. *Biochemistry* **34**: 1867–1877.
149. Smith CJ, Clarke AR, Chia WN, Irons LI, Atkinson T, Holbrook JJ. 1991. Detection and characterization of intermediates in the folding of large proteins by the use of genetically inserted tryptophan probes. *Biochemistry* **30**:1028–1036.
150. Otto MR, Lillo MP, Beechem JM. 1994. Resolution of multiphasic reactions by the combination of fluorescence total-intensity and anisotropy stopped-flow kinetic experiments. *Biophys J* **67**:2511–2521.
151. Ballew RM, Sabelko J, Gruebele M. 1996. Direct observation of fast protein folding: the initial collapse of apomyoglobin. *Proc Natl Acad Sci USA* **93**:5759–5764.
152. Service RF. 1996. Folding proteins caught in the act. *Science* **273**: 29–30.
153. Eftink MR. 1994. The use of fluorescence methods to monitor unfolding transitions in proteins. *Biophys J* **66**:482–501.
154. Eftink MR, Ionescu R, Ramsay GD, Wong C-Y, Wu JQ, Maki AH. 1996. Thermodynamics of the unfolding and spectroscopic properties of the V66W mutant of staphylococcal nuclease and its 1-136 fragment. *Biochemistry* **35**:8084–8094.
155. Ropson IJ, Dalessio PM. 1997. Fluorescence spectral changes during the folding of intestinal fatty acid binding protein. *Biochemistry* **36**:8594–8601.
156. Royer CA, Mann CJ, Matthews CR. 1993. Resolution of the fluorescence equilibrium unfolding profile of *trp* aporepressor using single tryptophan mutants. *Protein Sci* **2**:1844–1852.
157. Szpikowska BK, Beechem JM, Sherman MA, Mas MT. 1994. Equilibrium unfolding of yeast phosphoglycerate kinase and its mutants lacking one or both native tryptophans: a circular dichroism and steady-state and time-resolved fluorescence study. *Biochemistry* **33**:2217–2225.
158. Sendak RA, Rothwarf DM, Wedemeyer WJ, Houry WA, Scheraga HA. 1996. Kinetic and thermodynamic studies of the folding/unfolding of a tryptophan-containing mutant of ribonuclease A. *Biochemistry* **35**:12978–12992.
159. Steer BA, Merrill AR. 1995. Guanidine hydrochloride-induced denaturation of the colicin E1 channel peptide: unfolding of local segments using genetically substituted tryptophan residues. *Biochemistry* **34**:7225–7234.
160. Clark PL, Liu Z-P, Zhang J, Gierasch LM. 1996. Intrinsic tryptophans of CRABPI as probes of structure and folding. *Protein Sci* **5**: 1108–1117.

161. Clark PL, Weston BF, Gierasch LM. 1998. Probing the folding pathway of a β-clam protein with single-tryptophan constructs. *Folding Des* **3**:401–412.
162. Meagher JL, Beechem JM, Olson ST, Gettins PGW. 1998. Deconvolution of the fluorescence emission spectrum of human antithrombin and identification of the tryptophan residues that are responsive to heparin binding. *J Biol Chem* **273**(36):23283–23289.
163. Hannemann F, Bera AK, Fischer B, Lisurek B, Lisurek M, Teuchner K, Bernhardt R. 2002. Unfolding and conformational studies on bovine adrenodoxin probed by engineered intrinsic tryptophan fluorescence. *Biochemistry* **41**:11008–11016.
164. Mansoor SE, Mchaourab HS, Farrens DL. 1999. Determination of protein secondary structure and solvent accessibility using site-directed fluorescence labeling: studies of T4 lysozyme using the fluorescent probe monobromobimane. *Biochemistry* **38**:16383–16393.
165. Kintrup M, Schubert P, Kunz M, Chabbert M, Alberti P, Bombarda E, Schneider S, Hillen W. 2000. Trp scanning analysis of tet repressor reveals conformational changes associated with operator and anhydrotetracycline binding. *Eur J Biochem* **267**:821–829.
166. Gasymov OK, Abduragimov AR, Yusifov TN, Glasgow BJ. 1997. Solution structure by site directed tryptophan fluorescence in tear lipocalin. *Biochem Biophys Res Commun* **239**:191–196.
167. Gasymov OK, Abduragimov AR, Yusifov TN, Glasgow BJ. 2001. Site-directed tryptophan fluorescence reveals the solution structure of tear lipocalin: evidence for features that confer promiscuity in ligand binding. *Biochemistry* **40**:14754–14762.
168. Wong C-Y, Eftink MR. 1998. Incorporation of tryptophan analogues into staphylococcal nuclease, its V66W mutant, and Δ137-149 fragment: spectroscopic studies. *Biochemistry* **37**:8938–8946.
169. Mohammadi F, Prentice GA, Merrill AR. 2001. Protein–protein interaction using tryptophan analogues: novel spectroscopic probes for toxin-elongation factor-2 interactions. *Biochemistry* **40**:10273–10283.
170. Li Q, Du H-N, Hu H-Y. 2003. Study of protein–protein interactions by fluorescence of tryptophan analogs: application to immunoglobulin G binding domain of streptococcal protein G. *Biopolymers* **72**: 116–122.
171. Acchione M, Guillemette JG, Twine SM, Hogue CWV, Rajendran B, Szabo AG. 2003. Fluorescence-based structural analaysis of tryptophan analogue–AMP formation in single tryptophan mutants of *B. stearothermophilus* tryptophanyl-tRNA synthetase. *Biochemistry* **42**: 14994–15002.
172. Das K, Ashby KD, Smirnov AV, Reinach FC, Petrich JW, Farah CS. 1999. Fluorescence properties of recombinant tropomyosin containing tryptophan 5-hydroxytryptophan and 7-azatryptophan. *Photochem Photobiol* **70**(5):719–730.
173. Hogue CWV, Rasquinha I, Szabo AG, MacManus JP. 1992. A new intrinsic fluorescent probe for proteins. *FEBS Lett* **310**:269–272.
174. Twine SM, Szabo AG. 2003. Fluorescent amino acid analogues. *Methods Enzymol* **360**:104–127.
175. Heyduk E, Heyduk T. 1993. Physical studies on interaction of transcription activator and RNA-polymerase: fluorescent derivatives of CRP and RNA polymerase. *Cell Mol Biol Res* **39**:401–407.
176. Laue TM, Senear DF, Eaton S, Ross JBA. 1993. 5-hydroxytryptophan as a new intrinsic probe for investigating protein-DNA interactions by analytical ultracentrifugation: study of the effect of DNA on self-assembly of the bacteriophage λ cI repressor. *Biochemistry* **32**:2469–2472.
177. Soumillion P, Jespers L, Vervoort J, Fastrez J. 1995. Biosynthetic incorporation of 7-azatryptophan into the phage lambda lysozyme: estimation of tryptophan accessibility, effect on enzymatic activity and protein stability. *Protein Eng* **8**:451–456.
178. Wong C-Y, Eftink MR. 1997. Biosynthetic incorporation of tryptophan analogues into staphylococcal nuclease: effect of 5-hydroxytryptophan and 7-azatryptophan on structure and stability. *Protein Sci* **6**:689–697.
179. Laws WR, Schwartz GP, Rusinova E, Burke GT, Chu Y-C, Katsoyannis PG, Ross JBA. 1995. 5-hydroxytryptophan: an absorption and fluorescence probe which is a conservative replacement for [A14 tyrosine] in insulin. *J Protein Chem* **14**:225–232.
180. Hogue CWV, Szabo AG. 1993. Characterization of aminoacyl-adenylates in *B. subtilis* tryptophanyl-tRNA synthetase, by the fluorescence of tryptophan analogs 5-hydroxytryptophan and 7-azatryptophan. *Biophys Chem* **48**:159–169.
181. Broos J, Gabellieri E, Biemans-Oldehinkel E, Strambini GB. 2003. Efficient biosynthetic incorporation of tryptophan and indole analogs in an integral membrane protein. *Protein Sci* **12**:1991–2000.
182. Guharay J, Sengupta PK. 1996. Characterization of the fluorescence emission properties of 7-azatryptophan in reverse micellar environments. *Biochem Biophys Res Commun* **219**:388–392.
183. Negrerie M, Gai F, Bellefeuille SM, Petrich JW. 1991. Photophysics of a novel optical probe: 7-azaindole. *J Phys Chem* **95**:8663–8670.
184. Rich RL, Negrerie M, Li J, Elliott S, Thornburg RW, Petrich JW. 1993. The photophysical probe, 7-azatryptophan, in synthetic peptides. *Photochem Photobiol* **58**(1):28–30.
185. Chen Y, Gai F, Petrich JW. 1994. Solvation and excited state proton transfer of 7-azindole in alcohols. *Chem Phys Lett* **222**:329–334.
186. Chen Y, Gai F, Petrich JW. 1994. Single-exponential fluorescence decay of the nonnatural amino acid 7-azatryptophan and the nonexponential fluorescence decay of tryptophan in water. *J Phys Chem* **98**:2203–2209.
187. Chen Y, Rich RL, Gai F, Petrich JW. 1993. Fluorescent species of 7-azindole and 7-azatryptophan in water. *J Phys Chem* **97**:1770–1780.
188. English DS, Rich RL, Petrich JW. 1998. Nonexponential fluorescence decay of 7-azatryptophan induced in a peptide environment. *Photochem Photobiol* **67**(1):76–83.
189. Hott JL, Borkman RF. 1989. The non-fluorescence of 4-fluorotryptophan. *Biochem J* **264**:297–299.
190. England PM. 2004. Unnatural amino acid mutageneis: a precise tool for probing protein structure and function. *Biochemistry* **43**(37): 11623–11629.
191. Noren CJ, Anthony-Cahill SJ, Griffith MC, Schultz PG. 1989. A general method for site-specific incorporation of unnatural amino acids into proteins. *Science* **244**:182–188.
192. Bain JD, Glabe CG, Dix TA, Chamberlin AR. 1989. Biosynthetic site-specific incorporation of a non-natural amino acid into a polypeptide. *J Am Chem Soc* **111**:8013–8014.
193. Heckler TG, Chang L-H, Zama Y, Naka T, Chorghade MS, Hecht SM. 1984. T4 RNA ligase mediated preparation of novel "chemically misacylated" $tRNA^{Phe}$s. *Biochemistry* **23**:1468–1473.
194. Taki M, Hohsaka T, Murakami H, Taira K, Sisido M. 2002. Position-specific incorporation of a fluorophore–quencher pair into single

streptavidin orthogonal four-base codon–anticodon pairs. *J Am Chem Soc* **124**:14586–14590.
195. Hohsaka T, Ashizuka Y, Taira H, Murakami H, Sisido M. 2001. Incorporation of nonnatural amino acids into proteins by using various four-base codons in an *Escherichia coli* in vitro translation systems. *Biochemistry* **40**:11060–11064.
196. Wang L, Brock A, Schultz PG. 2002. Adding L-3-(2-naphthyl)alanine to the genetic code of *E. coli*. *J Am Chem Soc* **124**:1836–1837.
197. Anderson RD, Zhou J, Hecht SM. 2002. Fluorescence resonance energy transfer between unnatural amino acids in a structurally modified dihydrofolate reductase. *J Am Chem Soc* **124**:9674–9675.
198. Wang L, Brock A,, Herberich B, Schultz PG. 2001. Expanding the genetic code of *Escherichia coli*. *Science* **292**(5516):498–500.
199. Murakami H, Hohsaka T, Ashizuka Y, Hashimoto K, Sisido M. 2000. Site-directed incorporation of fluorescent nonnatural amino acids into streptavidin for highly sensitive detection of biotin. *Biomacromolecules* **1**:118–125.
200. Hohsaka T, Muranaka N, Komiyama C, Matsui K, Takaura S, Abe R, Murakami H, Sisido M. 2004. Position-specific incorporation of dansylated non-natural amino acids into streptavidin by using a four-base codon. *FEBS Lett* **560**:173–177.
201. Strasser F, Dey J, Eftink MR, Plapp BV. 1998. Activation of horse liver alcohol dehydrogenase upon substitution of tryptophan 314 at the dimer interface. *Arch Biochem Biophys* **358**(2):369–376. (The original data were courtesy of Dr. BU Plopp.)

PROBLEMS

P16.1. *Determination of Protein Association and Unfolding by Fluorescence*: Suppose you have a protein that consists of a single subunit with a molecular weight of 25,000 daltons. The protein contains a single-tryptophan residue near the central core of the protein and several tyrosine residues. The protein also contains a single reactive sulfhydryl residue on the surface.

A. Assume that the monomeric protein can be unfolded by the addition of denaturant. Explain how the fluorescence spectral properties of the unmodified protein could be used to follow the unfolding process.

B. Describe the use of collisional quenchers to probe the accessibility of the tryptophan residue to the solvent.

C. Assume that the unmodified protein self-associates with another subunit to form a dimer. How could fluorescence spectroscopy be used to follow the association process?

D. Describe how you would use fluorescence spectroscopy to measure the distance from the tryptophan residue to the reactive sulfhydryl group. Be specific with regard to the experiments that you would perform and how the data would be interpreted.

E. Describe how you would use energy transfer to measure self-association of the protein after the protein has been modified on the sulfhydryl groups with dansyl chloride.

P16.2. *Detection of Protein Dimerization*: Suppose you have a small protein with a single-tryptophan residue that displays $r_0 = 0.30$, and that the protein associates to a dimer. The correlation times of the monomer and dimer are $\theta_M = 1.25$ and $\theta_D = 2.5$ ns, respectively. Upon dimer formation the lifetime increases from $\tau_M = 2.5$ to $\tau_D = 5.0$ ns, and the relative quantum yield increases twofold. Describe how you would detect dimer formation using the:

A. steady-state intensity,

B. intensity decay,

C. steady-state anisotropy, or

D. anisotropy decay.

E. What fraction of the emission is due to the monomers and dimers when 50% of the monomers have formed dimers? What is the steady-state anisotropy? What are the intensity and anisotropy decays?

P16.3. *Effect of Excitation Wavelength on Protein Fluorescence*: Section 16.9.3 described kinetic studies of the refolding of cellular retinoic acid biding protein I (CRABPI). The wild-type protein contains three tryptophan residues (Figure 16.57). Figure 16.74 shows emission spectra of the native and denatured forms of CRABPI for various excitation wavelengths. The emission spectra of native CRABPI shift to longer wavelengths with increasing excitation wavelength. The emission spectra of denatured CRABPI do not depend on excitation wavelength. Explain these emission spectra. There may be more than one explanation.

P16.4. *Binding Between Calmodulin and a Protein Kinase C*: Myristoylated protein kinase (MRP) is a kinase that binds to calmodulin. MRP and CaM both lack tryptophan with wild-type sequence MRP. Emission spectra of wild-type and single-tryptophan mutants of MRP are shown in Figure 16.75. Explain these spectra.

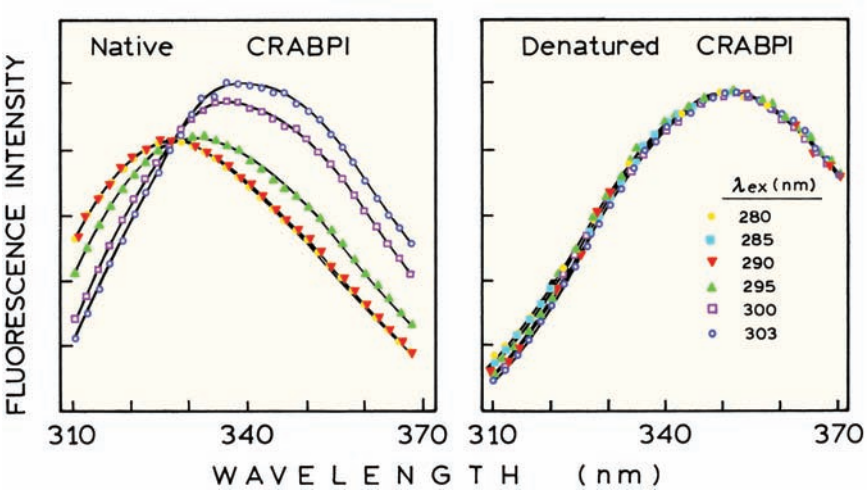

Figure 16.74. Emission spectra of cellular retinoic acid binding protein I (CRABPI) for various excitation wavelengths. Revised from [160].

P16.5. *Quenching of LADH and Its Mutants*: Liver alcohol dehydrogenase (LADH) contains two tryptophan residues at positions 15 and 314. Table 16.2 lists steady-state intensity quenching data for wild-type LADH and the mutant W314L containing only W15. Interpret these data in terms of the accessibility of each tryptophan residue to quenching, the Stern-Volmer quenching constants, and fractional accessibilities to quenching.

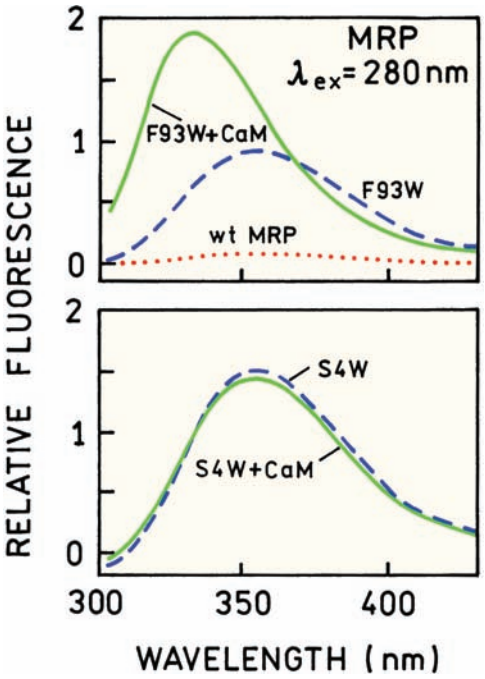

Figure 16.75. Emission spectra of wild-type myristoylated protein kinase C and single-tryptophan containing mutants, in the absence and presence of calmodulin. Revised from [119].

Table 16.2. Acrylamide and Iodide Quenching Data for the Wild-Type LADH and the W314F Mutant

	Wild-type LADH				
[Acrylamide]	F/F_0	$\Delta F/F_0$	[I^-]	F/F_0	$\Delta F/F_0$
0	1.00	0	0	1.00	0
0.025	0.86	0.14	0.061	0.96	0.04
0.050	0.77	0.23	0.122	0.93	0.07
0.074	0.71	0.29	0.181	0.89	0.11
0.098	0.67	0.33	0.238	0.863	0.137
0.120	0.63	0.36	0.294	0.856	0.144
0.146	0.60	0.40	0.349	0.84	0.16
0.170	0.57	0.43	0.402	0.83	0.17
0.190	0.55	0.45	0.455	0.82	0.18
0.238	0.51	0.49	0.506	0.80	0.20
0.280	0.49	0.51	0.556	0.77	0.23
0.370	0.45	0.54	0.604	0.76	0.23
0.450	0.42	0.58	0.652	0.75	0.25
0.550	0.40	0.60	0.700	0.74	0.26
0.650	0.38	0.62	0.745	0.73	0.27
0.745	0.34	0.66	0.790	0.72	0.28
0.830	0.33	0.67	0.833	0.71	0.29
1.000	0.31	0.69	0.876	0.70	0.296
			0.918	0.69	0.30
			0.960	0.69	0.31
			1.000	0.68	0.32
	W314F LADH				
[Acrylamide]	F/F_0	$\Delta F/F_0$	[I^-]	F/F_0	$\Delta F/F_0$
0	1	0	0	1	0
0.025	0.85	0.15	0.063	0.94	0.058
0.050	0.70	0.29	0.124	0.88	0.115
0.075	0.62	0.38	0.184	0.83	0.17
0.098	0.54	0.45	0.243	0.79	0.21
0.122	0.50	0.50	0.300	0.75	0.25
0.146	0.45	0.54	0.355	0.71	0.29
0.170	0.41	0.59	0.410	0.70	0.31
0.190	0.38	0.62	0.463	0.67	0.33
0.215	0.33	0.67	0.515	0.63	0.37
0.240	0.32	0.68	0.566	0.61	0.39
0.260	0.27	0.73	0.615	0.60	0.40
0.280	0.27	0.73	0.664	0.58	0.42
0.305	0.26	0.74	0.711	0.56	0.44
0.327	0.24	0.76	0.756	0.55	0.45
0.370	0.21	0.79	0.803	0.54	0.46
0.410	0.18	0.81	0.847	0.52	0.48
0.450	0.17	0.83	1.016	0.46	0.54
0.500	0.15	0.85			
0.540	0.14	0.86			
0.570	0.13	0.87			
0.650	0.11	0.89			
0.745	0.09	0.90			
0.833	0.08	0.92			
0.920	0.07	0.93			
1.080	0.05	0.95			

[a]From [201].